AN ABSTRACT OF THE DISSERTATION OF

Jayanthi J. Joseph for the degree of Doctor of Philosophy in Microbiology presented on August 10, 2022.

Title: Characterization of *Mycobacterium avium* subsp. *hominissuis* Interactions with Host Macrophages and Multinucleated Giant Cells

Abstract approved:

_____

Luiz E. Bermudez

Mycobacterium avium subsp. *hominissuis* (*M. avium*) is a ubiquitous environmental opportunistic pathogen that causes pulmonary disease humans. Pulmonary *M. avium* infections produce peribronchial granulomas which contain multinucleated giant cells (MGCs). Mycobacterial infection activates pro-inflammatory and anti-inflammatory pathways in macrophages. The balance of pro- and anti-inflammatory signals determine the outcome of bacterial survival. However, there is limited knowledge of the macrophage response to *M. avium* infection and the involvement of inflammasomes and the cGAS/STING pathway. Also, the mechanisms by which *M. avium* to modulates the macrophage inflammatory response need further clarification, specifically the role of eDNA. The involvement of MGCs in *M. avium* pathogenesis remains undefined and the shortcomings of current models pose a barrier to study these interactions. The main goals of this dissertation were to investigate the macrophage response to *M. avium*, examine the role of eDNA in the host, study MGC-*M. avium* interactions, and further describe MGCs.

To examine the macrophage response to *M. avium*, I compared inflammasome and cytosolic sensor expression and activation. My result demonstrated that virulent strains of *M. avium* (A5 and 104) suppress IL-1β production and induce IFN-β production in macrophages. *M. avium* mutants deficient at DNA export in the biofilm exhibited reduced intracellular survival and significantly higher IL-1β production than wildtype. IFN-β production appeared to be related to DNA export capability.

To further characterize MGCs, we developed a novel *in vitro* model which is comprised of a human-derived cell line (THP-1) and cytokine stimulation (IFN-γ and TNF-α). Examination of MGCs with transmission electron microscopy uncovered increased lipid droplets and elevated autophagy. My results showed that *M. avium* survived and replicated in MGCs and that host lipids play a role in intracellular replication. MGC-passaged bacteria were readily phagocytosed and exhibited normal intracellular replication. The mechanism of cell exit is still unclear.

The data presented in this dissertation significantly advance our understanding of the macrophage response to *M. avium*, and the features of MGCs, and how they interact with *M. avium*. Understanding these host-pathogen interactions has implications for NTM treatment. The idea that eDNA influences intracellular survival and anti-inflammatory signaling needs further study. However, DNA export genes could be a useful target for future therapies.

Characterization of *Mycobacterium avium* subsp. *hominissuis* Interactions with Host Macrophages and Multinucleated Giant Cells

by
Jayanthi J. Joseph

A DISSERTATION

submitted to

Oregon State University

in partial fulfillment of
the requirements for the
degree of

Doctor of Philosophy

Presented August 10, 2022
Commencement June 2023

Doctor of Philosophy dissertation of Jayanthi J. Joseph presented on August 10, 2022

APPROVED:

Major Professor, representing Microbiology

Head of the Department of Microbiology

Dean of the Graduate School

I understand that my dissertation will become part of the permanent collection of Oregon State University libraries. My signature below authorizes release of my dissertation to any reader upon request.

Jayanthi J. Joseph, Author

ACKNOWLEDGEMENTS

First, I want to thank Dr. Luiz Bermudez for giving me the opportunity to complete this research and dissertation. Throughout the years, he has provided me with constant and invaluable mentorship and taught me how to think critically about scientific data, which is an essential skill for independent scientists. I would also like to thank the other members of the Bermudez laboratory for their scientific insights, stimulating discussions, and support, as well as for their camaraderie and friendship. Special thanks to Dr. Sasha Rose, who trained me as an undergraduate student and taught me essential technical skills. Likewise, Amy Leestemaker-Palmer provided me with key scientific writing advice and taught me several new techniques that have served me well throughout graduate school. Lynette Hawthorne has been a positive presence in the office and helped guide me through the administrative side of graduate school. I would also like to thank Dr. Brian Dolan, Dr. Elain Fu, Dr. Daniel Rockey, and Dr. Martin Schuster for serving on my graduate committee.

My friends and family are a constant source of support and encouragement which has helped me tremendously. Special thanks to Dr. Lotisha Garvin for being a good friend and study partner during the hardest part of grad school. Finally, I would like to thank Amy Leestemaker-Palmer and Bailey Keefe for all the adventures that we have had over the years.

CONTRIBUTION OF AUTHORS

Chapter 1: Jayanthi J. Joseph wrote the General Introduction.

Chapter 2: Jayanthi J. Joseph designed and conducted the experiments, analyzed data, and wrote the manuscript. Soheila Kazemi helped design and perform the flow cytometry experiments. Lia Danelishvili performed siRNA and western blot experiments. Amy Leestemaker-Palmer assisted with experimental design and manuscript preparation and review. Luiz Bermudez designed experiments, performed siRNA experiments, provided important discussion and review of the manuscript, and funded the project.

Chapter 3: Jayanthi J. Joseph designed and conducted the experiments, analyzed data, and wrote the manuscript. Amy Leestemaker-Palmer assisted with experimental design, writing and manuscript preparation. Luiz Bermudez designed experiments and provided important discussion and review of the manuscript and funded the project.

Chapter 4: Jayanthi J. Joseph wrote the discussion and conclusion section. Luiz Bermudez provided important discussion.

TABLE OF CONTENTS

Page

TABLE OF CONTENTS (Continued)

Page

TABLE OF CONTENTS (Continued)

Page

LIST OF FIGURES

LIST OF FIGURES (Continued)

Figure Page

LIST OF TABLES

LIST OF APPENDICES

Chapter 1

General Introduction

Jayanthi J. Joseph

Characteristics of Mycobacteria

Mycobacterium is a genus of actinobacteria with 188 distinct species that range from obligate pathogens to environmental bacteria. Mycobacteria are aerobic bacilli that are typically nonmotile. The mycobacterial cell wall is thick and waxy, due to the abundance of hydrophobic mycolic acids (Jarlier & Nikaido, 1994). The unique composition of the mycobacterial cell wall contributes to the hardiness and virulence of this genus (Jarlier & Nikaido, 1994). Gram staining of mycobacteria yields a positive result but is not specific due to the high lipid content of the cell wall. The acid-fast stain is the preferred alternative for mycobacterial identification (Murray et al., 1980). Mycobacteria lack the type III secretion system, and instead utilize the type VII secretion system (ESX) to survive in diverse environments. Mycobacteria have five ESX systems, which vary depending on the pathogenicity of the species. In *Mycobacterium tuberculosis*¸ ESX-1 plays a vital role in cell entry, intracellular survival, DNA export, and phagosomal escape (Rivera-Calzada et al., 2021). ESX-3 and ESX-5 are also involved in virulence, with ESX-5 playing a major role in *M. avium* pathogenesis (Ates et al., 2016, p. 5; Li et al., 2005; McNamara et al., 2012, p. 5; Tufariello et al., 2016).

Nontuberculous Mycobacteria

Nontuberculous mycobacteria (NTM), also called atypical mycobacteria, are environmental bacteria that do not cause tuberculosis or leprosy. NTM are ubiquitous in the environment and are commonly found in natural water bodies, household plumbing, and soil (Gebert et al., 2018; Griffith et al., 2007; Honda et al., 2018). A recent survey identified NTM s in ice machines, rain water, showers, air conditioning

units, and dust from vacuum cleaners (Honda et al., 2018). NTM species are classified based on 16s RNA sequencing, which is also used as a diagnostic tool. NTM are further characterized as slow-growing or rapid-growing based on their growth rate on agar medium (Griffith et al., 2007). Rapid-growing NTM include *M. smegmatis, M. abscessus, M. chelonae,* and *M. fortuitum* (Griffith et al., 2007). Slow-growing NTM include *Mycobacterium avium* complex (MAC), *M. kansasii, M. xenopi, M. haemophilum,* and *M. simiae* (Griffith et al., 2007).

Biofilms are a significant source of NTM infections in immunocompetent patients (Griffith et al., 2007; Vega-Dominguez et al., 2020). NTM biofilms are ubiquitous in household plumbing and have been described in the lung during pulmonary NTM infections (Fig. 1.1) (Chakraborty et al., 2021; Gebert et al., 2018; Griffith et al., 2007). Bacteria released from the surface of environmental biofilms are aerosolized, and inhaled (Fig. 1.1) (Appelberg, 2006; Griffith et al., 2007; Yamazaki et al., 2006). NTM biofilms are composed of mycobacteria encased in a protective layer of extracellular polymeric substance (EPS) (Rose et al., 2015; Vega-Dominguez et al., 2020). The EPS of NTM biofilms contains glycopeptidolipids, extracellular DNA (eDNA), mycolyl-diacylglycerols, lipooligosaccharides, and lipopeptides (Freeman et al., 2006; Ojha et al., 2005; Rose et al., 2015). eDNA is a common ingredient of bacterial EPS, and has been described in *Listeria monocytogenes*, *Streptococcus pneumoniae*, and *Neisseria meningitidis* (Harmsen et al., 2010; Lappann et al., 2010; Moscoso et al., 2006). eDNA plays a role in biofilm formation, nutrient acquisition, structural support, and provides protection against antibiotics and antimicrobial peptides (Harmsen et al., 2010; Ilinov et al., 2021; Lappann et al., 2010;

Moscoso et al., 2006; Rose et al., 2015; Rose & Bermudez, 2016). *M. avium* exports eDNA during biofilm formation in the host and in the environment (Chakraborty et al., 2021; Rose & Bermudez, 2016). During early infection, *M. avium* biofilms trigger hyperstimulation and apoptosis of host macrophages, which significantly impedes bacterial clearance (Rose & Bermudez, 2014). Consequently, biofilms present a barrier for bacterial clearance by the host.

NTM Lung Disease

Transmission of NTM from environmental sources occurs when bacteria or bacterial aggregates are aerosolized and inhaled (Gebert et al., 2018; Griffith et al., 2007). Pulmonary NTM infections are characterized by the formation of non-necrotic and necrotic peribronchiolar granulomas, pulmonary nodules and lesions. Risk factors for pulmonary NTM disease include cystic fibrosis, chronic obstructive pulmonary disease (COPD), steroid therapy, vitamin D deficiency, being postmenopausal, or having a history of smoking (Griffith et al., 2007). NTM lung disease typically presents as nodular bronchiectasis in postmenopausal females (Griffith et al., 2007; Ratnatunga et al., 2020; Reich & Johnson, 1992; Wilińska & Szturmowicz, 2010). Classical presentation of NTM lung disease is apical fibrocavitary lung disease, which is most common in male patients (Ahn et al., 1982; Griffith et al., 2007). If left untreated, this presentation of pulmonary NTM infection can result in respiratory failure and extensive lung damage in 1-2 years (Ahn et al., 1982; Griffith et al., 2007).

Treatment of NTM Lung Disease

NTM lung disease is notoriously difficult to treat, partially due to the antibiotic tolerance of mycobacterial biofilms (Chakraborty et al., 2021). Treatment

yields inconsistent results even in immunocompetent patients (Griffith et al., 2007). Therapy involves a combination of antibiotics, including azithromycin or clarithromycin, rifampin, and ethambutol (Egelund et al., 2015; Griffith et al., 2007). The risk of adverse drug reactions or toxicity is heightened due to the use of multiple drugs. Major side effects include ototoxicity from aminoglycosides, gastrointestinal disturbance from macrolides and rifampin, leukopenia and hepatitis from rifampin, and optic neuritis from ethambutol. However, mono-macrolide treatment is not recommended because of the risk of developing macrolide-resistant NTM. Thrice-weekly treatment lasts for at least 12 months after the first negative sputum results and is ineffective in 40-50% of patients (Griffith et al., 2007).

M. avium Complex

The *Mycobacterium avium* complex (MAC) is comprised of *M. avium*¸ *M. chimaera,* and *M. intracellulare* (Griffith et al., 2007; Johansen et al., 2020). *Mycobacterium avium* subsp. *hominissuis* (*M. avium*) is an opportunistic pathogen that causes pulmonary, and systemic infection in humans. *M. avium* strain 104 and A5 were originally isolated from the blood of an AIDS patient (Rose et al., 2015). Strain 104 is the reference strain for *M. avium*. A5 forms robust biofilms and exports large amounts of extracellular DNA (eDNA) during biofilm formation (Rose et al., 2015; Rose & Bermudez, 2016). Additionally, A5 possesses a unique 50-kBp genomic region associated with DNA export (Rose & Bermudez, 2016). This region is present in *M. abscessus, M. chelonae, M. intracellulare, M. avium* subsp. *hominissuis* strain 3388, which are all of concern in human infections (Rose & Bermudez, 2016). The MAC

lacks ESX-1, but has ESX-2, ESX-3, ESX-4 and ESX-5 (Jeffrey et al., 2017). ESX-5 has been linked to virulence in MAC (McNamara et al., 2012, p. 5).

MAC Pathogenesis

Members of the MAC are facultative intracellular pathogens and preferentially infect antigen presenting cells such as macrophages and monocytes (Appelberg, 2006). MAC can enter host macrophages through receptor-mediated phagocytosis or macropinocytosis (L. E. Bermudez et al., 1999, 2004). MAC utilizes variety of receptors for receptor-mediated phagocytosis, including complement receptors, mannose receptor, and type A scavenger receptors (Appelberg, 2006; L. E. Bermudez et al., 1999; Polotsky et al., 1997). Once inside the macrophage, MAC survives and replicates within a vacuole by suppressing phagosome acidification and inhibiting lysosome fusion (Fig. 1.1) (Frehel et al., 1986; Oh & Straubinger, 1996; Sturgill-Koszycki et al., 1994). The MAC vacuole regularly fuses with non-lysosomal vesicles, which provide nutrients to intra-vacuolar bacteria (Russell et al., 1996). MAC triggers apoptosis of the host macrophage, escape, and infects neighboring cells (Fig. 1.1) (Early et al., 2011). MAC bacteria that exit host macrophages in this manner are taken up in significantly higher numbers by naïve macrophages (L. E. Bermudez et al., 1997, 2006). Additionally, a large percentage of these bacteria enter the next host cell by macropinocytosis, rather than receptor-mediated phagocytosis (L. E. Bermudez et al., 2004, 2006; Danelishvili et al., 2018).

Macrophages kill intracellular pathogens through a variety of mechanisms, including the production of reactive oxygen species (ROI), nitric oxide (NO), phagosome acidification and maturation, cell death (apoptosis, pyroptosis or

necroptosis), and autophagy (Weiss & Schaible, 2015). Intracellular MAC bacteria are resistant to ROS and NO (L. E. M. Bermudez & Young, 1989; Doi et al., 1993). In fact, recent research suggests the NO plays a pro-pathogen role in the grand scale of host-pathogen interactions during MAC infection, at least in part due to its role in the formation of giant cells (Gharun et al., 2017). MAC induces macrophage apoptosis as a strategy for cell-to-cell spread in host macrophages which leads to dissemination (Early et al., 2011).

Cell-to-Cell Transmission

Intracellular bacterial pathogens utilize several different pathways to exit the host cell. Vacuolar bacteria enter the cytosol to trigger cellular escape via apoptotic or necrotic cell death, cell lysis, direct transmission via actin-mediated protrusion, or nonlytic ejection or exocytosis (Flieger et al., n.d.). Once extracellular, the bacteria spread to neighboring cells. *M. abscessus* and MAC induce apoptotic cell death in host macrophages as a mechanism of cellular escape (Early et al., 2011; Flieger et al., n.d.). *M. marinum* utilizes actin motility to move directly from cell-to-cell (Stamm et al., 2003). *M. tb* and *M. marinum* can exit macrophages without host cell lysis by utilizing autophagy to leave the cell (Gerstenmaier et al., 2015). As the infection spreads, infected macrophages secrete pro-inflammatory cytokines which activate and recruit lymphocytes to the site of infection. In this way, innate inflammatory signaling initiates the adaptive response and paves the way for granuloma formation.

Mycobacterial Granulomas

Granulomas are the host-pathogen interface during chronic pulmonary mycobacterial infections (Fig. 1.1). Proinflammatory cytokines TNF-α produced by

macrophages, and IFN-γ produced by T cells, are instrumental in granuloma formation during mycobacterial infection (Smith et al., 1997). Several types of immune cells are involved in granuloma formation, which requires a persistent antigen, foreign body, or pathogen to form (Ehlers & Schaible, 2013). Mycobacteria, infected macrophages, uninfected macrophages, dendritic cells, multinucleated giant cells, and foamy macrophages form the center of the mycobacterial granuloma (Fig. 1.1) (Cronan et al., 2016; Ehlers & Schaible, 2013; Peyron et al., 2008). Lymphocytes (T cells and B cells) and fibroblasts surround the core of the granuloma (Ehlers & Schaible, 2013). As the infection progresses, infected macrophages in the core may become apoptotic or necrotic, releasing mycobacteria into the extracellular space. The necrotic center of the granuloma is lipid-rich and supplies bountiful nutrients for bacterial replication. The extracellular bacteria released by dying host cells infect neighboring uninfected macrophages, dendritic cells, or NK cells (if present), maintaining the chronic infection (Davis & Ramakrishnan, 2009; Early et al., 2011).

In the past, granulomas were assumed to be host-protective structures that dealt with intractable mycobacteria by cordoning them off from the rest of the body. However, the last decade of research has demonstrated that mycobacterial granulomas are dynamic structures with replicating bacteria and newly recruited host cells (Ehlers & Schaible, 2013). It is now understood that mycobacteria survive and persist in granulomas, and in some cases prefer the granuloma environment over the extra-granuloma environment (Cosma et al., 2004). In *M. marinum* infections of zebrafish embryos, granulomas have been shown to facilitate cell-to-cell spread of mycobacteria, aiding in dissemination and bacterial growth (Davis & Ramakrishnan,

2009; Volkman et al., 2004). Dispersion of granulomas reduced bacterial loads and increased host survival in *M. marinum* infections (Cronan et al., 2016).

Multinucleated Giant Cells

Langhans multinucleated giants cells (MGCs) are a feature of mycobacterial granulomas (Brodbeck & Anderson, 2009). However, the precise role of multinucleated giant cells in NTM pathogenesis is poorly understood. Histology of granulomatous lung tissues from rabbits, mice, and humans revealed a high bacterial load in MGCs *in vivo* (Gharun et al., 2017; Klotz et al., n.d.; S. N. Kumar et al., 2013; Langhans, 1868; Ufimtseva, 2015). In the granuloma, monocytes fuse to form MGCs with multiple nuclei, which range from 2-20 depending on the mycobacterial strain (Brooks et al., 2019; Gharun et al., 2017). MGCs from MAC infections retain the ability to phagocytose bacteria, and in some cases are more phagocytic than macrophages (Braune et al., 2021; Gharun et al., 2017; Milde et al., 2015). MGCs are typified by a shift towards cholesterol metabolism, and the upregulation of iNOS (Gharun et al., 2017; Lösslein et al., 2021). The abundant host lipids in MGCs and granulomas provide nutrients to mycobacteria during infection.

Utilization of Host Lipids

Mycobacteria utilize a variety of host-derived lipids to fuel replication in the host (Wilburn et al., 2018). Mycobacteria are adapted to metabolize host triacylglycerols, cholesterol and sphingomyelin. Cholesterol and sphingolipids have been implicated in mycobacterial persistence, growth, and virulence (Keown, 2010; Pandey & Sassetti, 2008; Rolando & Buchrieser, 2019). Cholesterol is an important

structural component of the eukaryotic plasma membrane and is involved in intracellular bacterial survival (Wilburn et al., 2018).

Sphingolipids are a critical structural component of the plasma membrane, and act as signaling molecules in a variety of cellular processes, including cell growth and inflammation (Rolando & Buchrieser, 2019). Sphingolipids are involved in the reorganization of plasma membrane receptors, modulation of autophagy, intracellular vesicle transport, and uptake of *M. tb* by macrophages. Ceramide is central to sphingolipid metabolism and acts as a precursor for ceramide-1-phosphate, which is another signaling molecule. Ceramide synthesized *de novo* from serine and palmitate or generated by the degradation of sphingomyelin (Rolando & Buchrieser, 2019). Sphingomyelin synthase catalyzes the reverse, sphingomyelin from ceramide. In the catabolic pathway, ceramide is converted to sphingosine, which is phosphorylated to form sphingosine-1-phosphate. *M. tb* utilizes host sphingomyelin as a source of nutrients in the host (Speer et al., 2015). The availability of lipids during MAC infection is influence by pro-inflammatory signaling. In the next section, we will explore the pro-inflammatory pathways that promote granuloma formation.

Inflammasomes

Inflammasomes are multimeric cytosolic sensors of pathogen associated molecular patterns (PAMPS) and danger-associated molecular patterns (DAMPS). Pattern recognition receptors (PRRs) are key components of the inflammasome and fall into two main families: NOD-like receptors (NLRs) and absent in melanoma 2-like receptors (ALRs) (Guo et al., 2015). Each family of PRR is capable of sensing specific stimuli, which triggers oligomerization of the NLR or ALR into a scaffold

with the ability to activate caspase-1 (Guo et al., 2015). Apoptosis-associated speck-like protein containing a card (ASC) is an adaptor molecule that is central to the formation of these oligomers. This thesis will focus on the NLR-containing NLRP3 inflammasome, and ALR-containing AIM2 inflammasome (Fig. 1.2).

The NLRP3 Inflammasome

The NLRP3 inflammasome is a cytosolic multi-protein complex that has three components; NLRP3, ASC, and pro-caspase-1 (Fig. 1.2) (Guo et al., 2015). Prior to activation, the NLRP3 inflammasome requires priming (Fig. 1.2). Priming involves NF-κB activation (e.g. through LPS binding to TLR4), which induces transcription of NLRP3 and IL-1β (Guo et al., 2015). Following priming, NLRP3 activation is triggered by potassium efflux, ROS, cathepsin release, localization of NLRP3 to the mitochondria, calcium influx, or mitochondrial stress (ROS/DNA) (Guo et al., 2015). Multiple NLRP3 proteins oligomerizes in association with multiple ASC proteins, which interact with pro-caspase-1 filaments (Fig. 1.2). Inflammasome assembly induces the cleavage of pro-caspase-1 into active caspase-1. Cytosolic caspase-1 cleaves pro-IL-1β and pro-IL-18 and produces active IL-1β and IL-18, which are secreted by the cell (Guo et al., 2015). Caspase-1 induces pyroptotic cell death, mediated by gasdermin D.

Excessive activation of the NLRP3 inflammasome leads to cell death by pyroptosis or necroptosis (Swanson et al., 2019, p. 3; Wong & Jacobs Jr, 2011). Consequently, NLRP3 inflammasome activation is a tightly regulated process. Regulation of NLRP3 activation involves post-translational modifications of NLRP3, ASC, and associated proteins. These include phosphorylation, ubiquitination, de-

ubiquitination, and de-phosphorylation (Swanson et al., 2019). *M. tb* and *M. abscessus* activate the NLRP3 inflammasome through the action of spleen tyrosine kinase (Syk) (Wong & Jacobs Jr, 2011). ASC phosphorylation (Tyr146) is controlled by Spleen Syk, which allows for NLRP3 oligomerization (Hara et al., 2013). Deubiquitination of NLRP3 and adaptor protein ASC is required for their association and activation (Fig. 1.2) (Guo et al., 2015). BRCA1/BRCA2-containing complex E3 ubiquitin ligase (BRCC3) is involved in the deubiquitination of NLRP3 (Py et al., 2013). NO negatively regulates the NLRP3 inflammasome, leading to a drop in IL-1β production in response to increased IFN-γ (B. B. Mishra et al., 2013b). In contrast, cytosolic ROS have a positive effect on NLRP3 activation (Zhou et al., 2010). *M. tb* infection in macrophages triggers the release of activated cathepsin B (CTSB) from lysosomes, which also plays a role NLRP3 activation (Amaral et al., 2018). CTSB expression is elevated in macrophages infected with MAC or *M. tb*, and is one way that the NLRP3 inflammasome is activated by these bacteria (Amaral et al., 2018; Gutierrez et al., 2008).

M. tb utilizes several effectors to modulate NLRP3 inflammasome activation. NLRP3 activation by *M. tb* has been shown to involve ESX-1, ESXA, LpqH, and the RD-1 locus (Beckwith et al., 2020; Kurenuma et al., 2009; Rastogi & Briken, 2022; Xu et al., 2020). NLRP3 inhibition by *M. tb* involves Phosphokinase D (PknD) and serine hydrolase (Hip1) (Madan-Lala et al., 2011; Rastogi et al., 2021a). *M. tb* inhibits NLRP3 activation early on, in an effort to lessen proinflammatory signaling and avoid immune detection (Be et al., 2012; Madan-Lala et al., 2011). Late stage

NLRP3 activation is triggered to induce pyroptotic or necrotic cell death to enable cell-to-cell dispersal (Wong & Jacobs Jr, 2011).

Chronic *M. avium* pulmonary disease reduces NLRP3 activation and IL-1β secretion in human patients (Wu et al., 2019, p. 3). *M. kansasii* induces NLRP3 activation and subsequent IL-1β release in macrophages via potassium, efflux, lysosomal acidification, ROS, and cathepsin B (C.-C. Chen et al., 2012). NLRP3-dependent IL-1β secretion plays a major role in host defense against intracellular *M. kansasii* (C.-C. Chen et al., 2012).

The AIM2 Inflammasome

The AIM2 inflammasome is a cytosolic dsDNA sensor that consists of AIM2, ASC, and pro-caspase-1 (Fig. 1.2) (Guo et al., 2015). Priming is triggered by the detection of PAMPS or other NF-κB-activating signals (Rastogi & Briken, 2022). The HIN-200 domain of AIM2 can bind directly to cytosolic dsDNA, which triggers activation (Guo et al., 2015). The binding of AIM2 to dsDNA is nonspecific and the minimum length of dsDNA required for activation is 80 bp (Guo et al., 2015). Multiple AIM2 proteins oligomerizes in association with multiple ASC proteins, which interact with pro-caspase-1 filaments (Fig. 1.2). Pro-caspase-1 oligomerization induces the cleavage of pro-caspase-1 into active caspase-1. Cytosolic caspase-1 cleaves pro-IL-1β and pro-IL-18 and releases active IL-1β and IL-18, which are secreted by the cell (Guo et al., 2015). Caspase-1 induces pyroptotic cell death, mediated by gasdermin D.

Intracellular pathogens with cytosolic stages (e.g. *Listeria monocytogenes*) induce AIM2 inflammasome activation during infection (Briken et al., 2013). *M.*

smegmatis, M. fortuitum, M. kansasii induce AIM2 activation whereas *M. tb* inhibits AIM2 activation *in vitro* (Shah et al., 2013). Type I interferon signaling is involved in AIM2 activation (Shah et al., 2013). NTM infection induces significantly higher levels of IFN-β compared to *M. tb* (Shah et al., 2013). Interestingly, in *M. bovis,* AIM2 activation inhibits STING-dependent IFN-β production and autophagy (C. Liu et al., 2016).

The cGAS/STING Pathway

The cGAS/STING pathway is a cytosolic DNA sensing pathway that induces autophagy and the secretion of type I interferons (IFN-α and IFN-β) (Schoggins et al., 2014; Watson et al., 2015). Cytosolic DNA sensor cyclic guanosine monophosphate-adenosine monophosphate synthase (cGAS) recognizes and binds to pathogen or host dsDNA in the cytosol (Burdette & Vance, 2013). The DNA-cGAS association results in the activation of cGAS which produces the secondary messenger cGAMP (Burdette & Vance, 2013). cGAMP triggers Stimulator of Interferon Genes (STING) polymerization, which facilitates the transfer of STING from the endoplasmic reticulum to the golgi body. Downstream effects of STING activation include transcription and synthesis of IFN-β and IL-6 (Burdette & Vance, 2013; Ma et al., 2020). In *M. tb* infection, cytosolic mycobacterial DNA activates the cGAS-STING pathway, resulting in IFN-β secretion and bacteria protection (Wassermann et al., 2015; Watson et al., 2015). In the next section, we will describe the host response to *M. avium* infection, including the involvement of inflammasomes.

Host Immune Response to *M. avium*

M. avium infection triggers an assortment of pro-inflammatory responses, which promote anti-bacterial pathways such as apoptosis and superoxide production. However, anti-inflammatory pathways are also activated during *M. avium* infection. Anti-inflammatory signals promote the creation of a permissive environment for intracellular bacterial growth (Rocco & Irani, 2011).

Host macrophages possess a variety of intracellular sensors to detect pathogen associated pathogen associated molecular patterns (PAMPs) and danger-associated molecular patterns (DAMPs). Once detected, PAMPs and DAMPs activate inflammatory pathways in the host macrophage, which lead to the production of pro-inflammatory signaling molecules called cytokines. Pro-inflammatory cytokines released during *M. avium* infections include TNF-α, IL-1β, IL-6, IL-12, IFN-γ.

Mycobacterial cell wall glycopeptidolipids (GPLs) bind toll-like receptor 2 (TLR2), which is located on the host cell plasma membrane. TLR2 activation triggers TNF-α secretion by the infected macrophages (Sweet & Schorey, 2006). TNF-α is involved in inflammation, macrophage activation, T cell activation, and granuloma formation (Bean et al., 1999). The NLRP3 and AIM2 inflammasomes produce IL-1β upon activation. IL-1β mediates inflammation, and is involved in granuloma maintenance and host resistance to mycobacterial infection via host cell apoptosis and autophagy (Appelberg, 2006; Mayer-Barber et al., 2010; Rastogi & Briken, 2022).

IL-12 is produced by infected macrophages and dendritic cells, and is involved in bacterial clearance (Castro et al., 2018; Doherty & Sher, 1998). However, as infection progresses *M. avium* suppresses IL-12 production by host macrophages

(Corthay et al., 2005; Wagner et al., 2002). IFN-γ secreted by T cells and natural killer (NK) cells during *M. avium* infection is a key factor in macrophage and NK cell activation, cytotoxic T cell differentiation and granuloma formation (L. E. Bermudez et al., 1995; Castro et al., 2018; Smith et al., 1997). IFN-γ also triggers autophagy and the upregulation of MHC Class II molecules by antigen presenting cells, which increases $CD4^+$ T cell activation (Castro et al., 2018; Corthay et al., 2005; Steele et al., 2015). Macrophage activation by IFN-γ leads to increased nitric oxide (NO), TNF-α production and apoptosis, which aid in bacterial killing (Castro et al., 2018; C. H. Wang et al., 2001). However, intracellular *M. avium* is not susceptible to NO killing, and recent research suggests that NO may have a negative effect on host defense later in infection by T cell suppression (Appelberg & Orme, 1993; Gomes et al., 1999).

IL-6 is produced by activated macrophages, T cells, and endothelial cells at the site of infection, and can act as a pro-inflammatory or anti-inflammatory signal. IL-6 is an inducer of cytotoxic T cells, which act to remove infected macrophages during mycobacterial infection (Rocco & Irani, 2011). On the other hand, IL-6 blocks TNF-α receptors and suppresses antigen presentation, which aid in bacterial survival (Rocco & Irani, 2011).

IL-10 and IFN-β are key anti-inflammatory cytokines released by macrophages and dendritic cells during mycobacterial infection. IL-10 suppresses TNF-α activity, which inhibits apoptosis and creates a permissive niche for intracellular survival and growth (Balcewicz-Sablinska et al., 1999; L. E. Bermudez & Champsi, 1993; Coclet-Ninin & Burger, 1997). Activation of the cGAS/STING

pathway by cytosolic mycobacterial DNA induces IFN-β production. IFN-β plays a host-protective role in viral infections, but is detrimental to the host in mycobacterial infections (Sabir et al., 2017; Watson et al., 2015). IFN-β inhibits the inflammasome activation and triggers increased IL-10 production by host macrophages (Guarda et al., 2011). IFN-β also interferes with the pro-inflammatory effects of IFN-γ. The suppression of pro-inflammatory pathways by IFN-β leads to reduced inflammation. Additionally, IFN-β promotes autophagic activity. Host macrophages utilize autophagy to regulate inflammasome activation, recycle damaged organelles, and kill intracellular bacteria.

Autophagy

Autophagy is a eukaryotic, intracellular maintenance process used to recycle organelles, damaged cellular structures, and kill intracellular pathogens (Khandia et al., 2019; Stromhaug & Klionsky, 2001). During cellular stress, when nutrient availability is reduced, autophagy is a crucial mechanism by which host cells maintain sufficient nutrient levels (Khandia et al., 2019; Steele et al., 2015). The two main initiators of autophagy are the activation of AMP-activated protein kinase (AMPK; glucose deprivation) and inhibition of mammalian target of rapamycin (mTOR; amino acid deprivation or hypoxia) (Jung et al., 2010). Autophagy is downregulated by NO and glycolysis.

There are several types of autophagy, but the main categories are bulk (non-specific) and selective (specific) (Steele et al., 2015). Selective autophagy targets specific cellular or foreign structures such as lipids (lipophagy), mitochondria (mitophagy), or pathogens (xenophagy). Xenophagy is involved in recognition,

targeting, and subsequent degradation of intracellular pathogens (Khandia et al., 2019; Steele et al., 2015). Mitophagy and xenophagy play a key anti-inflammatory role by reducing NLRP3 inflammasome activation through removal of damaged mitochondria, intracellular pathogens, NLRP3 effectors, and other cellular components that trigger inflammatory pathways (Biasizzo & Kopitar-Jerala, 2020, p. 3).

Following activation of AMPK, AMPK activates ULK1 via phosphorylation. ULK1 phosphorylates Beclin-1 and VPS34, which form a complex and localize to the phagophore, which is the double-membraned origin of the autophagosome (Steele et al., 2015). The nascent phagophore is elongated and engulfs the cytosolic target, forming the early double-membraned autophagosome. Elongation is carried out by the ATG5-ATG-12-ATG16L complex. Autophagosome maturation is controlled by LAMP-1/2. Microtubule-associated protein1A/1B-light chain 3 (LC3) binds to the autophagosome membrane upon phagophore formation. Targets of selective autophagy are labeled with polyubiquitin and autophagic adaptors p62, which bind to LC3-II (Khandia et al., 2019; Steele et al., 2015). The next step in maturation is acidification, which is controlled by ATG9 and V-ATPase (Khandia et al., 2019). The final step in autophagosome maturation is fusion with lysosomes, which deliver digestive enzymes to degrade autolysosome contents (Khandia et al., 2019).

In some cases, autophagy is an effective killing mechanism against intracellular pathogens (Birmingham et al., 2006; Shin et al., 2010). However, several bacterial pathogens have evolved ways to escape autophagic killing by mimicking host protein, inhibiting autophagosome maturation, and the destruction or inhibition

of autophagy effectors (Steele et al., 2015). Other intracellular pathogens take it one step farther and repurpose autophagy for nutrient acquisition or as an escape pathway to exit the host cell (Birmingham et al., 2007; Deng et al., 2016). For example, *Francisella tularensis,* an intracellular bacterial pathogen, utilizes host autophagy to acquire nutrients to fuel intracellular replication (Steele et al., 2013). *M. tb* blocks autophagy in macrophages by suppressing the production of ROS (Shin et al., 2010). *M. marinum* inhibits autophagosome maturation and exploits host autophagy for cell-to-cell spreading (Gerstenmaier et al., 2015). *M. abscessus*, a rapidly growing NTM, induces autophagy and inhibits autophagosome-lysosome fusion, suggesting that autophagosomes may be permissive for bacterial replication under these conditions (S.-W. Kim et al., 2017).

Scope of Dissertation

Does *M. avium* modulate inflammasome expression and activation in host macrophages? Does mycobacterial eDNA play a role in immunomodulation and intracellular survival? What is the role of MGCs in *M. avium* infection? Are MGCs permissive to *M. avium* replication? How does the MGC environment differ from macrophages? These are the main questions that the following chapters aim to answer.

I examined the interaction of virulent and nonvirulent mycobacteria with pro-inflammatory and anti-inflammatory pathways in the host macrophage. I observed modulation of NLRP3 and AIM3 inflammasomes, and cGAS/STING pathway by *M. avium* and investigated the role of mycobacterial eDNA in intracellular immunomodulation. Together, my data suggest that *M. avium* modulates the

macrophage response early in infection to promote intracellular survival and induce anti-inflammatory pathways in tandem. Finally, mycobacterial eDNA may play a role in anti-inflammatory signaling via the cGAS/STING pathway.

I developed and characterized a novel *in vitro* model of MGCs using THP-1 macrophages and utilized this model to describe interactions of MGCs with *M. avium*. My model of MGCs exhibited large cellular volume, elevated autophagic activity, lipid droplet accumulation and increased bacterial replication. I characterized the phenotype of MGC-passaged *M. avium* to further understand the role of MGCs in pathogenesis. Collectively, my findings suggests that MGCs are permissive to intracellular replication, and act as a source for bacteria cell-to-cell spread.

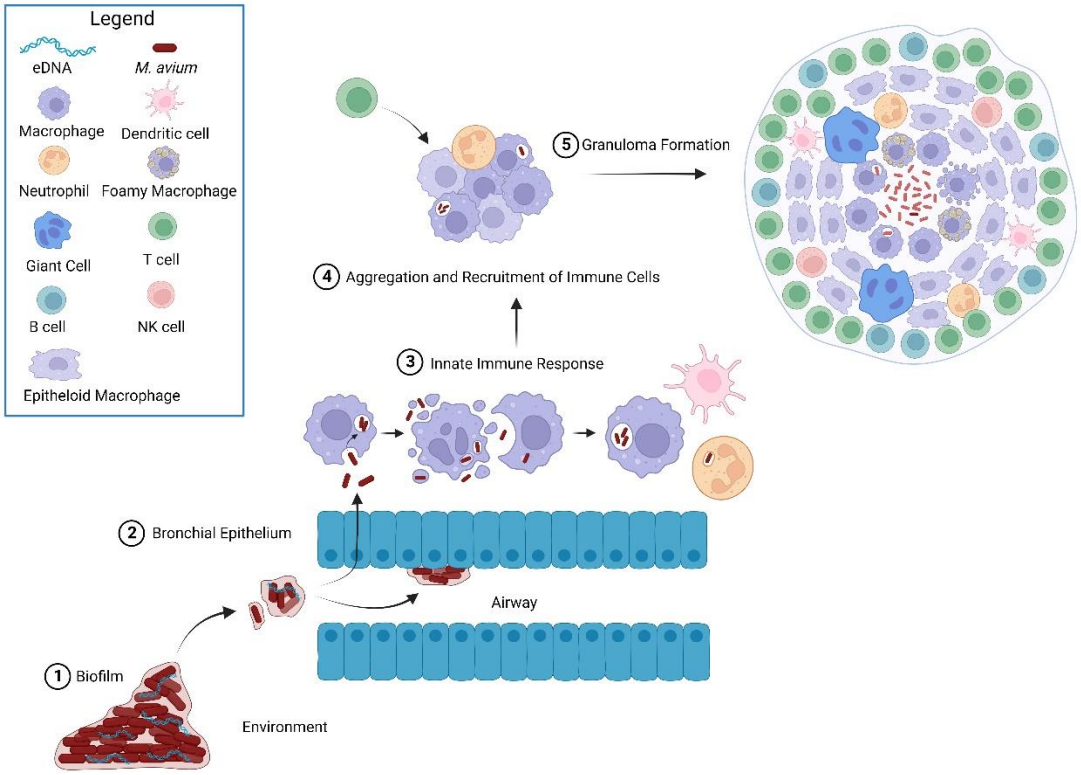

Fig. 1.1. Summary of *M. avium* Pathogenesis. (1) *M. avium* forms biofilms in the environment, which consist of bacteria surrounded by extracellular polymeric substance (EPS). EPS is composed of glycopeptidolipids, mycolyl-diacylglycerols, lipooligosaccharides, lipopeptides, and extracellular DNA (eDNA). (2) Once in the airway, *M. avium* translocates across the bronchial epithelium. (3) *M. avium* enters macrophages and evades intracellular killing by inhibiting phagosome maturation, which allows bacterial replication to proceed. As infection progresses, *M. avium* triggers apoptosis and uses this type of cell death as a tool for spreading to neighboring cells. (4) If *M. avium* bacteria are not cleared by the initial response, macrophages, infected macrophages, and neutrophils form cellular aggregates and recruit additional immune cells to the site of infection. (5) Over time, granulomas develop around innate immune cell aggregates. The lipid-rich core of the granuloma contains *M. avium*, infected macrophages, and foamy macrophages. Surrounding the core are epithelioid macrophages, multinucleated giant cells, neutrophils, NK cells, and dendritic cells. T cells and B cells form the outer layer of the granuloma. Created with BioRender.com.

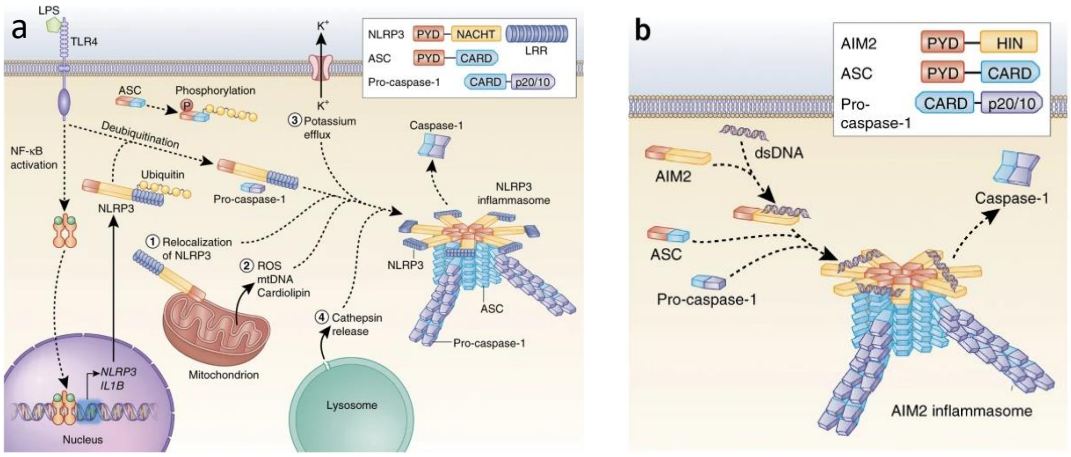

Fig. 1.2. Mechanism of NLRP3 and AIM2 Inflammasome Activation. The diagram shows an overview of the processes that activate the (a) NLRP3 and (b) AIM2 inflammasome and the downstream effect of inflammasome activation: caspase-1 activation and IL-1β release. A range of external and internal cellular stress signals can activate the NLRP3 inflammasome. Cytosolic double-stranded DNA (dsDNA) directly binds and activates the AIM2 inflammasome (Guo et al., 2015)**.**

Chapter 2

Mycobacterium avium Infection of Multinucleated Giant Cells Reveals Association of Bacterial Survival to Autophagy and Cholesterol Utilization

Jayanthi J. Joseph, Amy Leestemaker-Palmer, Soheila Kazemi, Lia Danelishvili, and Luiz E. Bermudez

Abstract

Mycobacterium avium subsp. *hominissuis* (*M. avium*) is an opportunistic environmental pathogen that typically infects immunocompromised patients and those with chronic lung conditions. Pulmonary *M. avium* infection generates peribronchial granulomas that contain infected macrophages and multinucleated giant cells (MGCs). The role of MGCs in host-pathogen interactions during mycobacterial pathogenesis is poorly understood. To shed light on the role of MGCs, we established a novel *in vitro* model utilizing THP-1 cells and a combination of IFN-γ and TNF-α. In this study, we show that MGCs can take up *M. avium,* which replicates intracellularly before leaving the cell. Characterization of MGCs with transmission electron microscopy revealed an accumulation of cytoplasmic lipid droplets, autophagic activity, and multiple nuclei. Autophagy is important of intracellular growth of *M. avium* in macrophages. Depletion of host cholesterol and sphingomyelin in MGCs reduced intracellular growth of *M. avium*. These processes potentially contribute to the formation of a supportive intracellular environment for the pathogen. *M. avium* bacteria exit the host macrophage early in infection and express several ESX proteins, as well as proteins associated with lipid and pyruvate metabolism. These MGC-passaged bacteria exhibit higher uptake by naïve macrophages and survive and replicate in macrophages. Collectively, our results suggest that *M. avium* is well adapted to replicate in MGCs and utilize them as a springboard for local spread.

Introduction

Mycobacterium avium subsp. *hominissuis* (*M. avium*) is an environmental opportunistic pathogen that causes pulmonary, and systemic infection in humans (Griffith et al., 2007). In recent years, the number of *M. avium* infections have been increasing worldwide (Prevots & Marras, 2015). Airway infections are chronic and characterized by the formation of pulmonary lesions, nodules, and both non-necrotic and necrotic peribronchiolar granulomas (Hong et al., 2016; Ohshimo et al., 2017). Treatment of pulmonary infections involves multiple antibiotics for a minimum of 12 months, and is only effective in 50-60% of patients (Griffith et al., 2007; Ingen et al., 2013). *M. avium* is a facultative intracellular bacterium and is ingested by macrophages and circulating monocytes. To survive the harsh intracellular conditions, *M. avium* inhibits phagosome acidification and prevents phagosome-lysosome fusion (Frehel et al., 1986; Oh & Straubinger, 1996). After replicating in the vacuole, *M. avium* triggers apoptosis of the host cell, escapes, and infects neighboring host cells (Early et al., 2011). Since activated macrophages can kill intracellular *M. avium*, the primary target of macrophage-passaged bacteria are newly arrived monocytes, which are unable to control intracellular bacterial growth. Previous studies have demonstrated that upon leaving the primary macrophage, *M. avium* exhibits increased uptake and that uptake by new macrophages occurs primarily via macropinocytosis (L. E. Bermudez et al., 1997, 2004, 2006; Danelishvili et al., 2018). It is clear that *M. avium* takes advantage of host macrophages for replication, increased uptake, and spread to surrounding host cells.

To sustain a chronic infection, mycobacteria must evade the immune system and find supportive niches to foster bacterial growth and dissemination. There is growing evidence that mycobacteria utilize the granulomatous response for their benefit. Traditionally, granulomas were assumed to be protective structures formed by the host immune system to contain pathogenic bacteria and prevent dissemination. Previous research, however, has shown that mycobacteria can survive and persist in granulomas, and work carried out by Cosma and colleagues showed that mycobacteria prefer the granuloma over the extra-granuloma environment (Cosma et al., 2004). Studies on *Mycobacterium marinum* infection in zebrafish, demonstrated that granulomas facilitate cell-to-cell spread, increase bacterial loads, and contribute to dissemination (Davis & Ramakrishnan, 2009; Volkman et al., 2004). Additionally, disruption of granulomas in zebrafish can promote host survival as shown in studies performed by Cronan and colleagues, suggesting that granulomatous inflammation is pro-pathogen (Cronan et al., 2016).

Langhans multinucleated giants cells (MGCs) are a characteristic feature of granulomas formed in response to pathogens, rather than foreign materials (Brodbeck & Anderson, 2009). MGCs in mycobacterial granulomas contain high bacterial loads *in vivo*, shown by histological examination of granuloma tissues from rabbits, mice, and humans (Gharun et al., 2017; Klotz et al., n.d.; S. N. Kumar et al., 2013; Langhans, 1868; Ufimtseva, 2015). Multinucleated giant cells are formed by the fusion of monocytes and are characterized by multiple nuclei (2-20), elevated cholesterol metabolism, and upregulation of iNOS (Gharun et al., 2017; Lösslein et al., 2021). The interactions between mycobacteria and multinucleated giant cells have

not been fully characterized. Previous studies have shown that *M. avium*-induced MGCs are able to take up bacteria (Gharun et al., 2017; Ufimtseva, 2015). Understanding the role of MGCs in mycobacterial pathogenesis may shed light into the balance of host-pathogen interactions during chronic infection. We developed an *in vitro* model of MGCs to facilitate understanding the contribution of MGCs in mycobacterial pathogenesis and the balance of the host-pathogen interaction during chronic infection of *M. avium*.

Cholesterol is required for persistence of *Mycobacterium tuberculosis (M. tb)* in the lungs of chronically infected mice and *Mycobacterium avium* subsp. *paratuberculosis* in human macrophages (Keown, 2010; Pandey & Sassetti, 2008). In humans, cholesterol accumulates in *M. tb* granulomas, accompanied by an increase in host lipid metabolism, and providing a nutrient rich environment for mycobacteria (M.-J. Kim et al., 2010). *M. avium* possesses genes involved in cholesterol metabolism, including several *mce* (mammalian cell entry) genes, which are associated with cholesterol uptake and utilization in mammalian hosts (Jeffrey et al., 2017; Pandey & Sassetti, 2008).

Sphingolipids are important components of eukaryotic cell membranes, and several intracellular pathogens have evolved mechanisms to utilize this class of lipids for growth (Rolando & Buchrieser, 2019). For example, *Pseudomonas aeruginosa* uses host sphingomyelin and ceramide as a nutrient by destroying them with a host-mimicking sphingomyelin synthase and ceramidase (Luberto et al., 2003; Okino et al., 1998). *M. tb* utilizes host sphingomyelin by expressing the SpmT (rv0888) gene to support intracellular replication in macrophages (Speer et al., 2015). While *M.*

avium lacks the SpmT gene, it possesses other genes involved in lipid uptake and degradation, which may play a similar role (Jeffrey et al., 2017).

In this study, we developed an *in vitro* MGC model and characterized the cellular morphology, which included multiple nuclei, accumulation of cytoplasmic lipid droplets, and the presence of autophagic activity. We determined the uptake and survival of *M. avium* in MGCs and found that *M. avium* is well adapted at intracellular survival and replication in MGCs. Increased autophagy and cytosolic lipid droplets could explain increased bacterial growth in MGCs. *M. avium* escapes from MGCs earlier than macrophages, and express ESX-5 as well as proteins associated with lipid metabolism and pyruvate metabolism. These MGC-passaged bacteria exhibit increased uptake by naïve macrophages and are able to survive and replicate in in macrophages. Together, these data point to the role of MGCs as permissive replicative niches that aid in cell-to-cell spread of *M. avium.*

Materials and Methods

Bacteria culture

Mycobacterium avium subsp. *hominissuis* strains 104 (*M. avium* 104), A5 (*M. avium* A5), 101 (*M. avium* 101), and 109 (*M. avium* 109) were originally isolated from the blood of AIDS patients (Aronson et al., 1999). *M. avium* 101 is the standard *M. avium* strain for susceptibility testing, and *M. avium* 109 has been used extensively in preclinical studies (Matern et al., 2018). *M. avium* A5 exhibits prolific biofilm formation, and eDNA export (Rose & Bermudez, 2016). *M. avium* 104 and *M. avium* A5 were grown on Middlebrook 7H10 agar supplemented with 10% w/v oleic acid, albumin, dextrose, and catalase (OADC, Hardy Diagnostics) for 7-10 days at 37°C.

Tissue Culture and formation of multinucleated giant cells

THP-1 (TIB-202) human monocytes were obtained from the American Type Culture Collection (ATCC) and maintained in RPMI 1640 supplemented with 10% heat-inactivated fetal bovine serum (FBS; Gemini Bio-Products) at 37°C with 5% CO_2. THP-1 cells were seeded in 48-well plates at a density of 3.5×10^5 cells per well and differentiated with 50 ng/ml of Phorbol 12-myristate 13-acetate (PMA; Sigma Aldrich) for 24 hours, followed by 24 hours in RPMI 1640 supplemented with 10% FBS without PMA, prior to use in experiments. Differentiated macrophages were treated with IFN-γ (100 ng/ml) (R&D Systems) and TNF-α (25 ng/ml) (VWR). The cytokines were used in combination to promote multinucleated giant cell (MGC) formation. Cytokines in RPMI 1640 supplemented with 10% FBS were added every 48 hours for 6 days after initial PMA treatment triggered differentiation. The fusion

index was calculated using the formula: (No. of Nuclei in MGCs)/ (Total No. of nuclei) x 100%.

Flow Cytometry

For CD40 surface marker analysis, THP-1 cells were seeded on a 6-well plate ($1x10^6$ cells/ml) and differentiated with 50 ng/ml PMA for 24 h. MGCs were formed as described above. Cells were detached from the plate using 0.25% EDTA-free trypsin (Thermo Fisher Scientific) in 1X Phosphate-buffered saline (PBS) for 5 min at 37˚C, followed by gentle pipetting. Cell suspensions were washed with PBS, and either left unstained, or stained with fluorochrome conjugated antibodies: CD40 FITC (5C3) (eBioscience), or Mouse IgG1 kappa Isotype Control (P3.6.2.8.1) (eBiosciene) FITC, for 1 hour at 20°C. After staining cells were fixed with 2% paraformaldehyde (PFA) for 10 min at 37˚C, washed, and analyzed immediately. Gating was performed to exclude dead cells. Flow cytometry was performed using an Accuri C6 flow cytometer (BD Biosciences). Data were analyzed using Accuri C6 software, FlowJo, and GraphPad Prism 9.

Mycobacterial infection and survival in MGCs

M. avium bacteria were added to multinucleated giant cells at an MOI of 10, synchronized by centrifugation for 10 min at 150 x g, and allowed to infect for 1 hour. Inoculums for these assays were formed in 1X HBSS supplemented with 0.05% Tween-20 (Sigma-Aldrich). Extracellular bacteria were removed by two wash steps with 1X HBBS followed by treatment with gentamicin sulfate (Sigma-Aldrich) for 1 hour (100 µg/ml) and an additional wash step with 1X HBSS to remove the antibiotic and dead extracellular bacteria. Cells were lysed at appropriate timepoints with 0.1%

Triton-X for 10 min and resulting lysates were diluted and plated. Colony forming units (CFUs) were enumerated at 1, 24, 48, and 72 hours post infection (h.p.i.). Potential extracellular bacteria escaping from cells were quantified at each timepoint via spot plating. Briefly, 5 µL of media removed from infected wells where plated on 7H10 agar. Colonies were counted after 7 days of incubation at 37°C.

Quantification PCR of Autophagy Associated Genes During MGC Infection

THP-1 and MGC RNA were isolated with the RNeasy mini kit (Qiagen), followed by treatment with DNase I recombinant (Roche Diagnostics) for 2 hours at 37°C to remove contaminating genomic DNA. The DNase was inactivated with Turbo DNase-inactivation reagent (Turbo DNA-free kit, Thermo Fisher Scientific) for 2 min at 37°C. Inactivation reagent was removed via centrifugation for 1 min at 10,000 x g, and RNA transferred to new collection tubes. RNA samples were stored at -4°C for future processing. cDNA was transcribed from host RNA using the iScript cDNA synthesis kit (Bio-Rad). The quality of cDNA was tested by PCR with Gold 360 master mix using the manufacturer's specifications (Thermo Fisher Scientific). The RT-qPCR reaction was performed using iQ SYBR Green Supermix (Bio-Rad) and an iCycler (CFX Connect Real-Time Systems, Bio-Rad) as previously described (Danelishvili et al., 2004). All gene expression data are presented as relative expression to beta-actin. Primers were designed in Primer3 using sequences from GenBank (National Center for Biotechnology Information). Primer sequences are as follows:

Beclin-1, 5'-AGCTGCCGTTATACTGTTCTG-3' (forward), and

5'-ACTGCCTCCTGTGTCTTCAATCTT-3' (reverse);

LC3-II, 5’-GATGTCCGACTTATTCGAGAGC -3’ (forward) and

5’-TTGAGCTGTAAGCGCCTTCTA-3’ (reverse); and

Beta-actin: 5’-CATGTACGTTGCTATCCAGGC-3’ (Forward),

5’-CTCCTTAATGTCACGCACGAT-3’ (Reverse) (J. Wang et al., 2013).

Fluorescent and transmission electronic microscopy of MGCs

Multinucleated giant cells were generated with cytokines in chamber slides (Falcon, VWR) and visualized by fluorescence microscopy. The cells were fixed in 2% PFA for 15 min, washed twice with 1X HBSS and permeabilized for 10 min with 0.1% Triton-X before staining with 1 µg/ml Hoechst 34580 (Invitrogen) for 15 min in the dark. Hoechst was removed, samples were washed twice with 1X HBSS, and stained with 0.165 µM Alexa Fluor 488 phalloidin (Thermo Fisher Scientific) for 15 min in the dark, followed by two wash steps with 1X HBSS. Slides were allowed to dry before affixing glass coverslips with cytoseal (Thermo Fisher Scientific). Slides were imaged with a Leica DM4000B fluorescent microscope (Leica Microsystems) and QICAM Fast 1394 camera (QImaging) at a magnification of 1000X under oil immersion. Images were acquired and processed with Qcapture Pro 7 software. For TEM, Cells were detached from 6-well plates by treatment with 5mM EDTA for 30 min, washed in 1X HBSS (HBSS, Cellgro), and suspended in fixative buffer with 2.5% glutaraldehyde, 1% formaldehyde, and 0.1 M sodium cacodylate for 24 hours prior to submission to the electron microscopy facility for processing. Samples were sectioned, dehydrated, and visualized by a FEIT Titan 80-200 TEM/STEM microscope at Oregon State University Electron Microscopy Facility.

siRNA targeting of autophagy genes during mycobacterial infection

To examine the role of ATG5 and Beclin-1 in activation of autophagy, we inhibited functionality of selected targets in THP-1 macrophages using siRNA technology in accordance with the manufacturer's recommendations (Santa Cruz Biotechnology, Inc). THP-1 cells were differentiated and seeded at 80% confluence in 6-well plates and, prior to infection, transfected with ATG5 and Beclin siRNAs. Briefly, siRNAs were diluted in RPMI without serum at a final concentration of 25 nM and 3μl of Continuum^{TM} transfection reagent (Gemini). Macrophage monolayers were washed once with siRNA transfection medium and replenished with new transfection medium containing target specific siRNA transfection reagent mixture. Cells were incubated at 37 °C in presence of 0.5% CO_2. Untreated and control siRNA (non-targeting sequences) transfected cells served as negative controls. After 48 h, monolayers were infected for different time-points, lysed and bacterial CFUs were recorded on Middlebrook 7H10 agar plates. Before infection, the ATG5, Beclin and β-actin protein levels from control and experimental wells were analyzed by semi-quantitative Western blotting. Lysed macrophages were resolved by electrophoresis on 12.5% SDS-PAGE gels, transferred to nitrocellulose membranes and blocked overnight with 5% Bovine Serum Albumin (BSA). After incubation with primary antibodies at a dilution of 1:200 for 2 h, membranes were washed three times with PBS and then probed with corresponding IRDye secondary antibody (Li-Cor Biosciences, Inc) at a dilution of 1:5000 for 1 h. Proteins were visualized using Odyssey Imager (Li-Cor).

Collection of MGC-passaged Bacteria

MGCs, formed as described previously, were infected with wild type *M. avium* A5 for 1h at an MOI of 10. The infection was carried out as described previously. Fresh media was replaced every 24h. Supernatants were collected at 72 h.p.i, and immediately kept on ice. Cell debris was removed by centrifugation for 5 min, 150 x g at 4 °C. The supernatant containing bacteria were pelleted by centrifugation for 15 min, 2000 x g at 4 °C. The supernatant was removed, and the pellet resuspended in 2ml of HBSS and stored at 4 °C for up to 7 days before use in experiments.

LC-MS

MGC-passaged bacteria and intracellular bacteria were collected as described above and washed twice with 1X HBSS. Plate bacteria were suspended in 1X HBSS and washed twice before protein isolation. Bacterial pellets were lysed with CelLytic B lysis buffer (company) supplemented with a protease inhibitor cocktail, phosphatase inhibitor cocktail (HALT), lysozyme (conc), and DNase I (Promega) for 15 min at room temperature. Lysates were transferred to a bead beating tube containing 100 µl of 0.1 mm disruption media (beads), followed by 2 minutes of disruption with a bead-beater. Debris was pelleted and supernatants were collected. Total protein was quantified using the Bradford assay. Samples were stored at -20 °C. Lysates were kept on ice between steps. To reduce disulfide bonds of the proteins, the samples were incubated at 56 °C for 1 hour with 5 mM dithiothreitol (ThermoFisher). Next, the samples were incubated with 10 mM iodoacetamide (MilliPore Sigma) for 1 hour at room temperature in the dark to carbamidomethylate cysteine residues. Samples were

digested overnight at 37 °C using Trypsin Gold (Mass Spectrometry Grade, Promega). After digestion, samples were spun down at 12000 rcf for 30 s to collect condensate, and the digestion was stopped by addition of 0.5% (v/v) trifluoroacetic acid. Samples were centrifuged at 12000 rcf for 10 minutes and then transferred to LC vials.

A Waters nanoAcquityTM UPLC system (Waters, Milford, MA) was coupled online to an Orbitrap Fusion Lumos mass spectrometer (Thermo Fisher Scientific). Peptides were loaded onto a trap 2G nanoAcquity UPLC Trap Column (180um, 50mm, 5um) at a flow rate of 5 µl/min for 5 minutes. The results were obtained on a commercially available Acquity UPLC Peptide BEH C18 column (100um, 100mm, 1.7um). Column temperature was maintained at 37 °C using the integrated column heater. Solvent A was 0.1% formic acid in LC-MS grade water and solvent B was 0.1% formic acid in LC-MS grade acetonitrile. The separation was performed at a flow rate of 0.5 µl/min and using linear gradients of 3–10% B for 10 minutes, 10–30% B for 10 minutes, 30–70% B for 5 minutes, 70–95% B for 3 minutes, 95–3% B for 4 minutes, 95–3% B for 3 minutes. Total method length was 35 minutes. The outlet of the column was connected to Thermo Nanospray Flex ion source and +2300V were applied to the needle.

MS1 spectra were acquired at a resolution of 120,000 (at m/z 200) in the Orbitrap using a maximum IT of 50 ms and an automatic gain control (AGC) target value of 2E5. For MS2 spectra, up to 10 peptide precursors were isolated for fragmentation (isolation width of 1.6 Th, maximum IT of 10 ms, AGC value of 2e4). Precursors were fragmented by HCD using 30% normalized collision energy (NCE) and analyzed in the Orbitrap at a resolution of 30,000. The dynamic exclusion duration

of fragmented precursor ions was set to 30 s. Raw files were processed in Thermo Proteome Discoverer 2.3. Precursor ion mass tolerance was set to 5 ppm, while fragment ion mass tolerance was 0.02 Da. The SequestHT search engine was used to search against the Swissprot human and M. abscessus protein database (). b and y ions only were considered for peptide spectrum matching. MS1 precursor quantification was used for label-free quantitation of the peptides. Protein abundances were calculated as a sum of abundances of unique peptides detected. LC-MS analysis was carried out by the mass spectrometry facility in the Center for Quantitative Life Sciences (CQLS) at Oregon State University.

Statistical Analysis

All described experiments were repeated at least three times and data shown are representative of the biological replicates. Comparisons between two groups were analyzed in Microsoft Excel using the two-tailed Student t test. Results with p-values below 0.05 were considered significant.

Results

IFN-γ and TNF-α induce multinucleated giant cell formation in vitro

To establish an *in vitro* MGC model THP-1 cells were differentiated with Phorbol 12-myristate 13-acetate (PMA) for 24 hours, followed by stimulation with a combination of TNF-α and IFN-ɣ for 6 days. After differentiation with PMA, THP-1 cells do not proliferate and become adherent. TNF-α and IFN-ɣ were selected because they have been shown to drive granuloma formation, and contribute to MGC formation *in vivo* (Epstein & Fukuyama, 1989; Fais et al., 1994; Mezouar et al., 2019; Tambuyzer & Nouwen, 2005). A fusion index of 56.5% was observed when cells were treated with 25 ng/ml TNF-α and 100 ng/ml IFN-ɣ over a 6-day period (Fig. 2.1A). The resulting mixed population of MGCs and activated THP-1 macrophages, was utilized for further experiments. MGCs formed with this protocol have 2-4 nuclei (Fig. 2.1B, C, and D). CD40 is a marker of MGCs associated with mycobacterial infection and is involved in MGC formation (Brooks et al., 2019; Sakai et al., 2012, p. 40). MGCs exhibited a large shift in mean fluorescent intensity (MFI) of FITC-CD40, indicating that 98% of MGCs are $CD40^+$ (Fig. 2.1E). THP-1 cells exhibited a small shift in fluorescent intensity, indicating a low percentage of $CD40^+$ cells (Fig. 2.1F). MGCs have an MFI of FITC-CD40 that is significantly higher than THP-1 macrophages, MGCs stained with a FITC-isotype control, and unstained MGCs (Fig. 2.1G). These results indicate that MGCs retain the CD40 marker and are biologically similar to MGCs observed *in vivo.*

Intracellular survival and growth of M. avium in multinucleated giant cells

The intracellular stages of mycobacteria in MGCs have not been fully described. Survival assays were performed to characterize the uptake and intracellular growth of *M. avium* in the *in vitro* MGC model and compared to THP-1 macrophages. *M. avium* A5 infected MGCs at a similar rate to THP-1 macrophages (Fig. 2.2A). Once cells were infected, bacterial survival was determined by CFU counts in either MGCs or THP-1 macrophages over 3 and 6 days respectively, and fold change relative to 1 h.p.i calculated. The time points selected for THP-1 survival assays are standard practice. The time points for MGC survival assays were selected from day 5 of stimulation up to the point where bacterial growth was observed. This happened to be at day 3 post-infection, so a day 6 time point was not necessary for MGCs. Additionally, the cells would have been on the plate for 12 days at the point, which would leave few viable cells to work with. At 4 d.p.i for THP-1 and 48 h.p.i for MGC, fold change of bacterial growth was 4 (Fig. 2.2B and C). In THP-1 macrophages, *M. avium* intracellular growth exhibited a fold change of 11 at 6 d.p.i, whereas *M. avium* intracellular growth in MGCs exhibited a fold change of 7 at 3 d.p.i (Fig. 2.2B and C). During the survival assay, CFU/mL of extracellular bacteria that exited MGCs was enumerated (Fig. 2.2D). The number of bacteria leaving MGCs was significantly greater at 72 h.p.i. compared to other timepoints. These data indicate that *M. avium* A5 can enter MGCs with the same efficacy as THP-1 macrophages. Additionally, *M. avium* A5 survives in the MGC environment and matches the level of intracellular growth in THP-1 macrophages in a shorter time. Our data support the idea of a favorable niche existing inside the MGC environment

that *M. avium* A5 can utilize to survive and eventually leave to infect other cells nearby.

Electron Microscopy Observations of M. avium A5 in MGCs

To increase our understanding of the behavior of bacteria inside MGCs, transmission electron microscopy (TEM) was used. MGCs were infected with *M. avium* over 72 h then processed for TEM. THP-1 macrophages that are not treated with cytokines or infected with bacteria show normal cellular structures including a single nucleus and cell size. After cytokine exposure, MGCs were formed and autophagosomes were visible in the cytosol, identified by double membranes (Fig. 2.3A). In MGCs infected with *M. avium* A5 for 72 h, bacteria can be seen inside autophagosomes (Fig. 2.3B), and bacterium-containing vacuoles can be seen interacting with autophagosomes (Fig. 2.3C and D). Comparing multiple cells, numerous autophagic vacuoles exist within MGCs, and once these cells are infected with *M. avium* A5 the number of autophagosomes increased substantially.

Prominent lipid droplets were observed in MGCs at multiple timepoints. The formation of MGCs causes several cellular changes and one of the changes observed was the accumulation of lipid droplets in the cytosol (Fig. 2.4A). At 1 h.p.i, bacteria were present the cytosol near lipid droplets (Fig. 2.4B) as well as in autophagosomes (Fig. 2.4C & E). Intracellular lipid inclusions were present in intracellular bacteria at several timepoints (Fig. 2.4B-E). Vacuoles containing multiple bacteria were observed at 72 h.p.i. (Fig. 2.4D). After 24 h bacteria started to leave MGCs and were observed near the plasma membrane (Fig. 2.4F).

in vitro multinucleated giant cells exhibit increased autophagic activity compared to macrophages

To determine autophagic activity in MGCs, we measured the mRNA levels of autophagy markers LC3 and Beclin-1 via real-time quantitative PCR. Beclin-1 controls phagophore formation and LC3 is involved in phagophore elongation (Glick et al., 2010). Beclin-1 gene levels after 4 h indicated that MGCs have naturally greater expression compared to THP-1 macrophages, and once infected, MGCs exhibited even greater gene expression of Beclin-1 (Fig. 2.5A). The trend continued through 24 h.p.i, except there was no difference between infected and uninfected MGCs gene expression. Later in the infection there was no difference in Beclin-1 gene expression between experimental groups. LC3 expression by MGCs at 4 h showed significant increase compared to LC3 expression by THP-1 macrophages (Fig. 2.5B). After 24 h LC3 gene expression by uninfected MGCS increase, and expression by infected MGCs decreased. After 72 h, LC3 gene expression was undetectable for all experimental groups. These data support our previous observation that infected MGCs have a greater number of autophagosomes than uninfected MGCs.

Silencing of Beclin and ATG5 reduces intracellular survival of M. avium in THP-1 macrophages

Since there is a clear tendency of MGCs cells to express autophagy upon *M. avium* infection we questioned if autophagy was an important occurrence for survival in macrophages. To assess the importance of increased autophagy during *M. avium* infection in THP-1 macrophages, siRNA technology was used to knockdown

expression of Beclin-1 and ATG5 host genes. THP-1 macrophages treated with siRNA targeting either Beclin, ATG5, empty vector, or no vector, showed reduced but not absent protein levels inside of cells, confirmed by western blot (Fig. 2.6A). These THP-1 macrophages where then infected with multiple strains of *M. avium* including, 101, 104, and 109 (Fig. 2.6B). Our results demonstrate that inhibition of ATG5 or Beclin, markers of autophagy, decreased the ability for bacteria to survive in macrophages over 4 days (Fig. 2.6B). These data suggest that *M. avium* uses autophagy for intracellular survival in resting macrophages.

Intracellular cholesterol transport and M. avium A5 survival in MGCs

The TEM micrographs show that *M. avium* is utilizing host lipids in MGC. We wanted to determine whether host cholesterol was essential for intracellular growth. Uptake and survival assays were carried out in MGCs treated with (3β)-3-[2-(Diethylamino) ethoxy] androst-5-en-17-one hydrochloride (U18666A), an intracellular cholesterol transport inhibitor. The final concentration was chosen based on previously published studies in mouse macrophages and human fibroblasts (Härmälä et al., 1994; Iftakhar-E-Khuda et al., 2009). As a control, it was determined that a concentration of 3 µg/ml of U18666A had no effect on the growth of *M. avium* A5 in 7H9 broth over 6 days (Fig. 2.7A). Since U18666A did not affect bacterial growth, we then used the inhibitor on MGCs infected with *M. avium* A5. U18666A was added 1 hour after infection of MGCs and replenished daily over 72 h. MGCs were lysed and CFUs were counted at 1, 24, and 72 h.p.i. In MGCs that were infected with *M. avium* A5, treatment with U18666A did not affect whether bacteria were taken up by the cells (Fig. 2.7B). *M. avium* A5 intracellular growth over 72 h was

significantly hindered by U18666A compared to without inhibition, with a reduction of about 25% (Fig. 2.7B). This shows that *M. avium* can utilize alternate sources of energy if cholesterol is unavailable in host cell during early stages of infection. However, *M. avium* is unable to overcome the lack of cholesterol later in infection and intracellular growth plateaus. Since the inhibition of intracellular cholesterol transport with U18666A reduces, but does not prevent intracellular growth of *M. avium*, we propose that cholesterol is not essential for intracellular growth.

Effect of sphingomyelin synthase inhibition on M. avium A5 survival in MGCs

Since sphingomyelin has been shown to be advantageous for TB in macrophages, we determined whether *M. avium* A5 utilizes sphingomyelin in MGCs to aid intracellular growth (Speer et al., 2015). MGCs were either treated with tricyclodecan-9-yl-xanthogenate (D609) or untreated. D609 is an inhibitor of sphingomyelin synthase that reduces intracellular diacylglycerol and sphingomyelin, and increases ceramide levels (Luberto & Hannun, 1998; A. Meng et al., 2004; Milhas et al., 2012). D609 was added to infected MGCs 1-hour post-infection and was replenished daily over the course of three days (Fig. 2.7C). The concentration of 100 µM was chosen based on previously established inhibitory concentrations in human lung fibroblast and monocyte cell lines (Luberto & Hannun, 1998; A. Meng et al., 2004). A concentration of 100 µM of D609 had no effect on the growth of *M. avium* A5 in 7H9 broth after 4 days of growth (Fig. 2.7A). To account for the effects of D609 on bacterial growth at day 6, all in vitro experimental timepoints were determined by day 3. MGCs were infected then lysed and CFUs were counted at 1, 24, and 72 h.p.i. In MGCs that were treated with 100 µM of D609, uptake of *M.*

avium A5 was not affected as D609 was added after infection. *M. avium* A5 intracellular growth was significantly hindered with treatment only at 72 h.p.i, with a reduction of about 30% (Fig. 2.7C). This shows that during early stages of infection *M. avium* can utilize alternate sources of energy if sphingomyelin is unavailable in host cell.

To determine the effect of sphingomyelin synthase inhibition after the infection had been more established, MGC survival assays were conducted in which D609 was added to the cells at either 24 h.p.i or 48 h.p.i (Fig. 2.7D). When D609 was added to *M. avium* A5-infected MGCS at 24 h.p.i, there was a reduction in bacterial survival at 48 h.p.i. However, *M. avium* A5 was able to overcome the effect of the inhibitor and resumed growth, which is shown by the increase in CFUs from 48- to 72 h.p.i. When D609 was added to *M. avium* A5-infected MGCS at 24 h.p.i, there was a reduction in bacterial survival at 72 h.p.i. The number of extracellular bacteria leaving the MGCs was counted for untreated, 24h D609, and 48h D609 groups (Fig. 2.7E). In both the untreated and 24h D609 groups, the number of extracellular bacteria increase between 48 and 72 h.p.i, however the 48h D609 group show no increase during this period. Our results show that *M. avium* A5 can overcome sphingomyelin depletion when it occurs at 24 h.p.i, but not 48 h.p.i. and suggest *M. avium* dependency on sphingomyelin at later stages of infection.

Passage through MGCs Increases Uptake, but not survival of M. avium A5 in naïve macrophages

To determine if the phenotype of MGC-passaged *M. avium* A5 is different than WT *M. avium* A5, uptake and survival assays were carried out in THP-1 macrophages.

To passage *M. avium* A5, MGCs were infected with WT *M. avium* A5 for 1h, and at 72 h.p.i, bacteria that exited the MGCs (MGC-passaged A5) were collected in cell culture media and kept on ice or at 4˚C while pelleted and washed. THP-1 cells were infected for 1 hour with MGC-passaged bacteria or *M. avium* A5 from a 7H10 streak plate. Uptake of *M. avium* A5 was tested by inhibiting macropinocytosis and receptor mediated phagocytosis. Wortmannin inhibits the macropinocytosis pathway by preventing complete closure of the cytoplasmic ruffles. Blocking complement receptor 3 (CR3) with a CD11b antibody inhibits complement receptor-mediated phagocytosis. MGC-passaged A5 exhibited a percent uptake approximately 3 times greater than *M. avium* A5 grown on a plate, under normal infection conditions (Fig. 2.8A). Blocking the CR3-receptor with an anti-CD11b antibody for 1 hour prior to infection led to a 52% reduction in uptake for both bacterial phenotypes (Fig. 2.8B). Inhibition of macropinocytosis with wortmannin for 2h prior to infection led to a 33% reduction in uptake for both bacterial phenotypes (Fig. 2.8B). Inhibiting uptake pathways reduced the uptake of both phenotypes, but did not completely block them, indicating that *M. avium* of either phenotype can circumvent the effect of the inhibitors and entering the macrophage via an alternate route. This suggests that MGC-passaged bacteria can enter THP-1 cells via alternate routes. Survival in THP-1 macrophages over 6 days with MGC-passaged A5 is comparable to A5 from the plate, thus once bacteria enter macrophages there was no added advantage to MGC-passaged bacteria (Fig. 2.8C). These data suggest that the MGC-environment increases the uptake of *M. avium* A5, but that they retain their ability to enter the next host cell in multiple ways.

Virulence and Metabolic Proteins Expressed by MGC-Passaged M. avium

To understand how *M. avium* exits the MGC, proteomic analysis MGC-passaged *M. avium* was performed. When compared to plate-grown bacteria, MGC-passaged bacteria did not express any unique proteins, and the abundance of all proteins was lower than in plate-grown bacteria. This could be due to the small size of the bacterial pellet used in the MGC-passaged LC-MS sample during preparation. Although the same total amount of protein was process for LC-MS in both samples, the MGC-passaged sample contained a significant number of human proteins as well. An alternate explanation is that bacteria that leave the cell adapt quickly to the extracellular environment. On-going proteomics work will look at intracellular *M. avium* from MGCs collected at 24 h.p.i, with the idea that proteins involved in escape from the host cell will be expressed intracellularly before exit. As a result of these limitations, the proteomic results discussed in this section are qualitative and will focus on proteins expressed by MGC-passaged bacteria.

- Increased uptake could be due to acquisition of host factor
- Change in bacteria lipid profile

Discussion

Multinucleated giant cells play an important role in the host-pathogen interaction during the granulomatous response to mycobacteria. Past studies have used *in vitro* multinucleated giant cell models that utilize mycobacteria or mycobacterial components, and a combination of primary lymphocytes and macrophages to trigger the formation of cellular aggregates with few MGCs (Gasser & Möst, 1999; Lay et al., 2007; Puissegur et al., 2004). The MGC model described in this study focuses on a single cell type, avoiding the use of bacterial components and complexities of cell-aggregate models (formed with several cell types) to detail characteristics of MGCs in the absence of confounding bacterial factors. The absence of bacterial components allows this model to have broader applications beyond mycobacterial studies. In addition, the model utilizes an immortalized cell line, rather than primary cells, this makes it affordable and reproducible. Foreign body multinucleated giant cell models induce macrophage fusion with IL-4 stimulation, however, these MGCs are typically found near medical implants and biomaterials, and are significantly different than MGCs found in mycobacterial granulomas (Aghbali et al., 2017; Anderson et al., 2008). In addition, MGCs formed in this model have the CD40 surface marker, which is present in MGCs during acute tuberculosis infection, and is required for MGC formation in tuberculosis (Brooks et al., 2019; Sakai et al., 2012, p. 40).

Multinucleated giant cells are a common feature of mycobacterial granulomas *in vivo,* and typically contain large bacterial loads (Gharun et al., 2017; Klotz et al., n.d.; Langhans, 1868; Ufimtseva, 2015). It is not clear whether multinucleated giant

cells play a host-protective role or act in favor of the pathogen. In previous studies, MGCs have been shown to exhibit increased phagocytic activity compared to macrophages (Braune et al., 2021; Gharun et al., 2017; Milde et al., 2015). Recent research by Gharun and colleagues supports the idea that multinucleated giant cells are permissive to mycobacterial replication (Gharun et al., 2017). In this study, we demonstrated that MGCs formed by the fusion of macrophages after IFN-γ an TNF-α stimulation can phagocytose *M. avium* and permit intracellular replication (Fig. 2.10).

After infection, *M. avium* survives in a cytoplasmic vacuoles of macrophages and prevents the acidification and vacuole fusion with lysosomes (Sturgill-Koszycki et al., 1994). The lack of Rab7 marker on *M. avium* late phagosomes influence the phago-lysosome fusion (Via et al., 1997). Furthermore, intracellular *M. avium* is resistant to ROS and nitric oxide and capable of subverting macrophage killing mechanisms (L. E. M. Bermudez & Young, 1989). Presumably, *M. avium* uses similar strategies for survival in MGCs.

Autophagy is a process used by eukaryotic cells to recycle organelles or to degrade damaged cellular structures (Stromhaug & Klionsky, 2001). In some cases, autophagy is used as a mechanism to kill intracellular pathogens, such as *Salmonella enterica* serovar *Typhimurium* and *M. tuberculosis* (Birmingham et al., 2006; Shin et al., 2010). However, some bacterial species have strategies to avoid autophagic clearance, while others utilize autophagy to fuel intracellular growth or to drive their escape from the host cell (Birmingham et al., 2007; Deng et al., 2016). For instance, *Francisella tularensis*, an intracellular pathogen that infects macrophages, exploits autophagy to amass nutrients for intracellular growth (Steele et al., 2013). *M.*

tuberculosis suppresses macrophage autophagy through the inhibition of production of reactive oxygen species (ROS) (Shin et al., 2010). *Mycobacterium marinum*, a model organism for *M. tuberculosis*, employs host autophagic machinery for cell-to-cell transmission of bacteria, and is able to prevent maturation to autophagolysosomes (Gerstenmaier et al., 2015). Our work demonstrates that the inhibition of autophagy using RNAi in THP-1 cells leads to a significant reduction in intracellular survival of *M. avium*. Altogether, data collected on the increased autophagy in MGCs, the presence of *M. avium* in autophagosomes, and the permissiveness for bacterial growth, suggest that *M. avium* utilizes autophagy to fuel intracellular growth in both macrophages and MGCs. However, further work is required to confirm the involvement of autophagy in intracellular *M. avium* replication in MGCs. This could be accomplished by inhibiting autophagy in MGCs with chemical inhibitor, or siRNA, and determining the effect on intracellular growth.

Lipids are a well-known source of nutrition for mycobacteria in the host (Wilburn et al., 2018). Host lipid metabolism shifts during mycobacterial infections, and the inhibition of lipid accumulation in mycobacterium-infected macrophages reduces bacterial survival (Gago et al., 2018; McClean & Tobin, 2020). Host lipids utilized by mycobacteria include triacylglycerols, cholesterol and sphingomyelin. Several intracellular pathogens manipulate host sphingolipid metabolism, including *M. tb, P. aeruginosa,* and *L. pneumophila* (Rolando & Buchrieser, 2019). *M. tuberculosis* possesses several genes involved in cholesterol metabolism, a neutral sphingomyelinase SpmT (Rv0888), and alkaline ceramidase (Rv0669c) (Lunge et al., 2020; Speer et al., 2015). Although *M. avium* lacks homologs for either of these

genes, it possesses several uncharacterized hypothetical genes that may have similar activity (Jeffrey et al., 2017; Pandey & Sassetti, 2008). When we inhibited intracellular cholesterol transport in MGCs, *M. avium* survival was significantly reduced at 72 h.p.i. These data indicate that cholesterol is not vital for intracellular survival, and that *M. avium* is able to overcome the lack of cholesterol and replicate in MGCs. Work from Stanley's group have indicated that accumulation of lipids in *M. tuberculosis* infected macrophages is not triggered by the bacteria but by the host (Knight et al., 2018). These findings agree with our observation that *M. avium* makes use of the cholesterol only because it is available; however, it does not affect bacterial survival if cholesterol is limited or absent. Depletion of host sphingomyelin with D609 during *M. avium* infection at different time points temporarily reduced bacterial intracellular growth in MGCs. *M. avium* was able to resume intracellular growth 24 hours after each D609 treatment, indicating that it may use host lipids as an energy source if they are present but can utilize alternative sources of energy if host lipids are not available. Improving our understanding of the role of host lipids in intracellular replication is an important avenue of future research. Characterization of MGC lipid droplets by lipidomics would provide further information about the MGC model and might point to specific lipids utilized by intracellular bacteria.

Additionally, *M. avium* that leaves the MGC readily enters neighboring macrophages. Previous work by Bermudez and colleagues has shown that macrophage-passaged *M. avium* exhibit higher uptake and induces apoptosis in macrophages as a mechanism of cell exit (Early et al., 2011). Apoptosis was not observed during visual inspection of macrophages infected with MGC-passaged *M.*

avium. To follow-up, an experiment is to measure apoptosis with an Annexin V assay is necessary to confirm this observation. The study published by Early et. al. shows that macrophage-passaged *M. avium* enters uninfected macrophages primarily via macropinocytosis rather than complement receptor-mediated phagocytosis, which is the typical pathway (Early et al., 2011). Our work demonstrates that blocking macropinocytosis or complement receptor-mediated phagocytosis significantly reduces the uptake of macrophages by MGC-passaged *M. avium,* suggesting that this phenotype uses multiple routes of entry. The precise escape mechanism of *M. avium* from MGCs remains unclear. *M. marinum* utilizes autophagy to escape from host macrophages in a nonlytic mechanism (Flieger et al., n.d.). *M. avium* may utilize a similar autophagy-mediated pathway of cell exit. Together, these findings demonstrate that exposure to the MGC environment increases the uptake of *M. avium,* by naïve macrophages which may help minimize the time spent in the extracellular space and maximize transmission. Further work is needed to describe the precise mechanism utilized by *M. avium* to exit MGCs.

Previous studies by Ramakrishnan and colleagues, in the *M. marinum* zebrafish model, demonstrated that infected macrophages control the bacterial burden, migrate into tissues, and recruit additional cells to form granulomas in early stages of infection (Clay et al., 2007). Additionally, granulomas themselves facilitate cell-to-cell spread of bacteria and increase bacterial burden (Davis & Ramakrishnan, 2009; Volkman et al., 2004). Our finding that *M. avium* exits multinucleated giant cells and exhibits higher uptake suggests that the intracellular environment of multinucleated giant cells may enhance and contribute to the bacterial replicative

niche and drive cell-to-cell spread. Characterizing the cell exit mechanism utilized by MGC-passaged *M. avium* is an important future direction. Probing the involvement of autophagy on bacterial cell exit would be a good starting point.

Using the *in vitro* model established in this study, we characterized some of the interactions between MGCs and *M. avium.* Bacterial survival assays in MGCs confirm a favorable intracellular environment promoting *M. avium* growth and escape. We also demonstrated that autophagy is elevated in MGCs, and its inhibition reduces *M. avium* survival in phagocytic cells. *M. avium* also appears to utilize host cholesterol and sphingomyelin to fuel intracellular growth. Further study is needed to define the role of lipids versus autophagy in nutrient acquisition by intracellular *M. avium.* Our data indicate that while *M. avium* is well adapted to replicate in MGCs, the host environment stimulates the uptake of bacteria and efficient escape from phagocytic cells likely for local spread (Fig. 2.10).

Figures

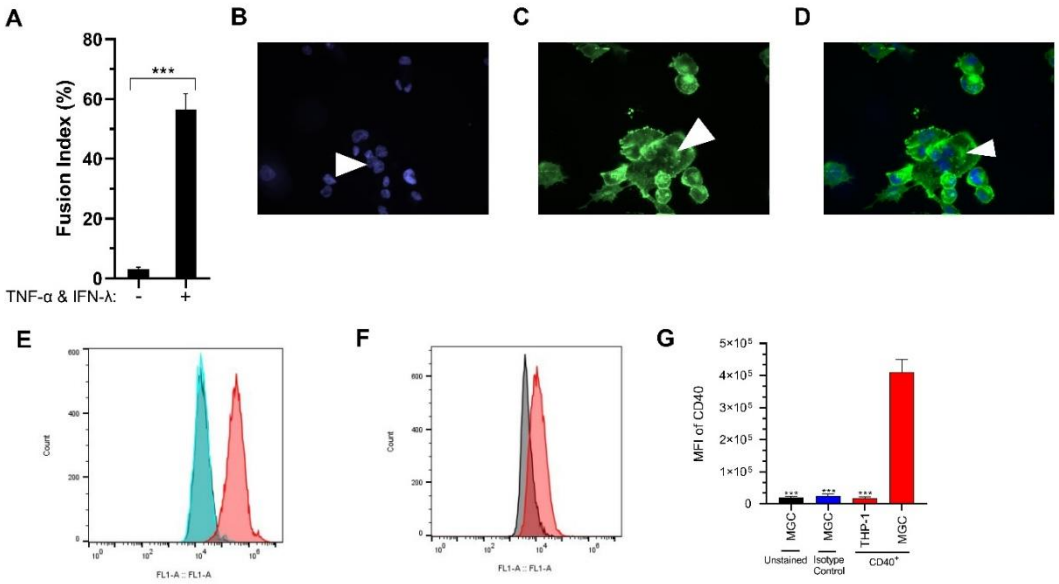

Figure 2.1. IFN-γ and TNF-α induce formation of multinucleated giant cells *in vitro*. THP-1 cells were fluorescently labeled after cytokine treatment to determine MGC formation via microscopy at 1000X magnification. The expression of CD40, a marker associated with classical macrophage activation and Langhans giant cells was measured via flow cytometry. (A) The macrophage fusion index determined the percentage of multinucleated cell having at least 2 nuclei in 10 fields of view. (B) Hoechst stain of MGC nuclei (white arrow). (C) Alexa Fluor Phalloidin 488 stain of actin cytoskeleton (white arrow). (D) Merged image of MGC (white arrow). (E) FITC-CD40 levels in MGCs (Black: unstained, Blue: Isotype control, Red: $CD40^+$). (F) FITC-CD40 levels in PMA-differentiated THP-1 cells (Black: unstained, Red: $CD40^+$). (G) Mean Fluorescent intensity of FITC-CD40 (Black: unstained, Blue: Isotype control, Red: $CD40^+$). All groups were compared to MGC $CD40^+$. Data are representative of 3 independent experiments. Statistical comparisons: *, $P < 0.01$, **, $P < 0.001$, ***, $P < 0.0001$.

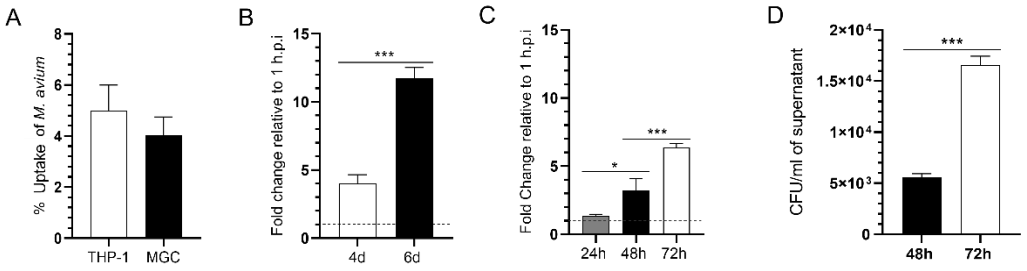

Figure 2.2. MGCs Phagocytose *M. avium* and Permit Intracellular Replication. (A) Percent uptake of *M. avium* A5 in THP-1 macrophages and MGCs after 1 hour of infection. (B) Fold change relative to 1 h.p.i (dashed line) of *M. avium* growth over 6 days in THP-1 macrophages. (C) Fold change relative to 1 h.p.i (dashed line) of *M. avium* growth over 3 days in MGCs. (D) Extracellular bacteria CFUs recovered after infection of MGCs. Data shown are representative of results from three independent biological replicates. Statistical comparisons: *, $P < 0.05$; **, $P < 0.005$; ***, $P < 0.0005$.

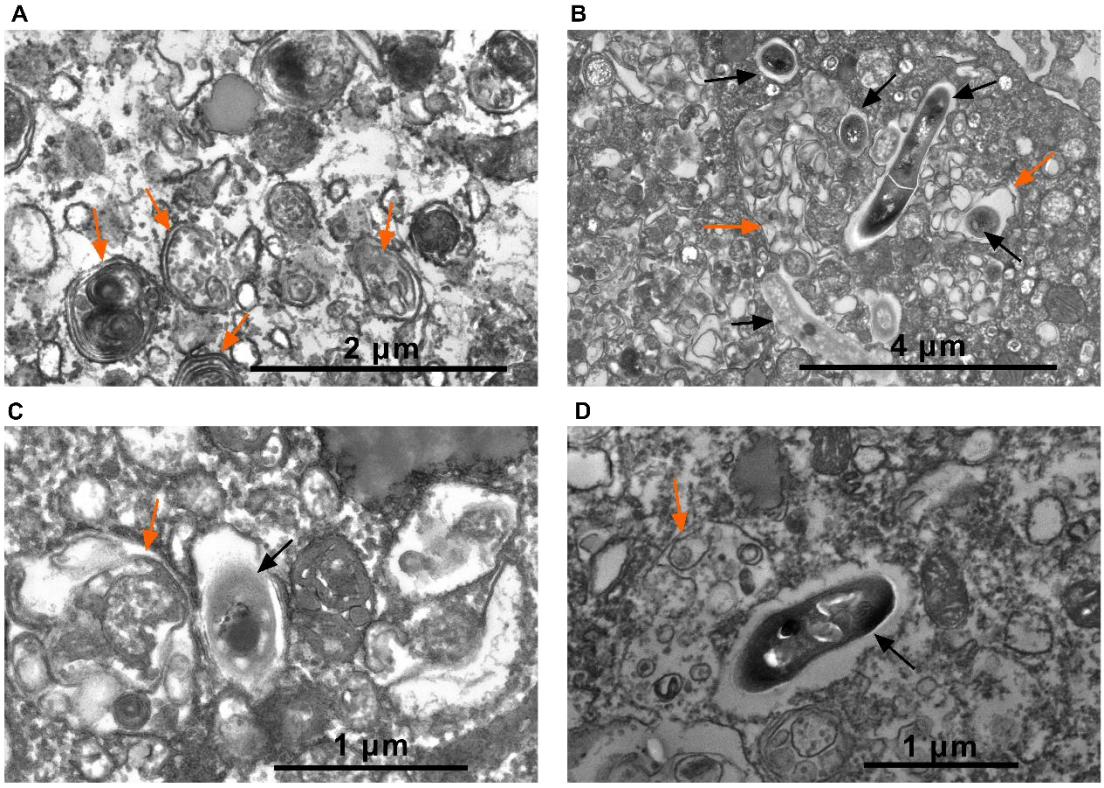

Figure 2.3. Autophagic Activity in MGCs. (A) Autophagosomes containing cellular components in uninfected MGCs (B) Autophagosomes containing *M. avium* 72 h.p.i. of MGCs. (C) At 72 h.p.i. vacuoles containing *M. avium* interacting with an autophagosome. (D) Same as (C). Black arrows: bacteria, orange arrows: autophagosomes.

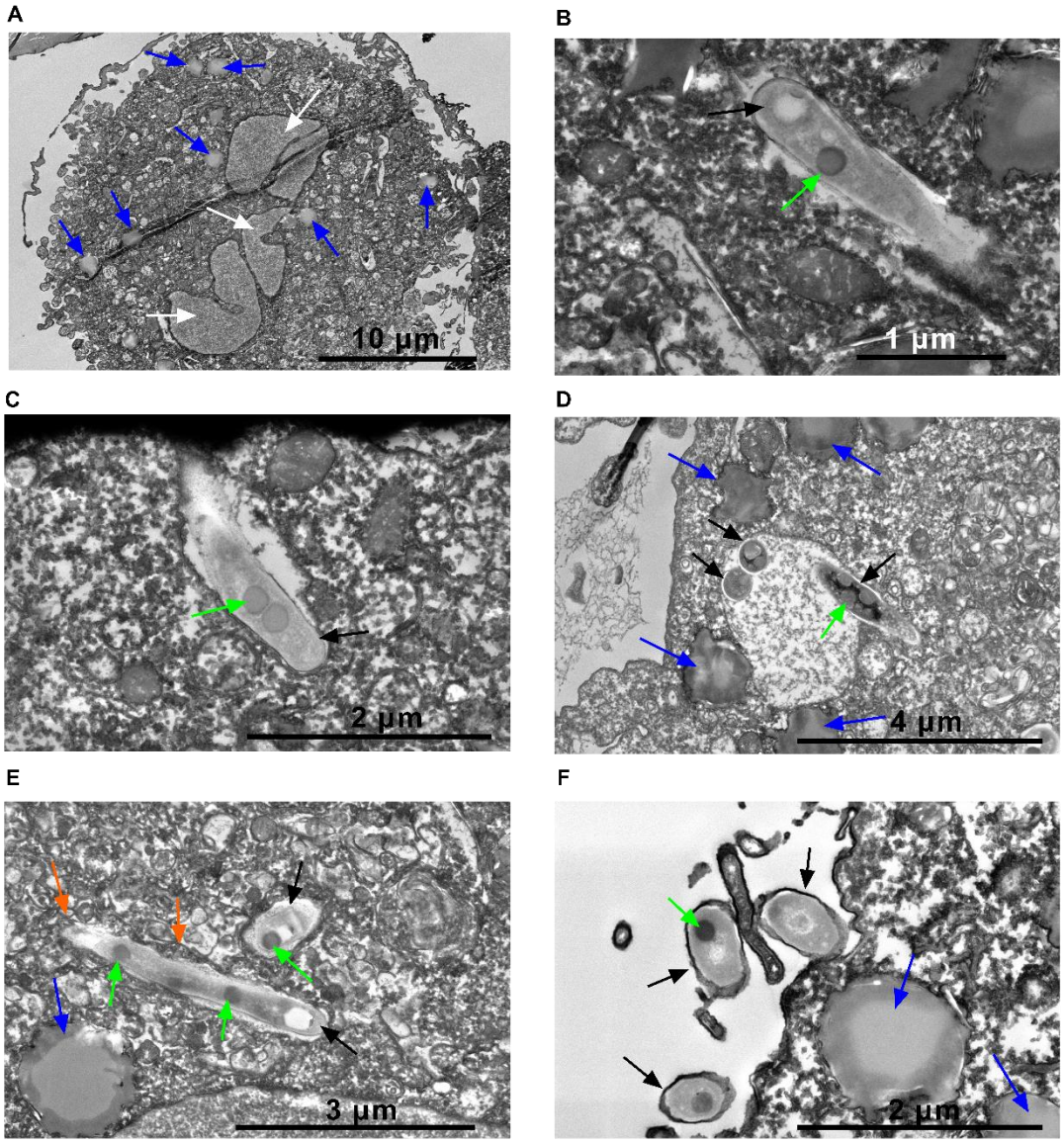

Figure 2.4. Characteristics of Intracellular *M. avium* in MGCs. (A) Uninfected MGC with three nuclei surrounded by lipid droplets. (B) Cytosolic *M. avium* inside MGCs at 1 h.p.i. (C) *M. avium* bacterium in a vacuole at 1 h.p.i in MGCs. (D) Vacuole containing multiple *M. avium* 72 h.p.i. inside MGCs. (E) Intracellular *M. avium* in autophagosome in MGC at 1 h.p.i. (F) 24 h.p.i., extracellular *M. avium* from an MGC. Blue arrows: host lipid droplets, black arrows: bacteria, green arrows: intra-bacterial lipid inclusions, white arrows: nuclei, and orange arrows: autophagosomes.

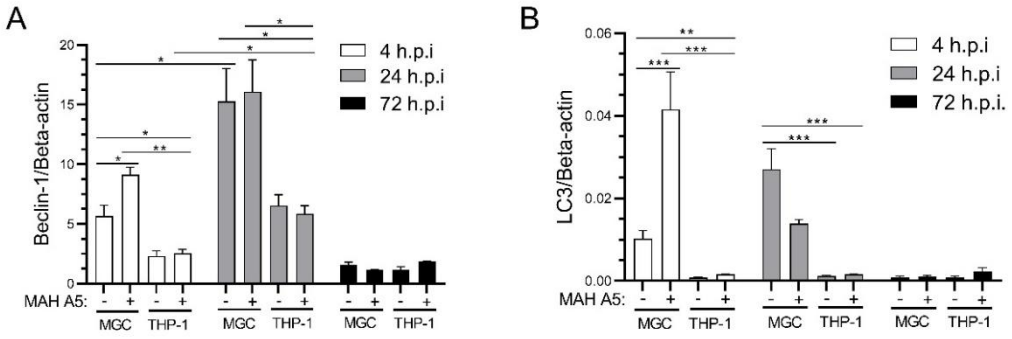

Figure 2.5. Gene expression of autophagic markers is elevated in MGCs. Either MGCs or THP-1 cells were infected with WT *M. avium* A5 for 4 h. (A) LC3 transcripts were measured by RT-qPCR at indicated times. mRNA levels are presented as relative expression to actin. (B) Beclin-1 transcripts were measured at indicated timepoints. mRNA levels are represented relative to actin expression. Data are representative of two independent experiments. Statistical comparisons: *, $P < 0.01$; **, $P < 0.001$; ***, $P < 0.0001$.

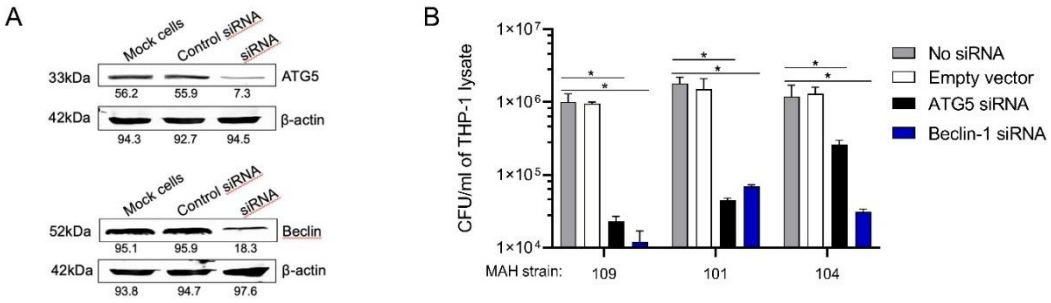

Figure 2.6: siRNA targeting of autophagy markers decreases protein levels. THP-1 cells were depleted of either ATG5 or Beclin-1 48 h after siRNA targeting. (A) Western blot band intensities were quantified using β-actin as a loading control by Odyssey imager software (Li-Cor). (B) Survival of *M. avium* strains 109, 101, and 104 at 48 h.p.i. in THP-1 macrophages transfected with ATG5 or Beclin-1 siRNA. CFU/ml of Data are representative of three experiments. Statistical comparisons: *, $P < 0.01$; **, $P < 0.001$; ***, $P < 0.0001$.

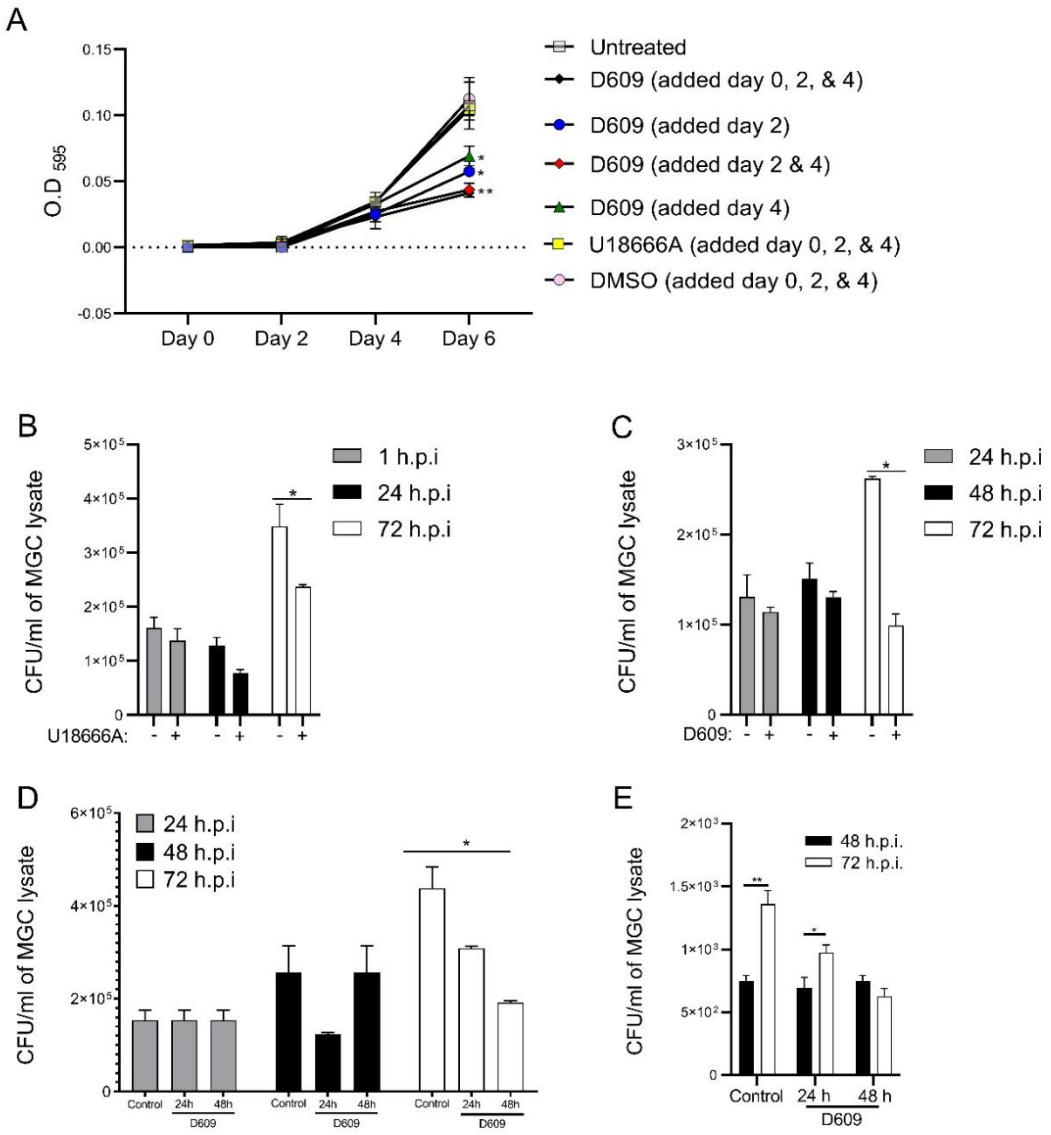

Figure 2.7. Effects of altering lipid cellular components during mycobacterial infection. (A) Growth curve of *M. avium* A5 in 7H9 supplemented with either DMSO, U18666A (3 µg/ml), or D609 (100 µM). D609 was added at specified timepoints after inoculation of growth media. (B) Survival of *M. avium* in MGCs in the presence of intracellular cholesterol transport inhibitor U18666A (3 µg/ml) or in media only. (C) Survival of *M. avium* in MGCs in the presence of sphingomyelin synthase inhibitor D609 (100 µM) or in media only. (D) D609 added to MGCs at 24, or 48h.p.i. then CFUs were determined over 72 h. (E) Extracellular CFUs from (D) supernatants from infected MGCs was plated at each time point. Statistically significant treatments are compared to untreated. Data shown are from 3 independent experiments. Statistical comparisons: *, $P < 0.01$; **, $P < 0.001$.

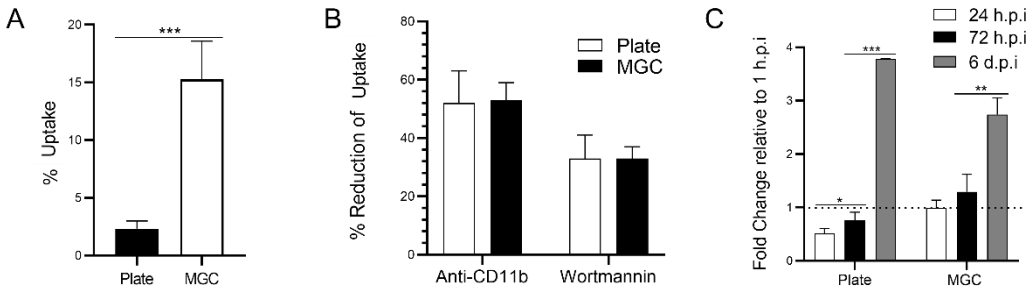

Fig. 2.8. Passage through MGCs Increases Uptake, but not survival of *M. avium* A5 in naïve macrophages. Uptake and survival of MGC-passaged *M. avium* A5 in THP-1 cells. (A) Percent Uptake of *M. avium* A5 inoculums in THP-1 cells after 1h of infection. THP-1 cells were treated with either wortmannin for 2h, or with a CD11b antibody for 1h, prior to infection. (B) Fold change relative to 1 h.p.i (dashed line) of bacterial survival by plate or MGC-passaged *M. avium* in THP-1 macrophages over 6 days. 'Plate' refers to *M. avium* A5 grown on a 7H10 plate, and 'MGC-passaged' refers to *M. avium* A5 that was collected from infected-MGCs at 72 h.p.i. Data are representative of three independent experiments. Statistical comparisons: *, $P < 0.01$, **, $P < 0.001$, ***, $P < 0.0001$.

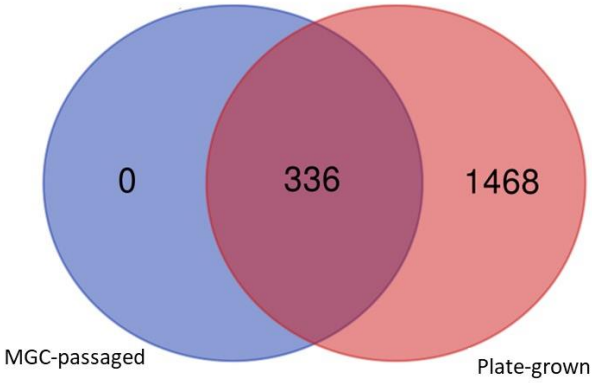

Fig. 2.9 Proteomics Analysis of MGC-Passaged versus Plate-Grown *M. avium*. MGC-passaged bacteria were collected at 72 h.p.i from the supernatant above infected MGCs. Plate-grown bacteria were collected from an agar streak plate. Total protein was isolated and sequenced. Data for MGC-passaged bacteria represents 8 pooled, independent experiments. Data for Plate-grown bacteria represent 3 pooled, independent experiments.

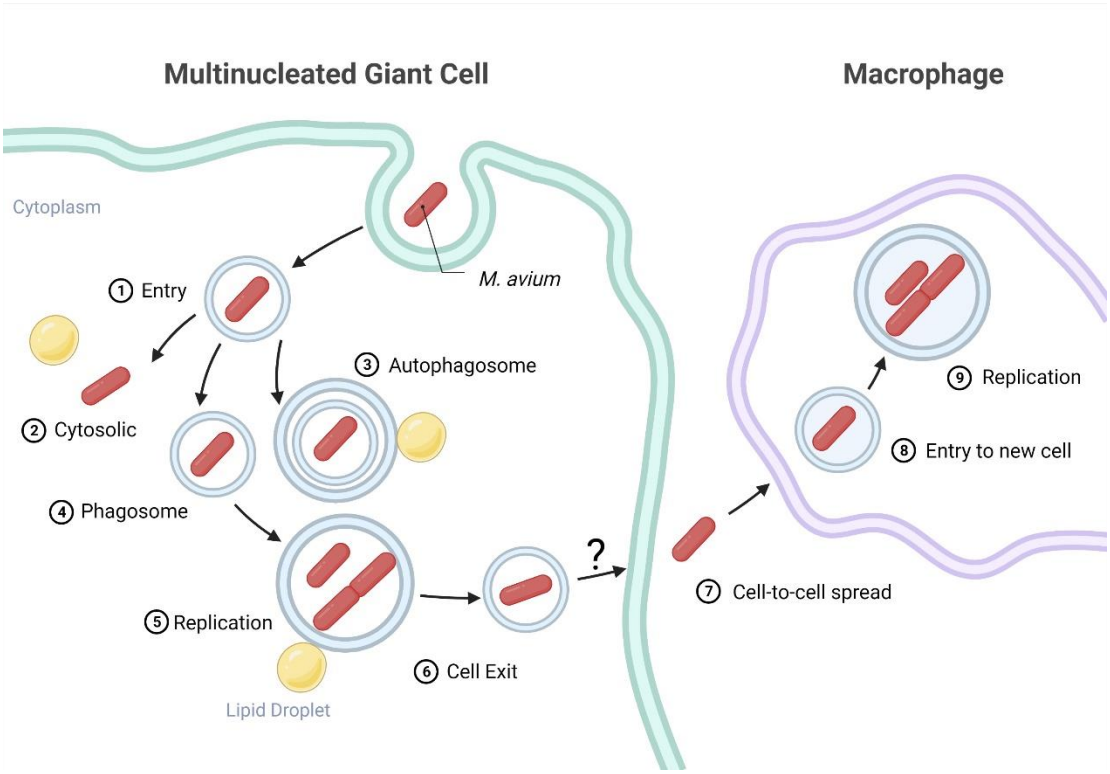

Fig. 2.10. Proposed *M. avium* Cell Cycle in Multinucleated Giant Cells. (1) *M. avium* enters MGC. (2) (3) (4) Intracellular bacteria are in phagosomes, autophagic vacuoles, and the cytosol. Some of these structures are near lipid droplets. (5) Intracellular bacteria replicate in phagosomes and autophagic vacuoles. (6) *M. avium* leaves the MGC by an unknown mechanism. (7) Extracellular *M. avium* infects neighboring macrophages. (8) Bacteria enter the macrophage through complement receptor 3-mediated phagocytosis, macropinocytosis, and may enter through other pathways as well. (9) Bacteria replicate in permissive phagosomes in the macrophage. Created with BioRender.com.

Acknowledgements

We thank Soheila Kazemi for her assistance with the flow cytometry experiments and Lia Danelishvili for performing the siRNA knockdown and western blot experiments. We acknowledge Teresa Sawyer and the Oregon State University Electron Microscopy Facility for their expertise and the use of their facility. The project described was supported, in part, the Oregon State University Research Office. The content is solely the responsibility of the authors and does not necessarily represent the official views of the OSU Mass Spectrometry Center. The authors acknowledge the OSU Mass Spectrometry Center at Oregon State University and specific institutional instrument grants. Orbitrap Fusion Lumos -NIH # 1S10OD020111-01, Waters Ion Mobility ToF Mass Spectrometer – NIH #1S10RR025628-01, Applied Biosystems 4000Qtrap- NIH # 1S10RR022589-01, ABSciex Triple ToF 5600-NIH #1S10RR027878-01.

Chapter 3

Understanding the Modulation of the Macrophage Inflammatory Responses During *Mycobacterium avium* Infection

Jayanthi J. Joseph, Amy Leestemaker-Palmer, Luiz E. Bermudez

Abstract

Mycobacterium avium subsp. *hominissuis* (*M. avium*) is an environmental opportunistic pathogen that causes pulmonary, and systemic infection in humans. Mycobacterial infection activates pro-inflammatory and anti-inflammatory pathways and bacteria must modulate these pathways to escape killing mechanisms of the host. Inflammasomes, such as NLRP3 and AIM2, play a crucial role in host immunity against *M. tuberculosis* infection through the production of pro-inflammatory IL-1β. NLRP3 detects a variety of cellular stress signals and AIM2 detects cytosolic dsDNA. The cGAS/STING pathway also detects cytosolic dsDNA but induces anti-inflammatory IFN-β secretion. eDNA is critical for environmental survival and biofilm formation of *M. avium.* We hypothesized that *M. avium* eDNA plays a role in intracellular survival via the cGAS/STING pathway. To investigate the macrophage response to *M. avium* and the involvement of eDNA, we utilized two virulent strains, *M. avium* 104 and A5, eDNA-deficient A5 mutants, and nonvirulent *M. smegmatis*. We demonstrated that *M. avium*, but not *M. smegmatis*, suppress IL-1β production and NLRP3 expression by host macrophages. eDNA-deficient mutants were attenuated at macrophage survival and yielded significantly higher IL-1β than wildtype. We also observed that *M. avium* A5, 104, *M.* smegmatis, and eDNA-deficient mutants triggered IFN-β production in a DNA-dependent manner but did not have an effect on cGAS expression. Taken together, these data indicate that *M. avium* strains modulate macrophage responses and is able to inhibit pro-inflammatory signaling pathways. Finally, our results suggest that eDNA found in *M. avium* strain

A5 plays a role in intracellular survival and manipulation of the macrophage responses to infection.

Introduction

In recent years, the number of *M. avium* infections have been increasing worldwide (Prevots & Marras, 2015). Treatment of pulmonary infections requires multiple antibiotics for a minimum of 12 months and is only effective in 50-60% of patients (Griffith et al., 2007; Ingen et al., 2013). Mycobacterial biofilms are ubiquitous in household plumbing, natural water sources, and the soil (Griffith et al., 2007). These biofilms are the primary source of infection in immunocompetent individuals (Griffith et al., 2007; Vega-Dominguez et al., 2020). To sustain a chronic infection, mycobacteria must evade the immune system and find supportive niches to foster bacterial growth and spreading. A key component of innate immunity is the ability for cells to sense stress or foreign material from viruses, bacteria, even dysregulated "self" material. To accomplish this the cell employs the inflammasome pathway to clear infections.

Manipulation of the host inflammasome response is a vital part of mycobacterial pathogenesis. The NLRP3 inflammasome was selected because it has been implicated in both bacterial clearance and bacterial dissemination in *M. tb* infection (Rastogi et al., 2021a; Xu et al., 2020). *M. tb* differentially modulates the NLRP3 inflammasome depending on the stage of infection. Early on, *M. tb* inhibits NLRP3 inflammasome activation in host macrophages via PknD and Hip1 (Madan-Lala et al., 2011; Rastogi et al., 2021a). During chronic infection, *M. tb* promotes NLRP3 activation to trigger cell death and bacteria cell-to-cell spread. Canonically, activation of the NLRP3 inflammasome leads to the secretion of pro-inflammatory IL-1β and can lead to pyroptosis (Guo et al., 2015). In patients with *M. avium* lung

disease, NLRP3 activation and IL-1β secretion are attenuated in PBMCS (Wu et al., 2019).

NLRP3 activation is a tightly regulated process involving phosphorylation of specific sites, ubiquitination control, and the interaction of specific effectors with NLRP3 (Swanson et al., 2019). Regulation of the ASC adaptor protein, is required for phosphorylation activation at Tyr146 by Spleen Tyrosine Kinase (Syk) (Hara et al., 2013). Syk has been implicated in NLRP3 activation during *M. tuberculosis* infection (H.-M. Lee et al., 2012). BRCA1/BRCA2-containing complex E3 ubiquitin ligase (BRCC3) deubiquitinates NLRP3, which promotes NLRP3 activation (Py et al., 2013). During *M. tuberculosis* infection of macrophages, lysosomal release of activated cathepsin B (CTSB) is required for NLRP3 activation (Amaral et al., 2018). Both *M. avium* and *M. tuberculosis* infection increase the expression of CTSB macrophages (Amaral et al., 2018; Gutierrez et al., 2008).

M. avium strain A5 is a high-biofilm producing strain of *M. avium* and unlike 104, exports large amounts of extracellular DNA (eDNA) in the biofilm (Chakraborty et al., 2021; Rose & Bermudez, 2016). The proteins for eDNA export in *M. avium* strain A5 was found within a unique 50-kbp genomic region and is present in other Mycobacterial species including, *M. abscessus*, *M. chelonae*, *M. intracellulare*, *M. avium* subsp. *hominissuis* strain 3388, which are all of concern in human infections (Rose & Bermudez, 2016). Previous work has shown that *M. avium* strain A5 bacteria are able to invade epithelial cells more efficiently than *M. avium* strain 104, forming aggregates on the cells surface, a precursor to biofilm formation; suggesting that biofilm-related genes play a role during infection (Yamazaki et al., 2006). eDNA is a

critical structural component of the extracellular matrix in *M. avium* strain A5 biofilms, and forms a protective barrier against antimicrobial peptides and antibiotics (Rose et al., 2015). With this added component of eDNA it is important for this strain and others to be able to manipulate DNA sensing pathways that lead to host killing mechanism evasion. To piece together the role of eDNA in the host macrophage we looked at a pro-inflammatory DNA sensor (AIM2) and an anti-inflammatory DNA sensor (cGAS/STING).

The AIM2 inflammasome is a cytosolic dsDNA sensor, which induces cleavage of pro-IL-1β by caspase 1 upon activation, similar to NLRP3 (Guo et al., 2015). *M. smegmatis, M. fortuitum, M. kansasii* induce AIM2 activation whereas *M. tuberculosis* inhibits AIM2 activation *in vitro* (Shah et al., 2013). To demonstrate AIM2 importance, knockout mice given *M. tuberculosis* are highly susceptible to infection compared to wildtype, which suggests that AIM2 plays a vital role in host defense for specific mycobacterial strains (Saiga et al., 2012). Additionally, both NLRP3 and AIM2 require Syk phosphorylation for IL-18 secretion, another pro-inflammatory cytokine (Hara et al., 2013). AIM2 is not the only DNA sensor within a cell. The cGAS-STING pathway also senses cytosolic dsDNA.

During *M. tuberculosis* infection cytosolic bacteria DNA is detected by the cGAS-STING pathway, leading to the production of type I interferons which have a suppressive effect on NLRP3 activation and IL-1β secretion (Ma et al., 2020; Wassermann et al., 2015; Watson et al., 2015). The STING pathway is a cytosolic surveillance pathway typically involved in the antiviral response and is characterized by the production of type I interferons (IFN-α and IFN-β) and activation of autophagy

(Schoggins et al., 2014; Watson et al., 2015). Briefly, Cytosolic dsDNA binds to cyclic GMP-AMP synthase (cGAS), dimerizing stimulator of interferon genes (STING) to induce IFN regulatory factor 3 (*IRF3*), upregulating Type I interferons (Burdette & Vance, 2013). Type I interferons have a suppressive effect on the macrophage antibacterial response (Boxx & Cheng, 2016; Guarda et al., 2011, p. 1).

In this study we examine the interaction of eDNA producing *M. avium* strain A5 with host inflammasomes as well as modulation of DNA sensing mechanisms. We demonstrate that *M. avium* strain A5 modulates pro-inflammatory pathways during early infection. Additionally, we demonstrated the important role of bacterial eDNA in anti-inflammatory signaling during the intra-macrophage phase of infection.

Methods

Bacteria culture

Mycobacterium avium subsp. *hominissuis* strains 104 (*M. avium* 104) and A5 (*M. avium* A5), were originally isolated from the blood of AIDS patients (Aronson et al., 1999). *M. avium* 104 is the reference strain and *M. avium* A5 exhibits prolific biofilm formation and eDNA export (Rose & Bermudez, 2016). *M. avium* A5 MycomarT7 phagemid-based transposon mutants generated by Sasha Rose were screened for deficiency in eDNA export during biofilm formation (Rose & Bermudez, 2016). As previously published, the eDNA/optical density (OD) value for each mutant was calculated by normalizing the fluorescence reading for day 7 RFU of eDNA bound to propidium iodide to the starting OD of the respective sample (Rose & Bermudez, 2016). The eDNA/O.D. for wildtype A5 was 30,000 (Rose & Bermudez, 2016). Ligation mediated PCR (LMPCR) was used to sequence transposon locations. *M. avium* 104, *M. avium* A5, and *Mycobacterium smegmatis* strain MC^2-155 (MS) were grown on Middlebrook 7H10 agar supplemented with 10% w/v oleic acid, albumin, dextrose, and catalase (OADC, Hardy Diagnostics) for 7-10 days at 37°C. *M. avium* A5 transposon mutants were grown on 7H10 agar supplemented with 10% w/v OADC and 400 µg/ml Kanamycin.

Tissue Culture

THP-1 (TIB-202) human monocytes were obtained from the American Type Culture Collection (ATCC) and maintained in RPMI 1640 supplemented with 10% heat--inactivated fetal bovine serum (FBS; Gemini Bio-Products) at 37°C with 5% CO_2. THP-1 cells were seeded in 48-well plates at a density of 3.5×10^5 cells per well, 24-

well plates at $1x10^6$ cells/well, and 6-well plates at $2x10^6$ cells/well. THP-1 cells were differentiated with 50 ng/ml of Phorbol 12-myristate 13-acetate (PMA; Sigma Aldrich) for 24 hours, followed by 24 hours in media without PMA, prior to use in experiments.

MycomarT7 transposon Mutants

A library of MycomarT7 (Mmt7) was created and screened by Sasha Rose as previously described (Rose & Bermudez, 2016). Briefly, the Mmt7 phagemid was transduced into *M. avium* A5, and the resulting transposon mutant library was screened. The library was screened for deficiency in eDNA export in biofilms by Sasha Rose (Rose & Bermudez, 2016). The location of transposon insertion selected eDNA-deficient mutants was determined using ligation-mediated PCR (LMPCR) as previously described (Rose & Bermudez, 2016).

Survival Assay

M. avium 104 and A5, *M. smegmatis*, and eDNA-deficient mutants were added to THP-1 cells at an MOI of 10, synchronized by centrifugation for 10 min at 150 x g, and allowed to infect for 1 hour. Inoculums for these assays were formed in 1X HBSS supplemented with 0.05% Tween-20 (Sigma-Aldrich). Extracellular bacteria were removed by two wash steps with 1X HBBS followed by treatment with gentamicin sulfate (Sigma-Aldrich) for 1 hour (100 µg/ml) and an additional wash step with 1X HBSS to remove dead bacteria. Cells were lysed at appropriate timepoints with 0.1% Triton-X for 10 min and resulting lysates were diluted and plated. Colony forming units (CFUs) were enumerated at 1, 24, 48, and 72 hours post infection (h.p.i.). Potential extracellular bacteria escaping from cells were quantified at each timepoint via spot

plating. Briefly, 5 µL of media removed from infected wells where plated on 7H10 agar. Colonies were counted after 7 days of incubation at 37°C.

NLRP3 Inhibition Survival Assay

Infection with *M. avium* 104 and A5 was carried out as described above. THP-1 cells were treated with 1 µM MCC950 (Millipore, Sigma) for 24 hours after infection. Cells were lysed and CFUs enumerated at 1, 24, and 48 h.p.i.

Growth Curve

M. avium was cultured in 7H9 broth supplemented with 10% w/v OADC at 37˚ C in a shaking incubator. MCC950 was added at day 0 to a final concentration of 1 µM. Control tubes were left untreated. The absorbance at 595nm was measured at day 0, 2, 4 and 6.

qPCR

THP-1 cells and MGCs were infected with *M. avium* 104, A5, MS, and *M. avium* A5 mutants as described above. RNA was isolated using the RNeasy mini kit (Qiagen). Genomic DNA was removed by treatment with DNase I recombinant (Roche Diagnostics) for 1 hour at 37°C. The DNase was inactivated with Turbo DNase-inactivation reagent (Turbo DNA-free kit, ThermoFisher Scientific) for 2 min at 37°C. Inactivation reagent was removed via centrifugation for 1 min at 10,000 x g, and RNA transferred to new collection tubes. RNA samples were stored at -4°C until cDNA synthesis. cDNA was transcribed from host RNA using the iScript cDNA synthesis kit (Bio-Rad). The quality of cDNA was tested by PCR with Gold 360 master mix using the manufacturer's specifications (ThermoFisher Scientific). The qPCR reaction was performed using iQ SYBR Green Supermix (Bio-Rad) and an

iCycler (CFX Connect Real-Time Systems, Bio-Rad) as previously described (Danelishvili et al., 2004). Primers were designed in NCBI Blast using sequences from GenBank (National Center for Biotechnology Information).

Primer sequences are as follows:

NLRP3 Forward	CTTCTCTGATGAGGCCCAAG	J. Joseph
NLRP3 Reverse	GCAGCAAACTGGAAAGGAAG	J. Joseph
AIM2 Forward	CAACGTGCTGCACCAAAAGT	J. Joseph
AIM2 Reverse	GCTTGCCTTCTTGGGTCTCA	J. Joseph
SYK Forward	TGCACTATCGCATCGACAAA	J. Joseph
SYK Reverse	GATTATTCCACCCGCTGACC	J. Joseph
Cathepsin B Forward	TGTGGGGACGGCTGTAAT	J. Joseph
Cathepsin B Reverse	GCTATTGGAGACGCTGTAGG	J. Joseph
BRCC3 Forward	TGCTTCCAATCCATACAGGC	J. Joseph
BRCC3 Reverse	CAAGGCACACTTTCCCGATA	J. Joseph
cGAS Forward	GGAGCCCTGCTGTAACACTT	J. Joseph
cGAS Reverse	GTGAGAGAAGGATAGCCGCC	J. Joseph
STING Forward	CAGCCTTGGTTCTGCTGAGT	J. Joseph
STING Reverse	ACCCCGTTTAACAGCAGTCC	J. Joseph
Beta-actin Forward	CATGTACGTTGCTATCCAGGC	J. Joseph
Beta-actin Reverse	CTCCTTAATGTCACGCACGAT	Wang, 2013

ELISA

Supernatants from infections carried out as described above were collected at 1, 6, 24, and 48 h.p.i. Supernatants were immediately spun down to remove cell debris for 10 min at 150 x g and stored at -20˚C until analyzed. IL-1β concentration was quantified with the Human IL-1β ELISA kit according to manufacturer's specifications (ThermoFisher Scientific). IFN-β was quantified using the Human IFN-β ELISA kit according to manufacturer's specifications (ThermoFisher Scientific).

Statistical Analysis

All described experiments were repeated at least three times and data shown are representative of the biological replicates. Comparisons between two groups were analyzed in Microsoft Excel using the two-tailed Student t test. Results with p-values below 0.05 were considered significant.

Results

eDNA exporting M. avium strain A5 modulates NLRP3 expression differently than M. avium strain 104

To determine if eDNA export has an effect on host stress sensors we examined the gene expression of NLRP3. *M. avium* strain A5 (A5), high eDNA exporter, was compared to a low eDNA exporter *M. avium* strain 104 (104). Since regulation of the inflammasome response needs to occur early on during infection, time points were chosen between 1-48 h.p.i. *M. smegmatis* (MSMEG) was a control strain of mycobacteria that can be killed by macrophages by 48 h.p.i but produces eDNA. Uninfected macrophages (UN) determine normal cellular expression of genes. NLRP3 expression was upregulated significantly at 1 h.p.i in all strains tested (Fig. 3.1A) compared to uninfected macrophages. The most upregulation being observed in MSMEG. Over time, NLRP3 expression in all treatments beings to reduce and at 48 h.p.i 104 and A5 have similar levels to uninfected. MSMEG however greatly increases expression of NLRP3 at 48 h.p.i (Fig. 3.1A). This over expression is in response to intracellular killing of MSMEG and the release of PAMPs into the cytosol. This is not seen with *M. avium,* as both strains survive in macrophages and do no induce stress associated pathways.

Naïve macrophages are not the only type of cell mycobacteria will encounter in the host. Macrophages can be activated into M1 or M2 phenotypes depending on cell signaling (Yunna et al., 2020, p. 2). A stimulator of M1 macrophages, LPS, also induces upregulation of NLRP3 (Gritsenko et al., 2020; Zheng et al., 2013, p. 2). We compared A5 to 104 and MSMEG after LPS stimulation to determine what effects

they have on inflammasome regulation in activated macrophages. NLRP3 expression is upregulated by LPS stimulation in all treatment groups at 1 h.p.i (Fig. 3.1B) compared to untreated cells. *M. avium* 104 and MSMEG infected macrophages had a significant upregulation of NLRP3 after 1 h.p.i compared to uninfected cell. Interestingly, A5 does not increase NLRP3 expression beyond the effects of LPS stimulation, similar to uninfected macrophages after 1 h.p.i. Again, after early stimulation, NLRP3 expression decreases over time, until 48 h.p.i, where all strains of mycobacteria increase NLRP3 expression (Fig. 3.1B). In addition to NLRP3 upregulation due to TLR4 signaling, the LPS can lead to increased bacteria killing in macrophages which may lead to the observable NLRP3 increase.

NLRP3 leads to the activation of IL-1β, a pro-inflammatory cytokine, and ultimately pyroptosis in macrophages. We examined if the upregulation seen in NLRP3 expression affects the quantity of IL-1β protein secreted by macrophages. When naïve macrophages are infected with 104, A5 or MSMEG, IL-1β protein concentration significantly (~500 pg/ml) increases by 6 h.p.i. (Fig. 3.1C). After 6 h.p.i, IL-1β protein concentration drops down to background levels. At 48 h.p.i, *M. avium* strain reduce protein levels while MSMEG increases protein concentration compared to uninfected macrophages. When macrophages are activated with LPS, IL-1β protein levels increase in uninfected cells and stay elevated (~500 pg/ml) over 48 h.p.i (Fig. 3.1D). Macrophage activation via LPS stimulation and measurable IL-1β production takes 2-4 hours (Gritsenko et al., 2020). However, LPS-induced NLRP3 inflammasome activation occurs within 15 min (Song et al., 2017). Activated macrophages infected with mycobacteria initially reduce IL-1β protein levels at 1

h.p.i, but after 6h, IL-1β levels increase to uninfected amounts. Interestingly, after 6h IL-1β protein levels in all mycobacterial strains tested are suppressed, diminishing this pro-inflammatory pathway (Fig. 3.1D). We wanted to investigate how A5 might be mitigating the NLRP3 pathway via regulation of NLRP3 activation.

NLRP3 Inflammasome Regulatory Protein SYK is Upregulated by M. avium strain A5

NLRP3 inflammasomes are tightly regulated by multiple checkpoints. For example, SYK protein phosphorylates ASC, an adaptor protein in the inflammasome complex. BRCC3 is a deubiquitinating enzyme that modulates the activity of NLRP3 by deubiquitinating NLRP3, which leads to activation. Another avenue of regulation is by affecting levels of NLRP3 activators like cathepsin B, which is upregulated in *M. kansasii* infection (C.-C. Chen et al., 2012). We investigated the gene expression of SYK, BRCC3, and Cathepsin B at 24 h.p.i via qPCR. A5 significantly increased the expression of Syk compared to uninfected macrophages (Fig. 3.2A). MSMEG also increased levels of Syk but to a lesser extent than A5. 104 did not increase this regulatory protein. Upon infection with A5, Syk is greatly increased presumably allowing ASC phosphorylation and further NLRP3 activation potentially leading to increased IL-1β. However, the increase of IL-1β protein level is not observed. A5 is suppressing pro-inflammatory signaling in an unknown manner. Expression of BRCC3 was not upregulated by mycobacterial infection compared to uninfected macrophages (Fig. 3.2B). Cathepsin B, an activator of the NLRP3 inflammasome, was not upregulated by mycobacterial strains when compared to uninfected macrophages (Fig. 3.2C). Overall, we observe an increase of regulatory Syk protein at

24 h.p.i, however this increase does not affect NLRP3 expression significantly as seen previously. Next, we determined how chemical inhibition of NLRP3 affected *M. avium* survival.

Chemical Inhibition of NLRP3 Activation does not affect early survival of M. avium in macrophages

We investigated whether inhibition of NLRP3 with compound MCC950 affected *M. avium* A5 and 104 infection and survival in macrophages. *M. avium* strain 104 and A5 were grown in 7H9 broth with or without NLRP3 inhibition to determine if this compound affects bacterial replication directly (Fig. 3.3A). Over 6 days of culture, there was no observable difference in growth capacity of either strain. To confirm the inactivation of NLRP3, IL-1β protein levels were determined for LPS stimulated macrophages, LPS and MCC 950 treated macrophages, and untreated macrophages. LPS again increased IL-1β (~350 pg/ml), while MCC950 significantly reduced IL-1β levels to ~100 pg/ml (Fig. 3.3B). After confirming reduction of NLRP3 activation by MCC950, we investigated the survival of *M. avium* strains in THP-1 macrophages. Treatment with MCC950 had no effect on 104 (Fig. 3.3C) survival compared to no inhibition of NLRP3. This observation was also seen in A5 (Fig. 3.3D). These data indicate that NLRP3 inflammasome activation does not affect infection or early survival in macrophages. However, since *M. avium* possesses the ability to actively reduce NLRP3 activation early in infection, so the effects of external NLRP3 inhibition may be indistinguishable from bacteria-induced suppression.

Expression of eDNA Sensors AIM2 and cGAS/STING after M. avium strain A5 infection

The NLRP3 inflammasome is only one pathway that produces IL-1β. The mechanism by which A5 reduces IL-1β production may be due to AIM2 inflammasome activation. The AIM2 inflammasome senses foreign and host dsDNA in the cytosol. To determine the effects that eDNA producing mycobacteria have an AIM2, gene expression was determined by qPCR. Early infection of naïve THP-1 with MSMEG showed an increasing amount of AIM2 over 48 h.p.i (Fig. 3.4A). A5 initially increased AIM2 over 6 h.p.i but then gradually decline after 48 h.p.i (Fig. 3.4A). 104 significantly upregulated AIM2 up to 24 h.p.i but less than high eDNA producing strain A5 and after 48 h.p.i upregulation was reduced (Fig. 3.4A). A5 exports higher quantities of extracellular DNA in the biofilm, which could explain why the initial spike in AIM2 expression differs from 104 (Rose & Bermudez, 2016). When THP-1 macrophages are pre-stimulated with LPS, uninfected cells upregulated AIM2 at 1h, then expression remained relatively low (Fig. 3.4B). Like NLRP3, AIM2 inflammasome expression was initially upregulated by LPS stimulation, but was reduced over 48 h.p.i. MSMEG upregulation of AIM2 increases over 48 h.p.i and is much more than uninfected macrophages (Fig. 3.4B). Both *M. avium* strains have significantly elevated AIM2 over 48 h.p.i but there was no difference between eDNA exporting strain (Fig. 3.4B). With high expression of AIM2 we would expect increased levels of IL-1β, but as observed previously, IL-1β is suppressed.

dsDNA can also be detected by the cGAS/STING pathway. Activation of this pathway leads to the production of IFN-β, an anti-inflammatory cytokine, and has

been shown to act in a host detrimental manner during chronic bacterial infections. IFN-β may counteract the effects of pro-inflammatory cytokine signaling. Since cGAS/STING is a multistep pathway, we investigated cGAS and STING expression. cGAS is the cytosolic sensor that binds to dsDNA and produces a secondary messenger (cGAMP) that leads to STING activation downstream. THP-1 macrophages infected with *M. avium* strains showed no increase in cGAS expression while MSMEG led to a significant increase (Fig. 3.4C). Macrophages stimulated with LPS showed an increase of cGAS overall but a significant increase in 104 and MSMEG at 24 h.p.i (Fig. 3.4C). A5 did not increase cGAS expression after 24 h.p.i. STING activation leads to the IFN-β transcription. STING expression in macrophages is not upregulated in *M. avium* infections. LPS stimulated macrophages demonstrated the upregulation of STING expression while all mycobacterial strains tested actively reduced STING expression (Fig. 3.4D). IFN-β ELISA were used o determined effects on cGAS/STING modulation by mycobacteria. Macrophages infected with eDNA generating mycobacteria produce high levels of IFN-β, A5 (~65 pg/ml) and MSMEG (~77 pg/ml) while 104 induces much lower levels (~30 pg/ml) (Fig. 3.4E). LPS stimulation reduces IFN-β levels for eDNA mycobacteria but increased IFN-β for 104 (Fig. 3.4E). Since LPS stimulates pro-inflammatory cytokines, a reduction in anti-inflammatory IFN-β would allow for host killing mechanism to prevail. Mycobacteria may use IFN-β to reduce the pro-inflammatory state of the macrophage especially when these bacteria actively reduce levels of IL-1β as seen previously. eDNA has been demonstrated to effectively modulate the inflammatory state of macrophages so

to understand these effects more in depth we utilized mutants deficient in eDNA export.

eDNA-deficient Mutants are Attenuated in THP-1 Macrophages

eDNA has been previously shown to be important for A5 biofilm formation. A library of *M. avium* strain A5 Mmt7 transposon mutants was previously screened for eDNA-deficiency during biofilm formation (Rose & Bermudez, 2016). We selected three mutants with varying eDNA deficiencies summarized in Table 3.1. Mutant 11e7 being the most deficient while mutant 9e11 is the least deficient at eDNA export. We tested the three mutants for their capacity to infect and survive in THP-1 macrophages, 7d3 (metal-dependent hydrolase), 9e11 (PknB-serine/threonine kinase) and 11e7 (Ftsk/SpoIIIE-DNA pore ATPase) compared to A5 (WT). All three mutants infected macrophages similarly to WT (Fig. 3.5A). After infection, mutants were extracted from THP-1 macrophages at 24 h.p.i and CFUs enumerated. All three mutants showed significantly reduced survival compared to WT whether in naïve or LPS stimulated macrophages (Fig. 3.5B). Replication of mutants 7d3 and 9e11 bacteria was similar to WT at day 2, however mutant 9e11 was significantly lower than WT at day 4 (Fig. 3.5C). Replication of mutant 11e7 was lower than WT at day 2, but similar to WT at day 4 (Fig. 3.5C). The slower rate of growth exhibited by mutant 11e7 at day 2 is not as pronounce at day 1, so it might only partially affect the intracellular survival at 24 h.p.i. Taken together these data demonstrate the importance of eDNA for survival of A5 in macrophages. Since we have eDNA deficient mutants that are attenuated in macrophages, inflammasome modulation was determined.

eDNA-deficient Mutants Alter IL-1β Secretion Through Inflammasome Pathways

A5 can modulate the expression of NLRP3 and AIM2 as seen previously. In naïve macrophages, eDNA deficient mutants had no upregulation of NLRP3 expression at 24 h.p.i (Fig. 3.6A). Interestingly, mutant 7d3 significantly upregulated NLRP3 with LPS stimulation (Fig. 3.6A). When investigating AIM2, mutant 7d3 had upregulated expression similar to A5 after LPS stimulation while all other mutants had no effect on the expression of AIM2 (Fig. 3.6B). Since NLRP3 and AIM2 stimulate IL-1β production, we determined cytokine protein levels. In naïve macrophages all mutants increased IL-1β levels compared to WT and uninfected macrophages. While LPS macrophages demonstrated that mutants still suppressed IL-1β but not as significantly as WT (Fig. 3.6C). eDNA export appears to play an important role in controlling IL-1β protein levels, especially mutant 7d3, which upregulated both NLRP3 and AIM2. These mutants can help narrow down specific interactions that affect pro-inflammatory cytokine levels in macrophages. The observation that NLRP3 expression did not correlate with the increased IL-1β during mutant infection, indicates that *M. avium* is affecting NLRP3 activation somewhere between expression and IL-1β production.

M. avium A5 eDNA-deficient Mutants are Downregulate STING Expression in LPS stimulated Macrophages and Modulate IFN-β Production

eDNA-deficient mutants effect the secretion of IFN-β through the cGAS/STING pathway. A5 previously showed no effect on cGAS upregulation compared to uninfected THP-1 macrophages. Whether or not these cells were primed by LPS addition. Attenuated mutants did not stimulate the upregulation of cGAS in

naïve macrophages similar to WT (Fig. 3.7A). This pattern was also seen in LPS stimulated macrophages. eDNA export did not affect the expression of cGAS in THP-1 macrophages. STING expression was greatly reduced only after LPS stimulation of macrophages similar to WT A5 (Fig. 3.7B). cGAS/STING stimulates IFN-β production when dsDNA is sense. Mutant 7d3 and 11e7 had significantly reduced levels of IFN-β compared to WT A5 in naïve macrophages (Fig. 3.7C). Mutant 9e11, the serine/threonine kinase, greatly stimulated anti-inflammatory activation and IFN-β production. In LPS stimulated macrophages, IFN-β levels were reduced compared to WT, likely due to the heightened inflammatory environment generated by LPS (Fig. 3.7C). However, these levels of IFN-β were still higher than uninfected macrophages, demonstrating that *M. avium* is still able to induce anti-inflammatory signaling. These data indicate an importance for eDNA export to promote anti-inflammatory signal expression during infection of macrophages to over host killing mechanisms. More work is needed to pinpoint what is truly affecting the modulation of inflammatory responses in host macrophages.

Discussion

Intracellular pathogens, like mycobacteria, modulate cytosolic sensing pathways to avoid macrophage killing mechanisms and premature cell death. The NLRP3 and AIM2 inflammasomes and cGAS/STING are cytosolic sensors of importance during mycobacterial infection. In this chapter, we found that *M. avium* 104 and A5 modulate NLRP3 inflammasome expression and activation early in infection. IL-1β secretion spiked early in infection but dropped to background levels up to 48 h.p.i. *M. abscessus* triggers high levels of NLRP3 activation, but the subsequent IL-1β secretion is countered by cGAS-STING dependent IFN-β production (B.-R. Kim et al., 2020). This is one possible explanation for the observed reduction of IL-1β during *M. avium* infection. In LPS stimulated macrophages IL-1β levels in *M. avium* infected macrophages increased at 48 h.p.i compared to uninfected macrophages. This could be due to increased bacterial killing after LPS stimulation. LPS is a potent macrophage activator and induces autophagy, pro-inflammatory cytokine secretion, nitric oxide, and enhance bacterial killing (F. Meng & Lowell, 1997). LPS also activates NLRP3 through a non-canonical pathway (Guo et al., 2015). LPS has also been shown to induce AIM2 and STING expression in macrophages (Lugrin & Martinon, 2018, p. 2; Ning et al., 2020). This explains the upregulation of NLRP3, AIM2, and STING expression and IL-1β production in uninfected cells stimulated with LPS.

Nonvirulent *M. smegmatis* induced significantly higher expression of NLRP3 and IL-1β production at 48 h.p.i than *M. avium*. However, IL-1β production by MSMEG-infected macrophages at 48 h.p.i was not increased in LPS-stimulated cells.

MSMEG is not adapted to survival in human macrophages. Macrophages clear MSMEG infection by 24-48 hours post-infection. MSMEG inhibits phagosome acidification during early infection, but after 5 hours, phagosome maturation continues (Kuehnel et al., 2001). Thus, phagosome maturation and subsequent intracellular killing of MSMEG could lead to increased cytosolic PAMPS which explains the upregulation of NLRP3 and AIM2 at 48 h.p.i. MSMEG matched *M. avium* A5 and 104 NLRP3 expression and IL-1β secretion at 6 h.p.i. The inhibition of phagosome maturation by MSMEG, while attenuated compared to *M. avium*, extends long enough to explain the similar macrophage response at early time points. At later timepoints, macrophage killing of MSMEG could explain the increase in inflammasome expression and IL-1β production due to increased cytosolic PAMPs.

The activation of the NLRP3 inflammasome may play different roles at different stages of infection. A previous study demonstrated that the early macrophage response to *M. avium* infection is pro-inflammatory, but is reversed once the bacteria are internalized (Greenwell-Wild et al., 2002). *M. tb* induces NLRP3 activation during chronic infection to facilitate cell-to-cell spread (Xu et al., 2020, p. 2). We observed no effect on intracellular *M. avium* survival in the presence of an NLRP3 inhibitor. This gives credence to the idea that *M. avium* possesses mechanisms by which to evade early inflammasome activation and modulate the pro-inflammatory response to further intracellular replication. One such strategy is employed by *M. tb* to inhibit NLRP3 activation during early stages of infection (Be et al., 2012). NLRP3 inhibition by *M. tb* involves Phosphokinase F (PknF) (Rastogi et al., 2021a). *M. avium* A5 has a homolog for PknF, and which is the gene disrupted in

mutant 9e11 (MAVA5_13430; PknB). MAVA5_13430 is in an operon that contains several hypothetical proteins, efflux pump, and transporter. Mutant 9e11 induces significantly higher IL-1β production than WT A5, which could be due to the lack of functional PknB. However, the same upregulation was observed for other eDNA-deficient mutants, so increased IL-1β may be a result of bacterial killing.

Next, we examined the modulation of DNA-sensing pathways AIM2 and cGAS/STING in the macrophage during *M. avium* and MSMEG infection. Activation of the AIM2 inflammasome leads to pro-inflammatory IL-1β production, which increases anti-bacterial activity. Activation of the cGAS/STING pathway leads to the production of type I interferon IFN-β. The role of type I interferons in NTM infection is inconclusive. Prolonged expression contributes to persistence during chronic viral and bacterial infections. IFN-β promotes chronic mycobacterial infections by inducing anti-inflammatory IL-10 production and suppressing pro-inflammatory IL-12 and IFN-γ (Boxx & Cheng, 2016; Teles et al., 2013). This limits inflammation-related tissue damage but slows bacterial clearance.

While the role of STING in *M. tb* is well-described, the importance of STING in NTM infection is still unclear. Recent research demonstrated that *M. abscessus,* a rapidly growing NTM, induces high levels of cGAS/STING-derived IFN-β, which counteracts NLRP3-derived IL-β, and facilitates bacterial survival (B.-R. Kim et al., 2020). During *M. tb* infection, the cGAS/STING pathway is activated by cytosolic mycobacterial DNA, and mycobacterial c-di-AMP (N. Liu et al., 2022; Watson et al., 2015). This activation induces autophagy, which has a negative effect on inflammasome activation and bacterial survival (Watson et al., 2015). However, *M. tb*

is able to survive by inhibiting autophagy and reducing the availability of STING via mycobacterial protein MmsA (Maphasa et al., 2021; Sun et al., 2020). *M. avium* has a homolog of the MmsA gene and may be able to utilize a similar mechanism. Further work could determine if MmsA is involved in the modulation of STING during *M. avium* pathogenesis.

We found that high eDNA-producing *M. avium* strain A5 induced significantly higher AIM2 expression and IFN-β production than low eDNA-producing 104 in naïve macrophages. However, LPS stimulation reduced these differences, indicating crosstalk between inflammasomes and cGAS/STING. We found that *M. avium* A5 eDNA-deficient mutants induced varied responses in human macrophages. All three mutants inhibited the LPS-induced upregulation of STING expression similar to WT A5. This suggests that eDNA may not be involved in the modulation of STING expression. Unfortunately, there is no evidence of intracellular eDNA export by *M. avium*, which is a significant gap in our understanding of this interaction. Intracellular DNA export has been established during *M. tb* infection, so it is feasible for mycobacteria to accomplish this in the host. However, the observation of reduced IFN-β during mutant 7d3 and 11e7 infection, compared to the increased IFN-β induced by WT A5, supports the hypothesis that eDNA is being secreted in the host macrophage. Future work could examine cGAS/STING activation and DNA export at later time points to shed light on this question.

All three mutants were attenuated at intracellular survival in human macrophages. Mutant 11e7 (MAVA5_03380; DNA pore ATPase) is the most attenuated at DNA export, which explains the reduction in AIM2 expression and IFN-

β production compared to wildtype. These differences are likely due to lower amounts of cytosolic mycobacterial DNA. The homolog of MAVA5_03380, *M. tb* gene Rv3871, encodes an ESX-1 Type VII secretion system protein EccB, which contains a FtsK/SpoIIIE domain, similar to MAVA5_03380, and is involved in protein secretion by the type VII secretion system, interaction with the host, and evasion of the host immune response (Brodin et al., 2006; Stanley et al., 2003). EccB interacts with EspL (Rv3876), which is the only ESX-1 protein found in *M. avium* (MAVA5_16875) (Jeffrey et al., 2017). EspL is essential for *M. tb* virulence and mediates ESX-1 function. Given the similarity of the ESX secretion systems, EspL may interact with an alternate ESX secretion system that is present in the *M. avium* genome. This could explain the attenuation of macrophage survival observed by mutant 11e7 (Fig. 3.5).

Mutant 9e11 is the least eDNA-deficient mutant used in this study, which could mean that there is sufficient cytosolic DNA to trigger the cGAS/STING pathway. This could explain the unexpected increase in IFN-β production induced by 9e11. Additionally, intracellular killing could release increased DNA into the cytosol. The gene disrupted in mutant 9e11, MAVA5_13430, has a serine/threonine protein kinase B domain (PknB), which is essential for growth, stress response and metabolic regulation in *M. tb* (Grundner et al., 2005). Additionally, MAVA5_13430 has three homologs in the *M. tb* genome: Rv2914c (PknI), Rv2088 (PknJ), and Rv1746 (PknF). All three genes encode serine/threonine protein kinases, which carry out a range of function in the host. PknI regulates bacterial growth in the host and specifically slows bacterial growth in the macrophage (Gopalaswamy et al., 2009). PknJ phosphorylates

several substrates in the host, including pyruvate kinase, and macrophage-entry associated protein GroEL2 (Arora et al., 2010; Vinod et al., 2021). PknF interacts with an ABC transporter encoded by Rv1747, to inhibit the NLRP3 inflammasome during *M. tb* infection (Rastogi et al., 2021a). The lack of any of these functions could explain the significant attenuation of extracellular and intracellular growth displayed by the 9e11 mutant (Fig. 3.5). This gene would be an ideal candidate for further study since it appears to be central to survival in the host and environment.

Mutant 7d3 (MAVA5_10275; hydrolase) is not as DNA deficient as 11e7, so there may be sufficient cytosolic DNA to induce AIM2 expression, cGAS/STING activation, and IFN-β production. Unexpectedly, 7d3 induced significant upregulation of NLRP3 and AIM2 in LPS pre-treated macrophages, but IL-1β production was unaffected. Mutant 7d3 induced significantly lower IFN-β than WT A5 in naïve macrophages and significantly higher levels in LPS stimulated macrophages. The neighboring genes upstream and downstream of MAVA5_10275 are involved in glycolysis and cellular metabolism. Additionally, the homolog of MAVA5_10275 in *M. abscessus,* MAB_2069, is a metal-dependent hydrolase involved in fatty acid metabolism. MAB_2069 interacts with AraC transcriptional regulator appY, which regulates the response to oxidative stress, acid stress and antibiotics in *E. coli* (Dale et al., 2022). AraC transcriptional regulators are known to be important for the regulation of virulence and response to stress (Gallegos et al., 1997). Disruption of MAVA5_10275 and surrounding genes in mutant 7d3 could interfere with the utilization of host lipids, and adaptation to intracellular conditions, leading to the observed attenuation of this mutant in the macrophage, but not extracellular growth

(Fig. 3.5). Complementation of these mutants is on-going and is needed to confirm that the interrupted gene is the cause of the observed effects.

A limitation of this study lies in the methodology used to determine inflammasome activation. The activation of both the NLRP3 and AIM2 inflammasome leads to IL-1β production by the macrophage, so additional controls are needed to rule out the contribution of each inflammasome. Comparing gene expression of each inflammasome partially addressed this issue, however, the activation of each inflammasome must be examined individually using chemical inhibitors, siRNA, or knockout cell lines. This limitation will be tackled in on-going work. Given our observation of low NLRP3 expression and IL-1β production, is important to explore the mechanisms, if any, employed by *M. avium* to modulate expression and activation of the NLRP3 inflammasome. On-going work is examining the effect of *M. avium* infection on NLRP3 phosphorylation, which is a key step in inflammasome activation. Future work should expand this idea to investigate mechanisms of AIM2 and cGAS/STING regulation and activation.

We started to explore the role of the NLRP3 inflammasome on bacterial survival. Next, it is important to investigate the effect of AIM2 inflammasome activation and cGAS/STING activation on bacterial survival. Knockout cell lines would be a useful tool and would allow us to determine bacterial survival and growth in the absence of each inflammasome or sensor. Alternatively, siRNA or chemical inhibition would allow us to investigate the involvement of inflammasomes and sensors at different points during infection. Now that we have begun to establish the macrophage response, we plan to investigate the MGC response to *M. avium*

infection. It is also important to look at AIM2 and cGAS/STING expression in MGCs, since we observed cytosolic *M. avium* in MGCs as early as 24 h.p.i. Cytosolic bacteria increase the amount of dsDNA available to activated DNA sensing pathways and this may reveal additional roles for eDNA in a cell type associated with chronic infection (MGCs).

Figures

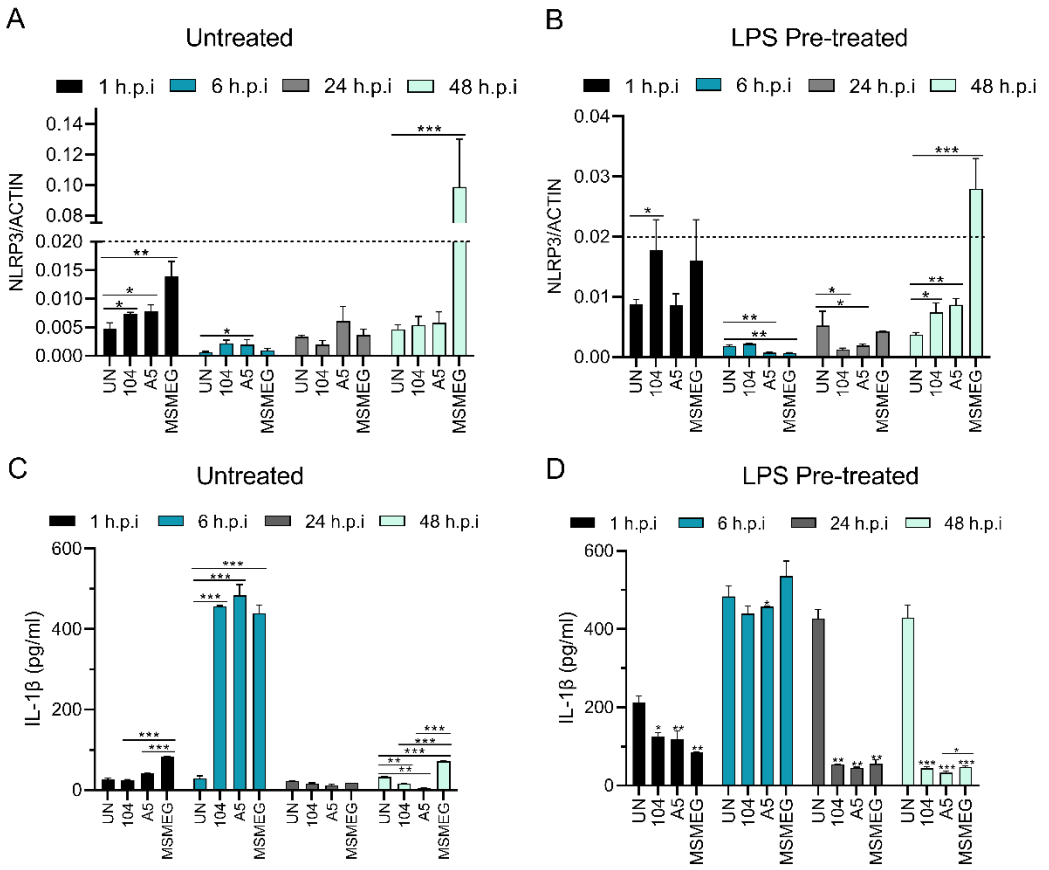

Figure 3.1. *M. avium* Suppresses NLRP3 Expression and IL-1β Secretion by THP-1 Macrophages. THP-1 cells were stimulated with 10 ng/ml LPS for 2h prior to infection with *M. avium* A5, 104, or MSMEG. Supernatants and RNA were collected at 1, 6, 24, and 48 h.p.i. NLRP3 expression was quantified by qPCR and IL-1β levels were quantified by ELISA. NLRP3 expression in (A) Untreated THP-1 cells. (B) LPS pre-treated THP-1 cells. IL-1β levels in supernatants from (C) Untreated THP-1 cells and (D) LPS-pre-treated THP-1 cells. Statistical comparisons represent significant difference from uninfected cells at each timepoint. The dashed line indicates 0.02 NLRP3/ACTIN in (A) and (B). Data are representative of three independent experiments. Statistical comparisons: *, $P < 0.05$; **, $P < 0.005$, ***, $P < 0.0005$.

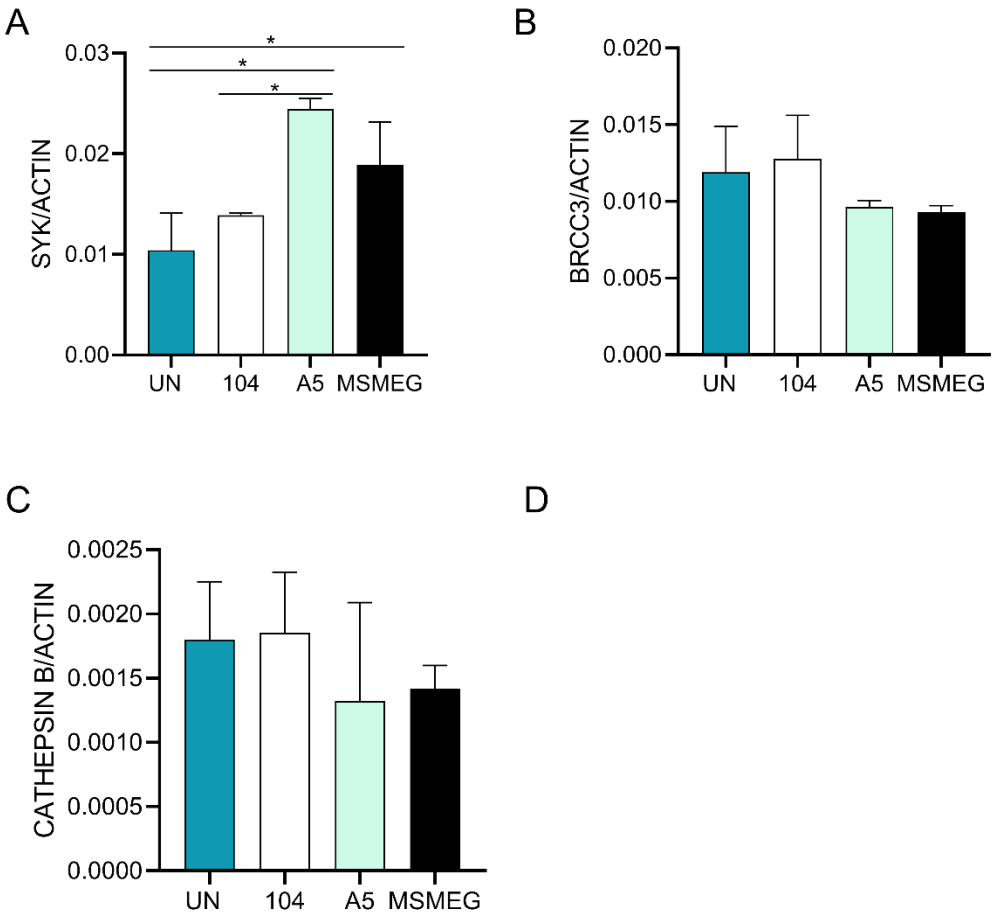

Figure 3.2. *M. avium* Infection Upregulates Expression of Syk and IL-1β, but not BRCC3 or Cathepsin B in THP-1 Macrophages. THP-1 cells infected with *M. avium* A5, 104, or MSMEG. RNA was isolated at 24 h.p.i. Expression of (A) Syk (B) BRCC3 and (C) Cathepsin B. Data are representative of two independent experiments. Statistical comparisons: *, $P < 0.05$; **, $P < 0.005$, ***, $P < 0.0005$.

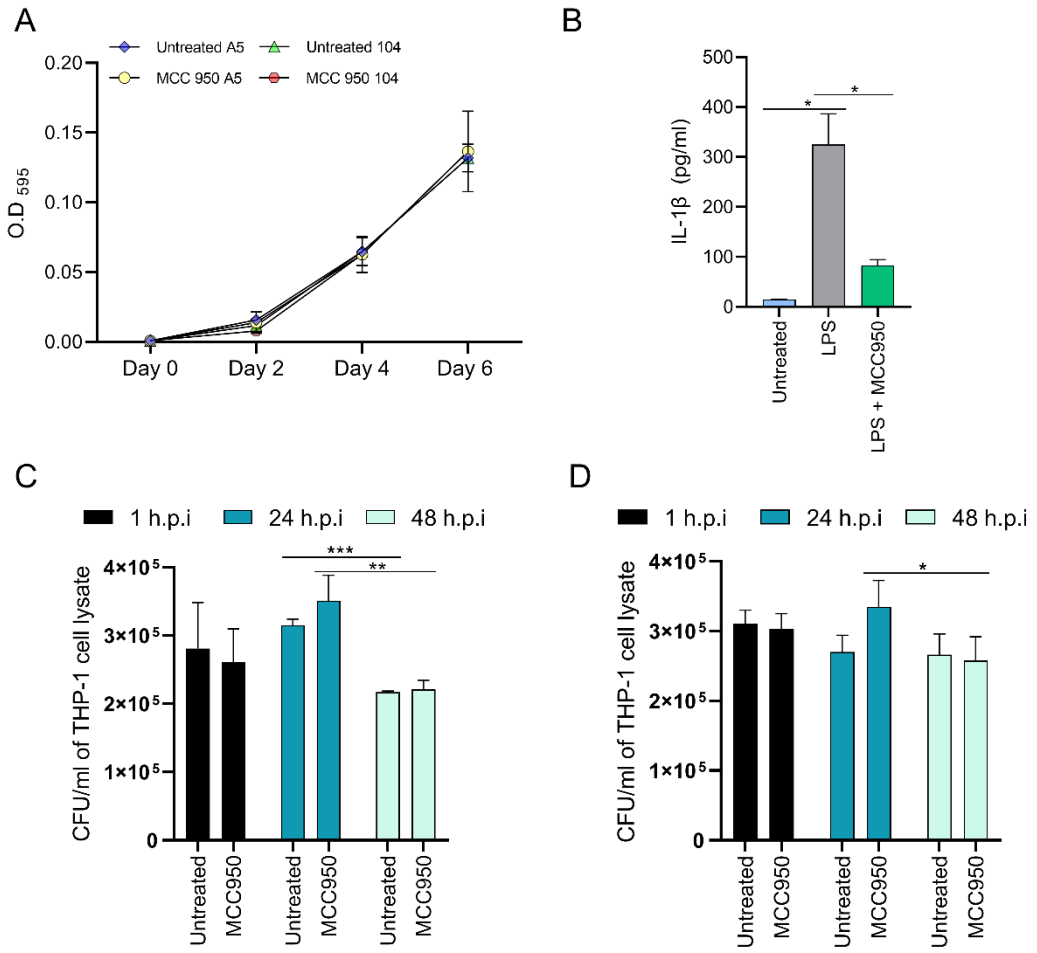

Figure 3.3. Chemical Inhibition of NLRP3 Activation Does Not Reduce *M. avium* Survival in Macrophages. (A) Growth curve of *M. avium* 104 and A5in 7H9 broth. MCC950 at a final concentration of 1µM was added at day 0. Absorbance was measured at 595 nm over 6 days. (B) Inhibition of NLRP3 activation was measured by IL-1β ELISA. THP-1 cells were treated with LPS (10 ng/ml) for 2 hours, followed by MCC950 (1 µM) for 24 hours. THP-1 cells were infected with (C) *M. avium* 104, or (B) *M. avium* A5 and treated with MCC950 (1µM) at 1 h.p.i. Statistical comparisons: *, $P < 0.05$; **, $P < 0.005$, ***, $P < 0.0005$.

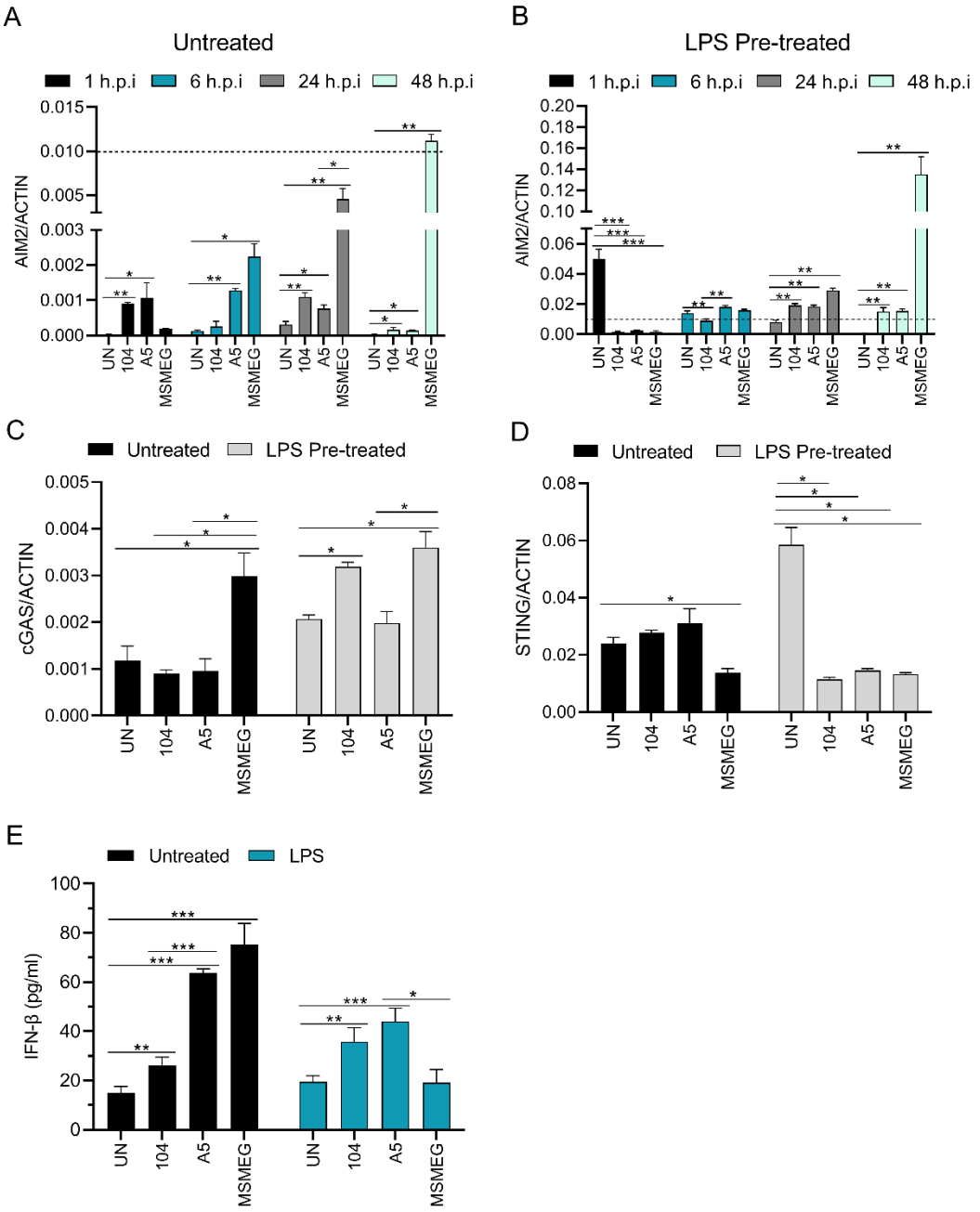

Figure 3.4. *M. avium* Suppresses the Expression of DNA sensors AIM2, cGAS, and STING, and triggers IFN-β Secretion. AIM2, cGAS and STING expression was quantified by qPCR and IFN-β levels were measured by ELISA. Expression of AIM2 in (A) Untreated THP-1 cells and (B) LPS pre-treated THP-1 cells infected with *M. avium* A5, 104, or MSMEG. Expression of (C) cGAS and (D) STING by untreated and LPS pre-treated THP-1 cells. Statistical comparisons (E) IFN-β secretion by untreated and LPS pre-treated THP-1 cells. THP-1 cells were treated with 10ng/ml LPS for 2 hours prior to infection. Data are representative of at least two independent experiments. Statistical comparisons: *, $P < 0.05$; **, $P < 0.005$, ***, $P < 0.0005$.

Table 3.1. eDNA-deficient *M. avium* A5 mutants.

Location of Transposon	Mutant	eDNA* (d7/O.D)	G-C Content	Conserved Domain	Neighboring Genes (MAVA5_XXXXX)***
MAVA5_03380	11e7	6177	61.6	FtsK/SpoIIIE (DNA pore ATPase)	Hypothetical, plasmid replication, integration, and excision activator. *Integrase, tRNA-Phe, tRNA-Asp, tRNA-glu, tRNA-Lys.*
MAVA5_10275**	7d3	9918	57.8	Metal-dependent hydrolase	TetR family transcriptional regulator. *Acetyl-CoA carboxylase, acetyl-CoA carboxylase subunit alpha, acyl-CoA dehydrogenase, long-chain fatty acid-CoA ligase, TetR family transcriptional regulator.*
MAVA5_13430	9e11	19286	71.8	PknB (serine/threonine kinase)	*Hypothetical, hypothetical, hypothetical, excinuclease ABC subunit UvrB/DNA Polymerase III, EmrB efflux pump/Major Facilitator Superfamily*

*WT A5 eDNA (d7/O.D) was ~30,000.
**Gene is in 50 kb genomic region that is associated with DNA export.
****Italics: downstream*, Normal: upstream.

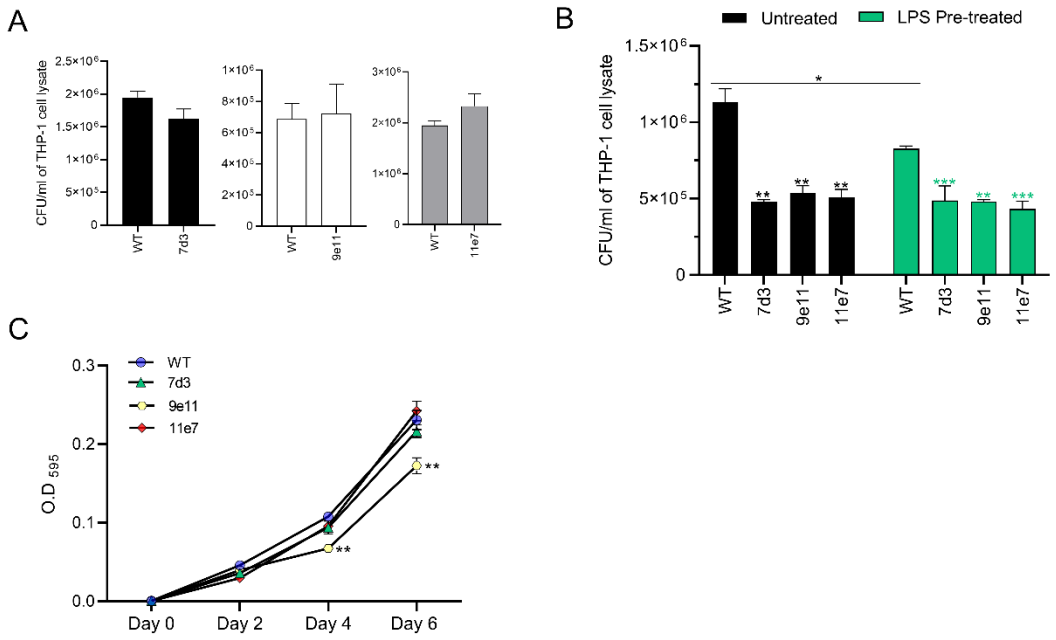

Figure 3.5. eDNA-deficient Mutants are Attenuated in THP-1 Macrophages. Untreated and LPS-primed THP-1 cells were infected with *M. avium* A5 and eDNA-deficient mutants 7d3, 9e11, 11e7 and c11e7. CFUs were enumerated and supernatants were collected at 24 h.p.i. (A) Uptake assays of eDNA-deficient mutants at wildtype A5 at 1 h.p.i. (B) Survival assay of eDNA-deficient A5 mutants compared to WT A5 in THP-1 cells at 24 h.p.i. Statistical comparisons: all mutants compared to WT in each condition. (C) Growth curve of wildtype A5 and eDNA mutants in 7H9 broth. Absorbance at 595nm was read at day 0, 2, 4, and 6. Statistical comparisons are between WT and mutants. Data are representative of three independent experiments. Statistical comparisons: *, $P < 0.05$; **, $P < 0.005$, ***, $P < 0.0005$.

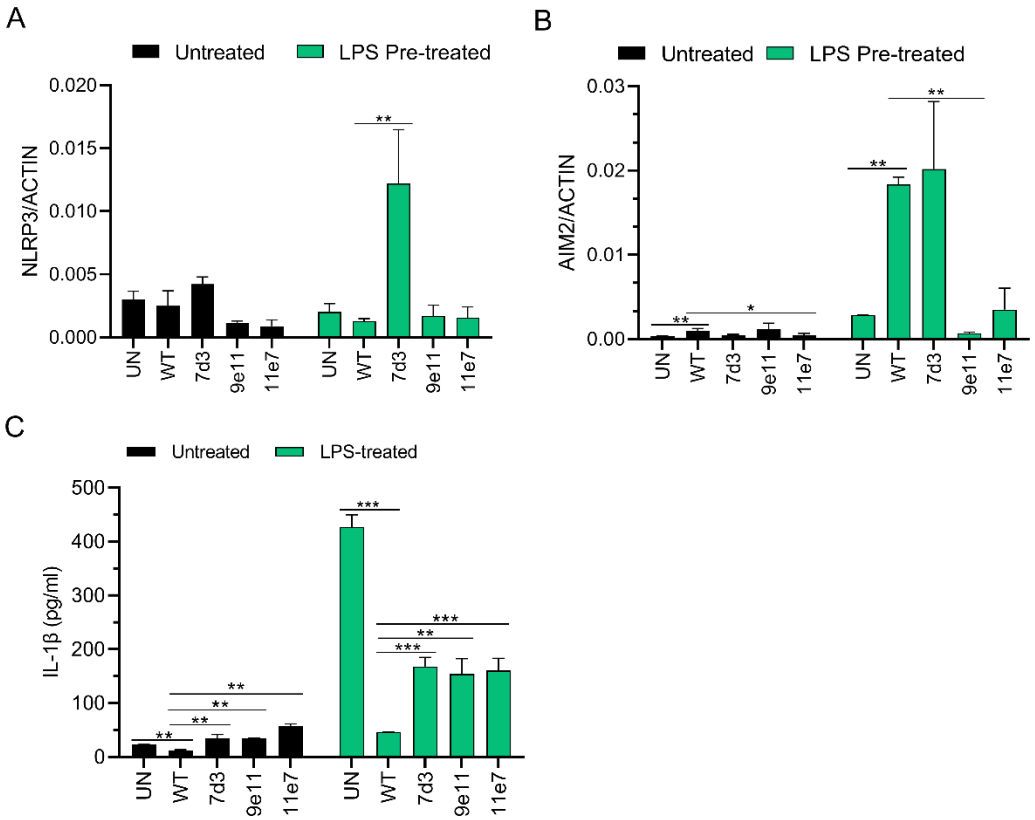

Figure 3.6. eDNA-deficient Mutants Alter IL-1β Secretion Through Inflammasome Pathways. THP-1 cells were stimulated with 10 ng/ml LPS for 2h prior to infection with *M. avium* A5 and eDNA-deficient mutants 7d3, 9e11, and 11e7. Supernatants and RNA were collected at 24 h.p.i. NLRP3 and AIM2 expression were quantified by qPCR and IL-1β levels were quantified by ELISA. (A) NLRP3 expression and (B) AIM2 expression by untreated and LPS pre-treated THP-1 cells (c) IL-1β secretion by untreated and LPS pre-treated THP-1 cells infected as describe above. Data are representative of three independent experiments. Statistical comparisons: *, $P < 0.05$; **, $P < 0.005$, ***, $P < 0.0005$.

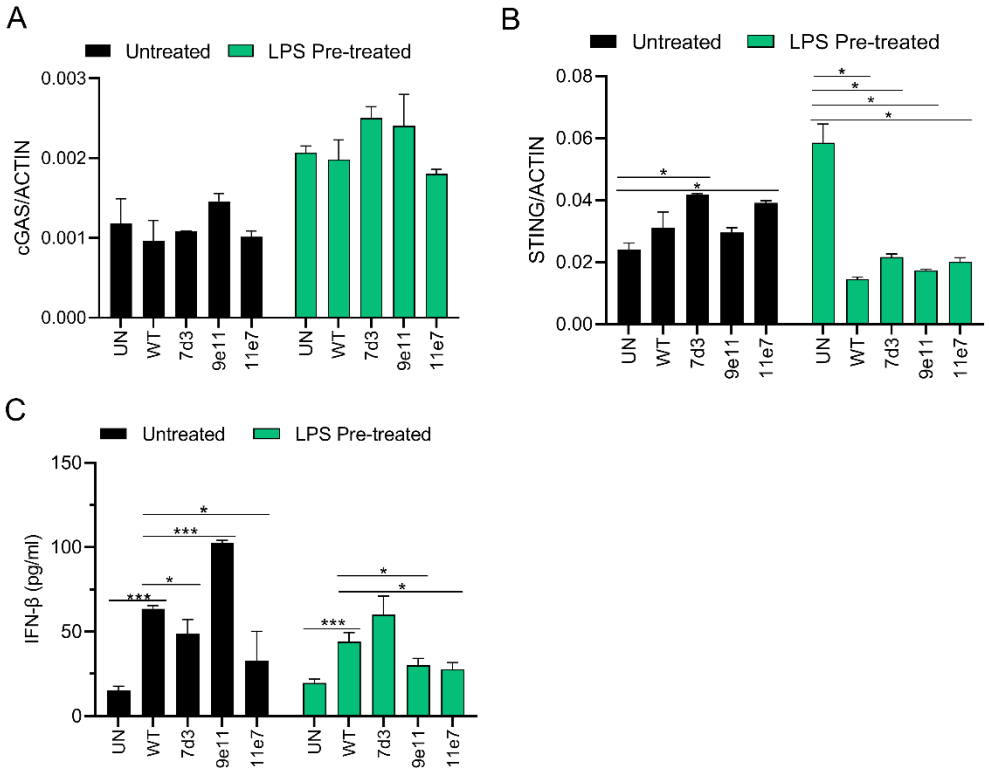

Figure 3.7. *M. avium* A5 eDNA-deficient Mutants Downregulate STING Expression in LPS stimulated Macrophages and Modulate IFN-β Production. Untreated and LPS-primed THP-1 cells were infected with *M. avium* A5 and eDNA-deficient mutants 7d3, 9e11, 11e7 and c11e7. The expression of cGAS and STING was quantified by qPCR and IFN-β levels were measured by ELISA at 24 h.p.i. (A) cGAS expression and (B) STING expression in untreated and LPS pre-treated THP-1 cells. (C) IFN-β levels in supernatants from untreated and LPS-primed THP-1 cells. Data are representative of three independent experiments. Statistical comparisons: *, $P < 0.05$; **, $P < 0.005$, ***, $P < 0.0005$.

Chapter 4

Discussion and Conclusions

Jayanthi J. Joseph

Overview

Nontuberculous mycobacteria (NTM) are ubiquitous in the environment and cause pulmonary and disseminated disease in humans. NTM exhibit a wide range of pathogenicity, with *M. abscessus*, *M. chelonae,* and *M. avium* being some of the most virulent species. NTM are opportunistic intracellular pathogens that utilize biofilms, host macrophages, granulomatous inflammation to maintain chronic infections. Biofilms act as environmental sources of infection, as well as drivers of persistence in the host. Macrophages are involved with bacterial replication, dissemination, and MGC formation. MGCs in mycobacterial granulomas retain phagocytic activity and contain high bacterial loads *in vivo*. Innate and adaptive pro-inflammatory signals contribute to granuloma formation during NTM infection, and this process begins in the macrophage. The research presented in this dissertation has contributed to the understanding of *M. avium* pathogenesis, specifically the role of eDNA in modulating the macrophage response, and interactions with multinucleated giant cells.

MGC Model

Limitations of current *in vitro* models necessitated the development of the novel MGC model presented in Chapter 2. Existing MGC models are complex, and involved multiple cell types, bacteria, and primary cells. The ability of MGCs to uptake bacteria is generally accepted by the literature, however early *in vitro* granuloma-focused models generated MGCs that exhibited restriction of cell-to-cell spread and loss of phagocytic activity. These models utilized primary lymphocytes, macrophages, and *M. tb* or BCG, and MGCs were only one component of the model (Brooks et al., 2019; Byrd, 1998; Gasser & Möst, 1999; Lay et al., 2007). These

models are expensive and difficult to scale up due to the use of primary cells. Also, the high level of complexity generated by utilizing multiple cell types, *M. tb,* and cytokines limits the application of these models in NTM research.

In contrast, recent MGC-focused models demonstrated that MGCs associated with mycobacterial granulomas are phagocytic and exhibit reduced intracellular killing (Y. Chen et al., 2022; Gharun et al., 2017; Lösslein et al., 2021). One such model utilized primary bovine macrophage and BCG or mycobacterial glycolipid lipomannan, to generate MGCs, and reported that nitric oxide was important for MGC formation. MGCs from this model exhibited increased phagocytosis of bacteria and apoptotic macrophages (Gharun et al., 2017). Another recent model utilized primary monocyte progenitors from mice stimulated with BCG lipomannan (Lösslein et al., 2021). MGCs from this model exhibited elevated cholesterol levels and were permissive to mycobacterial survival.

My model of MGCs improves upon existing models by utilizing a single cell line and recombinant cytokines, instead of specific bacterial species or antigens. This reduces the complexity of the model and increases the potential applications of the model. Unlike previous models, my MGC model can be used to study the MGC-bacterial interactions of a wider range of mycobacterial species, including NTM which tend to be overlooked by other models. Additionally, the components of my MGC model are readily available and can be scale up for larger experiments, which is difficult to do with primary cells and BSL-3 bacteria. MGCs generated by my model are similar to recent primary cell derived MGCs in that they are phagocytic, permissive to intracellular survival, and lipid rich. A limitation of my model is the

lower number of nuclei in MGCs produced by this method compared to other models that utilized *M. tb*. However, MGCs induced by *M. avium* infection tend to have fewer nuclei than *M. tb* or BCG MGCs, so this does not detract from the use of this model for NTM infections (Brodbeck & Anderson, 2009).

The Role of Multinucleated Giant Cells in Pathogenesis

MGCs are granuloma-associated cells and are of interest due to the high levels of intracellular bacteria observed during chronic NTM lung infections. In Chapter 3, I developed and characterize a novel *in vitro* model representing MGCs. To form MGCs, human THP-1 macrophages were stimulated with TNF-α and IFN-γ for five days to recreate conditions during granuloma formation. The role of MGCs within mycobacterial granulomas and their involvement in host-pathogen interactions is poorly understood. TNF-α and IFN-γ are required for granuloma formation in response to mycobacteria and are induced upon infection (Bean et al., 1999; Hogan et al., 2001). Additionally, IFN-γ is known to be involved in MGC formation (Sakai et al., 2012). MGC produced in this method contained multiple nuclei and were CD40 positive. MGCs from acute tuberculosis are CD40 positive and CD40 is involved in Langhans MGC formation (Brooks et al., 2019; Sakai et al., 2012, p. 40). They exhibited lipid droplet accumulation, elevated autophagic activity, and large size. *M. avium* was readily phagocytosed by the MGCs and replicated intracellularly at a higher rate than macrophages. *M. avium* was observe in autophagosomes and in autophagosomes interacting with lipid droplets. Interestingly, *M. avium* started leaving the MGC as early as 24 h.p.i by an unknown nonlytic mechanism. Perhaps the heightened autophagy renders the intracellular MGC environment more permissive than the macrophage.

However, the acquisition of host lipids could also explain the enhanced growth of *M. avium* in MGCs. Further characterization of the MGC model is needed to clarify the involvement of host lipids versus autophagy in intracellular survival. Lipidomic analysis of the lipid droplets that accumulate in MGCs and intracellular *M. avium*, could shed light onto the role of host lipids on intracellular survival. Additionally, measuring the expression of mycobacterial genes related to lipid metabolism could point to specific host lipids that are utilized by *M. avium* in the MGC. siRNA inhibition of autophagy could shed light on the role of autophagy in intracellular survival in MGCs. Understanding the mechanism of cell exit from MGCs and the implications for *M. avium* pathogenesis was the next step.

Mechanisms of Host Cell Exit and Cell-to-Cell Transmission

Pathogenic intracellular bacteria utilize a range of mechanisms for cell-to-cell transmission: membrane-dependent exit, host cell death, host cell lysis, or direct cell-to-cell transmission via actin-mediated protrusion (Flieger et al., n.d.). Bacteria that escape from the host cell to the extracellular space are free to infect neighboring cells. In most cases, intracellular bacteria that reside within vacuoles must enter the cytosol to trigger cell exit pathways. *Listeria monocytogenes* utilizes a cytolysin for lytic vacuolar escape (Flieger et al., n.d.). Cytosolic bacteria have been observed in *M. tb, M. marinum* and *M. leprae* infections, and phagosomal exit is lytic and ESX-1 dependent (Flieger et al., n.d., 2018; van der Niet et al., 2021, p. 1). Mycobacterial translocation from the phagosome to the cytosol in increased in immunocompromised hosts (van der Niet et al., 2021, p. 1).

In Chapter 2, cytosolic *M. avium* were observed in MGCs which indicates that *M. avium* can leave the vacuole by an ESX-1-independent mechanism. Mycobacteria utilize several pathways to exit host cells and further infection. *M. tb, M. abscessus* escape the host cell by triggering apoptotic or necrotic cell death, and by actin-mediated nonlytic ejection (Flieger et al., n.d.; Hagedorn et al., 2009). *M. marinum* is the only mycobacterial species that employs actin motility to facilitate direct cell to cell spread (Stamm et al., 2003). *M. avium* disrupts the actin filament network to prevent phagosome maturation and is therefore unable to utilize actin for cellular egress (Guérin & de Chastellier, 2000). A recent study revealed a novel nonlytic egress mechanism in *M. marinum* which involves ESX-1-independent mechanisms (Gerstenmaier et al., 2015). *M. marinum* enters the autophagic pathway, blocks autophagosome maturation, and is ejected from the host cell in a nonlytic manner (Gerstenmaier et al., 2015). *M. avium* triggers apoptosis to exit host macrophages, but does not employ actin-dependent ejection (Early et al., 2011; Hagedorn et al., 2009). Our observation of elevated autophagy in MGCs, together with autophagosomal and extracellular *M. avium,* suggests that *M. avium* may be using autophagy to leave the host cell without triggering cell death. It is possible that an alternative mechanism may be involved, given the fact that our understanding of MGC-*M. avium* interaction is still developing.

Describing the mechanism of exit utilized by *M. avium* in MGCs is an important topic for future research to explore. To unravel the potential involvement of autophagy in *M. avium* escape from MGCs, it would be useful to determine the effect of autophagy on bacterial escape, as well as intracellular localization of bacteria

through the inhibition of autophagy. Proteomic analysis of MGCs during *M. avium* infection could also shed light on the role of autophagy in this process. It would be exciting to uncover a novel exit mechanism previously undescribed in *M. avium*.

Cell-to-cell spreading is facilitated by bacterial exposure to the intracellular environment, which leads to phenotypic changes that aid in host cell entry and pathogenesis. Previous studies in *M. avium* have demonstrated that intracellular replication in macrophages increases the efficiency of uptake through complement receptor 3-mediated phagocytosis (L. E. Bermudez et al., 1997). In *M. paratuberculosis,* passage through epithelial cells generates an inflammatory phenotype, alters lipid composition, and increases intracellular growth in macrophages (Everman et al., n.d.; Phillips et al., 2021). In *M. tb* macrophage-passaged bacteria exhibited increased vacuolar fusion compared to non-passaged bacteria, indicating that growth within the host macrophage leads to a change in bacterial phenotype (McDonough et al., 2000). Several intracellular pathogens utilize this phenotypic change as a strategy for cell-to-cell spread but must escape the host cell before this can occur.

Once *M. avium* escapes from the host cell, it enters neighboring macrophage and monocytes. *M. avium* that leave human macrophages by triggering apoptosis are readily taken up by naïve macrophages (Early et al., 2011). A recent study demonstrated that interactions between mycobacterial phthiocerol dimycocerosate (PDIM) and host epithelial membranes influenced infectivity and blocked immune activation (Cambier et al., 2020). Additionally, PDIM facilitates phagosomal permeabilization which permits translocation of bacteria from the phagosome to

cytosol (Osman et al., 2020). Given the observed accumulation of lipids in intracellular *M. avium* in MGCs, the expression of LppX could explain the enhance uptake exhibited by MGC-passaged bacteria. Further characterization of the interactions between MGC-passaged bacteria and different types of host cells could shed light on the role of MGCs in cell-to-cell spread of *M. avium*.

The Interaction between *M. avium* and host Macrophages

The observation of cytosolic bacteria at early time points in MGCs is similar to what is known about *M. tb* intracellular stages in macrophages. Cytosolic *M. tb* eDNA activates several host pathways and triggers cytokine production in host macrophages. In Chapter 2, the objective was to assess the macrophage response to *M. avium* infection and examine the role of eDNA in survival in the host. I originally planned to study the host response in MGCs as well, but I faced significant technical and logistical barriers that prevented me from completing this work in MGCs. It was difficult to get a sufficient RNA from MGCs, but this was solved by scaling up the number of cells. However, due to the COVID-19 pandemic, supply chain issues made the use of larger amounts of reagents and materials unsustainable and time consuming. So, I decided move to MGCs after establishing the system in macrophages, which are the preferred host cell type of *M. avium*. Macrophages are the key innate immune cells involved in the response to mycobacterial infections and initiate the adaptive immune response by the secretion of pro-inflammatory cytokines and antigen presentation. To survive in the host, *M. avium* must evade detection by intracellular sensors of PAMPS and DAMPS to facilitate bacterial replication and prevent premature cell death. The balance of pro-inflammatory and anti-inflammatory

signals is a crucial part of *M. avium* pathogenesis and survival in the host. The NLRP3 and AIM2 inflammasomes are key innate immune system sensors that trigger inflammation during infection. Prolonged activation of inflammasomes can lead to bacterial clearance, cell death and tissue damage. Anti-inflammatory pathways work to temper inflammation and limit cell death. The DNA-sensing cGAS/STING pathway is one such pathway. The macrophage inflammatory response decides the intracellular fate of *M. avium* and eDNA is a crucial part of the equation. eDNA is a major structural component of mycobacterial biofilms. Although well-studied in *M. tb,* DNA export by intracellular *M. avium* has not been established. With the use of eDNA-deficient *M. avium* mutants I was able to utilize their differential DNA export to approach the problem from a different perspective.

In Chapter 2, I investigated the macrophage response to *M. avium* infection with a focus on the NLRP3 and AIM2 inflammasomes, and the cGAS/STING pathway. My research shows that *M. avium* activates the NLRP3 inflammasome immediately upon entry into the macrophage but possesses a mechanism to inhibit activation as infection progresses. *M. abscessus* and *M. kansasii* also activate the NLRP3 inflammasome and induce IL-1β production at early time points in the host macrophage (<18 h.p.i), which is similar to what we observed (C.-C. Chen et al., 2012; B.-R. Kim et al., 2020, p. 3). However, these studies did not go beyond 18 h.p.i, so the downregulation of NLRP3 during NTM remains undescribed in the literature. NLRP3 activation and IL-1β production is important for bacterial clearance during acute mycobacterial infections, however it may help maintain chronic infections by promoting bacterial spread. *M. kansasii,* an NTM, induces NLRP3

activation and IL-1β release early in infection, which restricts bacterial replication (C.-C. Chen et al., 2012). *M. tb* activation of NLRP3 has been demonstrated at later time points and can lead to pyroptosis of the host macrophage, which facilitates cell-to-cell spread of bacteria (Beckwith et al., 2020; Xu et al., 2020, p. 3). A possible mechanism for NLRP3 inhibition could be shared with *M. tb,* which inhibits NLRP3 activation by the indirect action of serine/threonine kinase F (PknF) (Rastogi et al., 2021b). *M. avium* possesses a homolog for *M. tb* PknF, MAVA5_13430 (PknB), which could be involved in NLRP3 suppression. An A5 transposon mutant of MAVA5_13430, mutant 9e11, induced significantly higher IL-1β secretion than wildtype A5, indicating that MAVA5_13430 may play a similar NLRP3 inhibitory role in *M. avium.* However, significant work is needed to confirm that MAVA5_13430 inhibits NLRP3 activation in *M. avium* infection. Nitric oxide (NO) is another possible mechanism for NLRP3 inhibition during *M. avium* infection. *M. avium* infection triggers nitric oxide (NO) production in macrophages. NO attenuates NLRP3 inflammasome activity at the post-translational level by direct S-nitrosylation (B. B. Mishra et al., 2013a). This may account for the some of the reduction in NLRP3 expression and activation observed in this chapter. However, more work is needed to confirm the involvement of NO in NLRP3 modulation during *M. avium* infection.

The AIM2 and cGAS/STING response to *M. avium* were used to investigate the role of eDNA in intracellular survival and modulation of the macrophage response. The involvement of the AIM2 inflammasome and cGAS/STING in NTM pathogenesis is not well described (Shah et al., 2013). In Chapter 2, I found that *M.*

avium strain A5 significantly upregulated AIM2 expression at 6 h.p.i compared to 104, but AIM2 expression was comparable at all other time points. Interestingly A5, but not 104, significantly upregulated Syk in the host macrophage. Syk phosphorylates inflammasome adaptor ASC, which is necessary for NLRP3 and AIM2 inflammasome oligomerization and activation (Lin et al., 2015). *M. abscessus* utilizes Syk to induce NLRP3 activation and like A5, is an avid DNA exporter in the biofilm. Potentially, the enhanced DNA export ability of A5 is involved in this upregulation. Although I investigated Syk expression because of its role in NLRP3 activation, my results suggest that it may be involved in AIM2 activation as well during *M. avium* infection. Future work utilizing NLRP3$^{-/-}$ and AIM2$^{-/-}$ cell lines can separate the involvement of each inflammasome in the macrophage response to *M. avium.*

IFN-β production, the result of cGAS/STING activation, was induced by *M. avium* infection of macrophages. This points to cGAS/STING activation and suggests that mycobacterial DNA is in the cytosol. eDNA-deficient mutants 7d3 and 11e7 induced significantly less IFN-β than WT A5, which supports the assertion that mycobacterial eDNA is involved in cGAS/STING activation during *M. avium* infection. However, WT A5 and the eDNA-deficient mutants did not significantly modify cGAS expression compared to uninfected cells. cGAS may sense eDNA at the bacterial cell surface, which may be part of the targeting mechanism for cGAS/STING-induced autophagy (N. Liu et al., 2022). Even a small amount of extracellular DNA on the bacterial surface may be sufficient to initiate this response, which explains why my DNA deficient mutants were able to induce cGAS expression

that was equivalent to WTA5. Interestingly, WT A5 and all three mutants suppressed the LPS-induced upregulation of STING. The upregulation of STING expression and activation leads to increased NLRP3 activation in macrophages, which could explain why high STING levels could be detrimental to bacterial survival (Ning et al., 2020, p. 3). Investigating the interaction of STING and NLRP3 during *M. avium* infection could help explain this observation.

All three eDNA-deficient A5 mutants were attenuated at intracellular survival in the macrophage and induced a strong IL-1β response independent of NLRP3 upregulation. Two of the mutants, 7d3 and 11e7, were attenuated at IFN-β production, which lends support to the idea that *M. avium* secretes eDNA intracellularly. Collectively, these data suggest that eDNA is involved in the intracellular survival of *M. tb* in macrophages and induces IFN-β production via cGAS/STING. However, the mutant-related data needs to be supplemented with data from complemented mutants to confirm that complementation of the affected gene re-establishes the wildtype phenotype.

Pathogenic bacteria have evolved different mechanisms to evade or induce cGAS/STING activation. Activation of cGAS/STING triggers autophagy in *Listeria monocytogenes, Legionella pneumophila,* and *Burkholderia pseudomallei* (N. Liu et al., 2022; Whiteley et al., 2017). *L. monocytogenes* and *L. pneumophila* inhibit autophagy and escape intracellular killing (Birmingham et al., 2007; Watson et al., 2015). Activation of cGAS/STING increases bacterial replication in *Brucella abortus* and *Staphylococcus aureus* infection. Intracellular cytosolic eDNA modulates the macrophage response to *M. tb* by inducing IFN-β production and autophagy, which

promote bacterial survival and dissemination. Conversely, *M. tb* is also able to evade cGAS/STING activation by inhibiting autophagy and decreasing cytosolic STING levels (Maphasa et al., 2021; Sun et al., 2020). This suggests that the role of cGAS/STING fluctuates during mycobacterial infection.

Current research is not in agreement about the host protective versus bacterial protective role of Type I Interferons in NTM infections. Recent studies demonstrated that *M. abscessus* induces NLRP3 and cGAS/STING activation, and that cGAS/STING-induced IFN-β suppresses NLRP3-induced IL-1β, thus contributing to bacterial survival (B.-R. Kim et al., 2020). This could explain my observation of increased IFN-β and decreased IL-1β at 24 h.p.i during *M. avium* infection. Another study described the utilization of IFN-β signaling for cell to cell spread by *M. abscessus* (B.-R. Kim et al., 2019). In contrast, IFN-β produced during *M. abscessus* infection increased nitric oxide, which led to reduced intracellular survival. However, the behavior of these pathways in acute infection is different than in chronic infections (Brady et al., 2018). The cGAS/STING pathway has been shown to be detrimental to the host during chronic viral infections, and beneficial to the host during acute viral infections. If pro-inflammatory pathways are activated over prolonged periods, the extensive cell death and tissue damage would lead to significant pathology and mortality. In chronic infections pro-inflammatory pathways are diminished to preserve host tissues (Kurtz et al., 2017; Wu et al., 2019).

Due to the technical limitations of ELISAs I was only able to analyze a few cytokines in this thesis. Future work could improve upon this by utilizing new technology such as the Luminex assay, which can analyze multiple cytokines

simultaneously. This would provide a much fuller picture of the macrophage response to *M. avium* infection. Investigating the regulation of NLRP3 and AIM2 inflammasome activation could be improved using proteomic analysis to determine post-translational modifications of the inflammasomes.

Understanding the modulation of the macrophage response by *M. avium* will help tune medical treatment to match the phase of infection. For example, macrolides, the typically antibiotic of choice for NTM infections, have immunomodulatory effects on the host. Macrolides azithromycin, clarithromycin, roxithromycin, and erythromycin have been shown to reduce TNF-α, IL-1β, IL-12, IL-6, and IFN-γ levels in the host (Gualdoni et al., 2015; Kanoh & Rubin, 2010; Zimmermann et al., 2018). Early treatment with macrolides might inhibit granuloma formation and aid bacterial clearance. Although most NTM infections are not diagnosed until they become chronic, but advances in diagnostics may allow for the treatment of acute NTM infections in the future.

Conclusions and Future Directions

Our understanding immunomodulatory capacity of *M. avium* continues to deepen, however there still aspects of *M. avium*-host interactions that require further investigation. In this dissertation, I revealed the ability of *M. avium* to modulate host inflammasome and cGAS/STING expression, and subsequent IL-1β and IFN-β release. Additionally, I uncovered a potential role for eDNA in intracellular survival and immunomodulation in host macrophages. Finally, I established and characterized a novel MGC model which I used to investigate the role of MGCs *M. avium*

pathogenesis. The work presented in this dissertation has paved the way for future research in *M. avium* immunomodulation and escape from MGCs

The work presented in Chapter 3 revealed an immunomodulatory role of *M. avium* eDNA in the macrophage. An important next step is to investigate the inflammasome response to *M. avium* in MGCs, and to characterize the involvement of cGAS/STING and eDNA in this cell type. This especially interesting because of the observed upregulation of autophagy in MGCs during early infection. Autophagy suppresses the cGAS/STING pathway in a Beclin-1-mediated mechanism, which make it likely that the MGC response will be different than the macrophage response to *M. avium* (Xiong et al., 2018). The MGC model established in this dissertation will be a useful tool to accomplish this.

In Chapter 2, I developed and characterizer an *in vitro* model of MGCs which allowed me to investigate MGC-mycobacterial interactions. My work revealed that MGCs are permissive to intracellular survival and growth of *M. avium*, and host lipids and autophagy may be involved in the creation of the permissive environment. Additionally, MGCs may aid the cell-to-cell spread of bacteria in granulomas. My observation that *M. avium* escapes from MGCs in high numbers early in infection revealed a key difference between MGCs and macrophages. *M. avium* typically leaves host macrophages later in infection, and immediately triggers apoptosis in neighboring macrophages. In contrast, *M. avium* that escape from MGCs do not induce apoptosis in macrophages. By acting as a source for *M. avium*, MGCs could promote maintenance of chronic infection. The characterization of MGC-passaged bacteria is a new and exciting avenue for future research in *M. avium* pathogenesis.

Investigating the inflammatory response to MGC-passaged bacteria in naïve macrophages could further illuminate the involvement of MGCs in *M. avium* infections.

Bibliography

Aghbali, A., Rafieyan, S., Mohamed-Khosroshahi, L., Baradaran, B., Shanehbandi, D., & Kouhsoltani, M. (2017). IL-4 induces the formation of multinucleated giant cells and expression of β5 integrin in central giant cell lesion. *Medicina Oral, Patología Oral y Cirugía Bucal*, *22*(1), e1–e6. https://doi.org/10.4317/medoral.20935

Ahn, C. H., McLarty, J. W., Ahn, S. S., Ahn, S. I., & Hurst, G. A. (1982). Diagnostic Criteria for Pulmonary Disease Caused by Mycobacterium kansasii and Mycobacterium intracellulare. *American Review of Respiratory Disease*, *125*(4), 388–391. https://doi.org/10.1164/arrd.1982.125.4.388

Amaral, E. P., Riteau, N., Moayeri, M., Maier, N., Mayer-Barber, K. D., Pereira, R. M., Lage, S. L., Kubler, A., Bishai, W. R., D'Império-Lima, M. R., Sher, A., & Andrade, B. B. (2018). Lysosomal Cathepsin Release Is Required for NLRP3-Inflammasome Activation by Mycobacterium tuberculosis in Infected Macrophages. *Frontiers in Immunology*, *9*, 1427. https://doi.org/10.3389/fimmu.2018.01427

Anderson, J. M., Rodriguez, A., & Chang, D. T. (2008). Foreign body reaction to biomaterials. *Seminars in Immunology*, *20*(2), 86–100. https://doi.org/10.1016/j.smim.2007.11.004

Appelberg, R. (2006). Pathogenesis of Mycobacterium avium infection. *Immunologic Research*, *35*(3), 179–190. https://doi.org/10.1385/IR:35:3:179

Appelberg, R., & Orme, I. M. (1993). Effector mechanisms involved in cytokine-mediated bacteriostasis of Mycobacterium avium infections in murine macrophages. *Immunology*, *80*(3), 352–359.

Aronson, T., Holtzman, A., Glover, N., Boian, M., Froman, S., Berlin, O. G. W., Hill, H., & Stelma, G. (1999). Comparison of Large Restriction Fragments of Mycobacterium avium Isolates Recovered from AIDS and Non-AIDS Patients with Those of Isolates from Potable Water. *Journal of Clinical Microbiology*, *37*(4), 1008–1012.

Arora, G., Sajid, A., Gupta, M., Bhaduri, A., Kumar, P., Basu-Modak, S., & Singh, Y. (2010). Understanding the Role of PknJ in Mycobacterium tuberculosis: Biochemical Characterization and Identification of Novel Substrate Pyruvate Kinase A. *PLoS ONE*, *5*(5), e10772. https://doi.org/10.1371/journal.pone.0010772

Ates, L. S., Woude, A. D. van der, Bestebroer, J., Stempvoort, G. van, Musters, R. J. P., Garcia-Vallejo, J. J., Picavet, D. I., Weerd, R. van de, Maletta, M., Kuijl, C. P., Wel, N. N. van der, & Bitter, W. (2016). The ESX-5 System of Pathogenic Mycobacteria Is Involved In Capsule Integrity and Virulence through Its Substrate PPE10. *PLOS Pathogens*, *12*(6), e1005696. https://doi.org/10.1371/journal.ppat.1005696

Balcewicz-Sablinska, M. K., Gan, H., & Remold, H. G. (1999). Interleukin 10 Produced by Macrophages Inoculated with Mycobacterium avium Attenuates Mycobacteria-Induced Apoptosis by Reduction of TNF-α Activity. *The Journal of Infectious Diseases*, *180*(4), 1230–1237. https://doi.org/10.1086/315011

Be, N. A., Bishai, W. R., & Jain, S. K. (2012). Role of Mycobacterium tuberculosis pknD in the Pathogenesis of central nervous system tuberculosis. *BMC Microbiology*, *12*, 7. https://doi.org/10.1186/1471-2180-12-7

Bean, A. G., Roach, D. R., Briscoe, H., France, M. P., Korner, H., Sedgwick, J. D., & Britton, W. J. (1999). Structural deficiencies in granuloma formation in TNF gene-targeted mice underlie the heightened susceptibility to aerosol Mycobacterium tuberculosis infection, which is not compensated for by lymphotoxin. *Journal of Immunology (Baltimore, Md.: 1950)*, *162*(6), 3504–3511.

Beckwith, K. S., Beckwith, M. S., Ullmann, S., Sætra, R. S., Kim, H., Marstad, A., Åsberg, S. E., Strand, T. A., Haug, M., Niederweis, M., Stenmark, H. A., & Flo, T. H. (2020). Plasma membrane damage causes NLRP3 activation and pyroptosis during Mycobacterium tuberculosis infection. *Nature Communications*, *11*(1), 2270. https://doi.org/10.1038/s41467-020-16143-6

Bermudez, L. E., & Champsi, J. (1993). Infection with Mycobacterium avium induces production of interleukin-10 (IL-10), and administration of anti-IL-10 antibody is associated with enhanced resistance to infection in mice. *Infection and Immunity*, *61*(7), 3093–3097. https://doi.org/10.1128/iai.61.7.3093-3097.1993

Bermudez, L. E., Early, J., & Danelishvili, L. (2006). Mycobacteria and Macrophage Apoptosis: Complex Struggle for Survival. *Microbe Magazine*, *1*(8), 372–375. https://doi.org/10.1128/microbe.1.372.1

Bermudez, L. E., Goodman, J., & Petrofsky, M. (1999). Role of Complement Receptors in Uptake ofMycobacterium avium by Macrophages In Vivo: Evidence from Studies Using CD18-Deficient Mice. *Infection and Immunity*, *67*(9), 4912–4916. https://doi.org/10.1128/IAI.67.9.4912-4916.1999

Bermudez, L. E. M., & Young, L. S. (1989). Oxidative and non-oxidative intracellular killing of Mycobacterium avium complex. *Microbial Pathogenesis*, *7*(4), 289–298. https://doi.org/10.1016/0882-4010(89)90047-8

Bermudez, L. E., Parker, A., & Goodman, J. R. (1997). Growth within macrophages increases the efficiency of Mycobacterium avium in invading other macrophages by a complement receptor-independent pathway. *Infection and Immunity*, *65*(5), 1916–1925.

Bermudez, L. E., Petrofsky, M., & Sangari, F. (2004). Intracellular phenotype of Mycobacterium avium enters macrophages primarily by a macropinocytosis-

like mechanism and survives in a compartment that differs from that with extracellular phenotype. *Cell Biology International*, *28*(5), 411–419. https://doi.org/10.1016/j.cellbi.2004.03.010

Bermudez, L. E., Wu, M., & Young, L. S. (1995). Interleukin-12-stimulated natural killer cells can activate human macrophages to inhibit growth of Mycobacterium avium. *Infection and Immunity*, *63*(10), 4099–4104. https://doi.org/10.1128/iai.63.10.4099-4104.1995

Biasizzo, M., & Kopitar-Jerala, N. (2020). Interplay Between NLRP3 Inflammasome and Autophagy. *Frontiers in Immunology*, *11*. https://doi.org/10.3389/fimmu.2020.591803

Birmingham, C. L., Canadien, V., Gouin, E., Troy, E. B., Yoshimori, T., Cossart, P., Higgins, D. E., & Brumell, J. H. (2007). Listeria monocytogenes Evades Killing by Autophagy During Colonization of Host Cells. *Autophagy*, *3*(5), 442–451. https://doi.org/10.4161/auto.4450

Birmingham, C. L., Smith, A. C., Bakowski, M. A., Yoshimori, T., & Brumell, J. H. (2006). Autophagy Controls Salmonella Infection in Response to Damage to the Salmonella-containing Vacuole*. *Journal of Biological Chemistry*, *281*(16), 11374–11383. https://doi.org/10.1074/jbc.M509157200

Bottai, D., Di Luca, M., Majlessi, L., Frigui, W., Simeone, R., Sayes, F., Bitter, W., Brennan, M. J., Leclerc, C., Batoni, G., Campa, M., Brosch, R., & Esin, S. (2012). Disruption of the ESX-5 system of Mycobacterium tuberculosis causes loss of PPE protein secretion, reduction of cell wall integrity and strong attenuation. *Molecular Microbiology*, *83*(6), 1195–1209. https://doi.org/10.1111/j.1365-2958.2012.08001.x

Boxx, G. M., & Cheng, G. (2016). The Roles of Type I Interferon in Bacterial Infection. *Cell Host & Microbe*, *19*(6), 760–769. https://doi.org/10.1016/j.chom.2016.05.016

Brady, R. A., Mocca, C. P., Plaut, R. D., Takeda, K., & Burns, D. L. (2018). Comparison of the immune response during acute and chronic Staphylococcus aureus infection. *PLoS ONE*, *13*(3), e0195342. https://doi.org/10.1371/journal.pone.0195342

Braune, J., Lindhorst, A., Fröba, J., Hobusch, C., Kovacs, P., Blüher, M., Eilers, J., Bechmann, I., & Gericke, M. (2021). Multinucleated Giant Cells in Adipose Tissue Are Specialized in Adipocyte Degradation. *Diabetes*, *70*(2), 538–548. https://doi.org/10.2337/db20-0293

Briken, V., Ahlbrand, S. E., & Shah, S. (2013). Mycobacterium tuberculosis and the host cell inflammasome: A complex relationship. *Frontiers in Cellular and Infection Microbiology*, *3*, 62. https://doi.org/10.3389/fcimb.2013.00062

Brodbeck, W. G., & Anderson, J. M. (2009). GIANT CELL FORMATION AND FUNCTION. *Current Opinion in Hematology*, *16*(1), 53–57. https://doi.org/10.1097/MOH.0b013e32831ac52e

Brodin, P., Majlessi, L., Marsollier, L., de Jonge, M. I., Bottai, D., Demangel, C., Hinds, J., Neyrolles, O., Butcher, P. D., Leclerc, C., Cole, S. T., & Brosch, R. (2006). Dissection of ESAT-6 System 1 of Mycobacterium tuberculosis and Impact on Immunogenicity and Virulence. *Infection and Immunity*, *74*(1), 88–98. https://doi.org/10.1128/IAI.74.1.88-98.2006

Brooks, P. J., Glogauer, M., & McCulloch, C. A. (2019). An Overview of the Derivation and Function of Multinucleated Giant Cells and Their Role in Pathologic Processes. *The American Journal of Pathology*, *189*(6), 1145–1158. https://doi.org/10.1016/j.ajpath.2019.02.006

Burdette, D. L., & Vance, R. E. (2013). STING and the innate immune response to nucleic acids in the cytosol. *Nature Immunology*, *14*(1), 19–26. https://doi.org/10.1038/ni.2491

Byrd, T. F. (1998). Multinucleated giant cell formation induced by IFN-gamma/IL-3 is associated with restriction of virulent Mycobacterium tuberculosis cell to cell invasion in human monocyte monolayers. *Cellular Immunology*, *188*(2), 89–96. https://doi.org/10.1006/cimm.1998.1352

Cambier, C., Banik, S. M., Buonomo, J. A., & Bertozzi, C. R. (2020). Spreading of a mycobacterial cell-surface lipid into host epithelial membranes promotes infectivity. *ELife*, *9*, e60648. https://doi.org/10.7554/eLife.60648

Casabon, I., Swain, K., Crowe, A. M., Eltis, L. D., & Mohn, W. W. (2014). Actinobacterial Acyl Coenzyme A Synthetases Involved in Steroid Side-Chain Catabolism. *Journal of Bacteriology*, *196*(3), 579–587. https://doi.org/10.1128/JB.01012-13

Castro, F., Cardoso, A. P., Gonçalves, R. M., Serre, K., & Oliveira, M. J. (2018). Interferon-Gamma at the Crossroads of Tumor Immune Surveillance or Evasion. *Frontiers in Immunology*, *9*. https://www.frontiersin.org/article/10.3389/fimmu.2018.00847

Chakraborty, P., Bajeli, S., Kaushal, D., Radotra, B. D., & Kumar, A. (2021). Biofilm formation in the lung contributes to virulence and drug tolerance of Mycobacterium tuberculosis. *Nature Communications*, *12*, 1606. https://doi.org/10.1038/s41467-021-21748-6

Chen, C.-C., Tsai, S.-H., Lu, C.-C., Hu, S.-T., Wu, T.-S., Huang, T.-T., Saïd-Sadier, N., Ojcius, D. M., & Lai, H.-C. (2012). Activation of an NLRP3 Inflammasome Restricts Mycobacterium kansasii Infection. *PLOS ONE*, *7*(4), e36292. https://doi.org/10.1371/journal.pone.0036292

Chen, Y., Jiang, H., Xiong, J., Shang, J., Chen, Z., Wu, A., & Wang, H. (2022). Insight into the Molecular Characteristics of Langhans Giant Cell by

Combination of Laser Capture Microdissection and RNA Sequencing. *Journal of Inflammation Research*, *15*, 621–634. https://doi.org/10.2147/JIR.S337241

Clay, H., Davis, J. M., Beery, D., Huttenlocher, A., Lyons, S. E., & Ramakrishnan, L. (2007). Dichotomous Role of the Macrophage in Early Mycobacterium marinum Infection of the Zebrafish. *Cell Host & Microbe*, *2*(1), 29–39. https://doi.org/10.1016/j.chom.2007.06.004

Coclet-Ninin, J., & Burger, J.-M. D. and D. (1997). Interferon-beta not only inhibits interleukin-1α and tumor necrosis factor-α but stimulates interleukin-1 receptor antagonist production in human peripheral blood mononuclear cells. *European Cytokine Network*, *8*(4), 345–349.

Cohen, S. B., Gern, B. H., Delahaye, J. L., Adams, K. N., Plumlee, C. R., Winkler, J. K., Sherman, D. R., Gerner, M. Y., & Urdahl, K. B. (2018). Alveolar Macrophages Provide an Early Mycobacterium tuberculosis Niche and Initiate Dissemination. *Cell Host & Microbe*, *24*(3), 439-446.e4. https://doi.org/10.1016/j.chom.2018.08.001

Corthay, A., Skovseth, D. K., Lundin, K. U., Røsjø, E., Omholt, H., Hofgaard, P. O., Haraldsen, G., & Bogen, B. (2005). Primary Antitumor Immune Response Mediated by CD4+ T Cells. *Immunity*, *22*(3), 371–383. https://doi.org/10.1016/j.immuni.2005.02.003

Cosma, C. L., Humbert, O., & Ramakrishnan, L. (2004). Superinfecting mycobacteria home to established tuberculous granulomas. *Nature Immunology*, *5*(8), 828–835. https://doi.org/10.1038/ni1091

Cronan, M. R., Beerman, R. W., Rosenberg, A. F., Saelens, J. W., Johnson, M. G., Oehlers, S. H., Sisk, D. M., Jurcic Smith, K. L., Medvitz, N. A., Miller, S. E., Trinh, L. A., Fraser, S. E., Madden, J. F., Turner, J., Stout, J. E., Lee, S., & Tobin, D. M. (2016). Macrophage Epithelial Reprogramming Underlies Mycobacterial Granuloma Formation and Promotes Infection. *Immunity*, *45*(4), 861–876. https://doi.org/10.1016/j.immuni.2016.09.014

Dale, A. G., Porcu, A., Mann, J., & Neidle, S. (2022). The mechanism of resistance in Escherichia coli to ridinilazole and other antibacterial head-to-head bis-benzimidazole compounds. *Medicinal Chemistry Research*, *31*(7), 1176–1191. https://doi.org/10.1007/s00044-022-02918-7

Daleke, M. H., Cascioferro, A., Punder, K. de, Ummels, R., Abdallah, A. M., Wel, N. van der, Peters, P. J., Luirink, J., Manganelli, R., & Bitter, W. (2011). Conserved Pro-Glu (PE) and Pro-Pro-Glu (PPE) Protein Domains Target LipY Lipases of Pathogenic Mycobacteria to the Cell Surface via the ESX-5 Pathway *. *Journal of Biological Chemistry*, *286*(21), 19024–19034. https://doi.org/10.1074/jbc.M110.204966

Danelishvili, L., Poort, M. J., & Bermudez, L. E. (2004). Identification of Mycobacterium avium genes up-regulated in cultured macrophages and in

mice. *FEMS Microbiology Letters*, *239*(1), 41–49. https://doi.org/10.1016/j.femsle.2004.08.014

Danelishvili, L., Rojony, R., Carson, K. L., Palmer, A. L., Rose, S. J., & Bermudez, L. E. (2018). Mycobacterium avium subsp. Hominissuis effector MAVA5_06970 promotes rapid apoptosis in secondary-infected macrophages during cell-to-cell spread. *Virulence*, *9*(1), 1287–1300. https://doi.org/10.1080/21505594.2018.1504559

Daniel, J., Sirakova, T., & Kolattukudy, P. (2014). An Acyl-CoA Synthetase in Mycobacterium tuberculosis Involved in Triacylglycerol Accumulation during Dormancy. *PLoS ONE*, *9*(12), e114877. https://doi.org/10.1371/journal.pone.0114877

Davis, J. M., & Ramakrishnan, L. (2009). The Role of the Granuloma in Expansion and Dissemination of Early Tuberculous Infection. *Cell*, *136*(1), 37–49. https://doi.org/10.1016/j.cell.2008.11.014

Deng, Q., Wang, Y., Zhang, Y., Li, M., Li, D., Huang, X., Wu, Y., Pu, J., & Wu, M. (2016). Pseudomonas aeruginosa Triggers Macrophage Autophagy To Escape Intracellular Killing by Activation of the NLRP3 Inflammasome. *Infection and Immunity*, *84*(1), 56–66. https://doi.org/10.1128/IAI.00945-15

Doherty, T. M., & Sher, A. (1998). IL-12 Promotes Drug-Induced Clearance of Mycobacterium avium Infection in Mice. *The Journal of Immunology*, *160*(11), 5428–5435.

Doi, T., Ando, M., Akaike, T., Suga, M., Sato, K., & Maeda, H. (1993). Resistance to nitric oxide in Mycobacterium avium complex and its implication in pathogenesis. *Infection and Immunity*, *61*(5), 1980–1989. https://doi.org/10.1128/iai.61.5.1980-1989.1993

Early, J., Fischer, K., & Bermudez, L. E. (2011). Mycobacterium avium uses apoptotic macrophages as tools for spreading. *Microbial Pathogenesis*, *50*(2), 132–139. https://doi.org/10.1016/j.micpath.2010.12.004

Egelund, E. F., Fennelly, K. P., & Peloquin, C. A. (2015). Medications and Monitoring in Nontuberculous Mycobacteria Infections. *Clinics in Chest Medicine*, *36*(1), 55–66. https://doi.org/10.1016/j.ccm.2014.11.001

Ehlers, S., & Schaible, U. (2013). The Granuloma in Tuberculosis: Dynamics of a Host–Pathogen Collusion. *Frontiers in Immunology*, *3*. https://www.frontiersin.org/article/10.3389/fimmu.2012.00411

Epstein, W. L., & Fukuyama, K. (1989). Mechanisms of granulomatous inflammation. *Immunology Series*, *46*, 687–721.

Everman, J. L., Eckstein, T. M., Roussey, J., Coussens, P., Bannantine, J. P., & Bermudez, L. E. Y. 2015. (n.d.). Characterization of the inflammatory phenotype of Mycobacterium avium subspecies paratuberculosis using a novel

cell culture passage model. *Microbiology*, *161*(7), 1420–1434. https://doi.org/10.1099/mic.0.000106

Fais, S., Burgio, V. L., Silvestri, M., Capobianchi, M. R., Pacchiarotti, A., & Pallone, F. (1994). Multinucleated giant cells generation induced by interferon-gamma. Changes in the expression and distribution of the intercellular adhesion molecule-1 during macrophages fusion and multinucleated giant cell formation. *Laboratory Investigation; a Journal of Technical Methods and Pathology*, *71*(5), 737–744.

Flieger, A., Frischknecht, F., Häcker, G., Hornef, M. W., & Pradel, G. (n.d.). Pathways of host cell exit by intracellular pathogens. *Microbial Cell*, *5*(12), 525–544. https://doi.org/10.15698/mic2018.12.659

Freeman, R., Geier, H., Weigel, K. M., Do, J., Ford, T. E., & Cangelosi, G. A. (2006). Roles for Cell Wall Glycopeptidolipid in Surface Adherence and Planktonic Dispersal of Mycobacterium avium. *Applied and Environmental Microbiology*, *72*(12), 7554–7558. https://doi.org/10.1128/AEM.01633-06

Frehel, C., de Chastellier, C., Lang, T., & Rastogi, N. (1986). Evidence for inhibition of fusion of lysosomal and prelysosomal compartments with phagosomes in macrophages infected with pathogenic Mycobacterium avium. *Infection and Immunity*, *52*(1), 252–262.

Gago, G., Diacovich, L., & Gramajo, H. (2018). Lipid metabolism and its implication in mycobacteria-host interaction. *Current Opinion in Microbiology*, *41*, 36–42. https://doi.org/10.1016/j.mib.2017.11.020

Gallegos, M. T., Schleif, R., Bairoch, A., Hofmann, K., & Ramos, J. L. (1997). Arac/XylS family of transcriptional regulators. *Microbiology and Molecular Biology Reviews*, *61*(4), 393–410. https://doi.org/10.1128/mmbr.61.4.393-410.1997

Gasser, A., & Möst, J. (1999). Generation of Multinucleated Giant Cells In Vitro by Culture of Human Monocytes with Mycobacterium bovis BCG in Combination with Cytokine-Containing Supernatants. *Infection and Immunity*, *67*(1), 395–402. https://doi.org/10.1128/IAI.67.1.395-402.1999

Gebert, M. J., Delgado-Baquerizo, M., Oliverio, A. M., Webster, T. M., Nichols, L. M., Honda, J. R., Chan, E. D., Adjemian, J., Dunn, R. R., & Fierer, N. (2018). Ecological Analyses of Mycobacteria in Showerhead Biofilms and Their Relevance to Human Health. *MBio*, *9*(5), e01614-18. https://doi.org/10.1128/mBio.01614-18

Gerstenmaier, L., Pilla, R., Herrmann, L., Herrmann, H., Prado, M., Villafano, G. J., Kolonko, M., Reimer, R., Soldati, T., King, J. S., & Hagedorn, M. (2015). The autophagic machinery ensures nonlytic transmission of mycobacteria. *Proceedings of the National Academy of Sciences*, *112*(7), E687–E692. https://doi.org/10.1073/pnas.1423318112

Gharun, K., Senges, J., Seidl, M., Lösslein, A., Kolter, J., Lohrmann, F., Fliegauf, M., Elgizouli, M., Vavra, M., Schachtrup, K., Illert, A. L., Gilleron, M., Kirschning, C. J., Triantafyllopoulou, A., & Henneke, P. (2017). Mycobacteria exploit nitric oxide-induced transformation of macrophages into permissive giant cells. *EMBO Reports*, e201744121. https://doi.org/10.15252/embr.201744121

Glick, D., Barth, S., & Macleod, K. F. (2010). Autophagy: Cellular and molecular mechanisms. *The Journal of Pathology*, *221*(1), 3–12. https://doi.org/10.1002/path.2697

Gomes, M. S., Flórido, M., Pais, T. F., & Appelberg, R. (1999). Improved Clearance of Mycobacterium avium Upon Disruption of the Inducible Nitric Oxide Synthase Gene. *The Journal of Immunology*, *162*(11), 6734–6739.

Gopalaswamy, R., Narayanan, S., Chen, B., Jacobs, W. R., & Av-Gay, Y. (2009). The serine/threonine protein kinase PknI controls the growth of Mycobacterium tuberculosis upon infection. *FEMS Microbiology Letters*, *295*(1), 23–29. https://doi.org/10.1111/j.1574-6968.2009.01570.x

Greenwell-Wild, T., Vázquez, N., Sim, D., Schito, M., Chatterjee, D., Orenstein, J. M., & Wahl, S. M. (2002). Mycobacterium avium Infection and Modulation of Human Macrophage Gene Expression. *The Journal of Immunology*, *169*(11), 6286–6297. https://doi.org/10.4049/jimmunol.169.11.6286

Griffith, D. E., Aksamit, T., Brown-Elliott, B. A., Catanzaro, A., Daley, C., Gordin, F., Holland, S. M., Horsburgh, R., Huitt, G., Iademarco, M. F., Iseman, M., Olivier, K., Ruoss, S., von Reyn, C. F., Wallace, R. J., & Winthrop, K. (2007). An Official ATS/IDSA Statement: Diagnosis, Treatment, and Prevention of Nontuberculous Mycobacterial Diseases. *American Journal of Respiratory and Critical Care Medicine*, *175*(4), 367–416. https://doi.org/10.1164/rccm.200604-571ST

Gritsenko, A., Yu, S., Martin-Sanchez, F., Diaz-del-Olmo, I., Nichols, E.-M., Davis, D. M., Brough, D., & Lopez-Castejon, G. (2020). Priming Is Dispensable for NLRP3 Inflammasome Activation in Human Monocytes In Vitro. *Frontiers in Immunology*, *11*. https://www.frontiersin.org/article/10.3389/fimmu.2020.565924

Grundner, C., Gay, L. M., & Alber, T. (2005). Mycobacterium tuberculosis serine/threonine kinases PknB, PknD, PknE, and PknF phosphorylate multiple FHA domains. *Protein Science : A Publication of the Protein Society*, *14*(7), 1918–1921. https://doi.org/10.1110/ps.051413405

Gualdoni, G. A., Lingscheid, T., Schmetterer, K. G., Hennig, A., Steinberger, P., & Zlabinger, G. J. (2015). Azithromycin inhibits IL-1 secretion and non-canonical inflammasome activation. *Scientific Reports*, *5*, 12016. https://doi.org/10.1038/srep12016

Guarda, G., Braun, M., Staehli, F., Tardivel, A., Mattmann, C., Förster, I., Farlik, M., Decker, T., Du Pasquier, R. A., Romero, P., & Tschopp, J. (2011). Type I Interferon Inhibits Interleukin-1 Production and Inflammasome Activation. *Immunity*, *34*(2), 213–223. https://doi.org/10.1016/j.immuni.2011.02.006

Guérin, I., & de Chastellier, C. (2000). Pathogenic Mycobacteria Disrupt the Macrophage Actin Filament Network. *Infection and Immunity*, *68*(5), 2655–2662. https://doi.org/10.1128/IAI.68.5.2655-2662.2000

Guo, H., Callaway, J. B., & Ting, J. P.-Y. (2015). Inflammasomes: Mechanism of action, role in disease, and therapeutics. *Nature Medicine*, *21*(7), 677–687. https://doi.org/10.1038/nm.3893

Gutierrez, M. G., Mishra, B. B., Jordao, L., Elliott, E., Anes, E., & Griffiths, G. (2008). NF-κB Activation Controls Phagolysosome Fusion-Mediated Killing of Mycobacteria by Macrophages. *The Journal of Immunology*, *181*(4), 2651–2663. https://doi.org/10.4049/jimmunol.181.4.2651

Hagedorn, M., Rohde, K. H., Russell, D. G., & Soldati, T. (2009). Infection by Tubercular Mycobacteria Is Spread by Nonlytic Ejection from Their Amoeba Hosts. *Science*, *323*(5922), 1729–1733. https://doi.org/10.1126/science.1169381

Hara, H., Tsuchiya, K., Kawamura, I., Fang, R., Hernandez-Cuellar, E., Shen, Y., Mizuguchi, J., Schweighoffer, E., Tybulewicz, V., & Mitsuyama, M. (2013). Phosphorylation of the adaptor ASC acts as a molecular switch that controls the formation of speck-like aggregates and inflammasome activity. *Nature Immunology*, *14*(12), 1247–1255. https://doi.org/10.1038/ni.2749

Härmälä, A.-S., Pörn, M. I., Mattjus, P., & Slotte, J. P. (1994). Cholesterol transport from plasma membranes to intracellular membranes is inhibited by 3β-[2-(diethylamino) ethoxy]androst-5-en-17-one. *Biochimica et Biophysica Acta (BBA) - Lipids and Lipid Metabolism*, *1211*(3), 317–325. https://doi.org/10.1016/0005-2760(94)90156-2

Harmsen, M., Lappann, M., Knøchel, S., & Molin, S. (2010). Role of Extracellular DNA during Biofilm Formation by Listeria monocytogenes. *Applied and Environmental Microbiology*, *76*(7), 2271–2279. https://doi.org/10.1128/AEM.02361-09

Healy, C., Golby, P., MacHugh, D. E., & Gordon, S. V. (2016). The MarR family transcription factor Rv1404 coordinates adaptation of Mycobacterium tuberculosis to acid stress via controlled expression of Rv1405c, a virulence-associated methyltransferase. *Tuberculosis (Edinburgh, Scotland)*, *97*, 154–162. https://doi.org/10.1016/j.tube.2015.10.003

Hogan, L. H., Markofski, W., Bock, A., Barger, B., Morrissey, J. D., & Sandor, M. (2001). Mycobacterium bovis BCG-induced granuloma formation depends on gamma interferon and CD40 ligand but does not require CD28. *Infection and*

Immunity, *69*(4), 2596–2603. https://doi.org/10.1128/IAI.69.4.2596-2603.2001

Honda, J. R., Virdi, R., & Chan, E. D. (2018). Global Environmental Nontuberculous Mycobacteria and Their Contemporaneous Man-Made and Natural Niches. *Frontiers in Microbiology*, *9*. https://www.frontiersin.org/article/10.3389/fmicb.2018.02029

Hong, S. J., Kim, T. J., Lee, J.-H., & Park, J.-S. (2016). Nontuberculous mycobacterial pulmonary disease mimicking lung cancer. *Medicine*, *95*(26). https://doi.org/10.1097/MD.0000000000003978

Iftakhar-E-Khuda, I., Koide, N., Hassan, F., Noman, A. S. M., Dagvadorj, J., Tumurkhuu, G., Naiki, Y., Komatsu, T., Yoshida, T., & Yokochi, T. (2009). Novel mechanism of U18666A-induced tumour necrosis factor-α production in RAW 264·7 macrophage cells. *Clinical and Experimental Immunology*, *155*(3), 552–558. https://doi.org/10.1111/j.1365-2249.2008.03779.x

Ilinov, A., Nishiyama, A., Namba, H., Fukushima, Y., Takihara, H., Nakajima, C., Savitskaya, A., Gebretsadik, G., Hakamata, M., Ozeki, Y., Tateishi, Y., Okuda, S., Suzuki, Y., Vinnik, Y. S., & Matsumoto, S. (2021). Extracellular DNA of slow growers of mycobacteria and its contribution to biofilm formation and drug tolerance. *Scientific Reports*, *11*, 10953. https://doi.org/10.1038/s41598-021-90156-z

Ingen, J. van, Ferro, B. E., Hoefsloot, W., Boeree, M. J., & Soolingen, D. van. (2013). Drug treatment of pulmonary nontuberculous mycobacterial disease in HIV-negative patients: The evidence. *Expert Review of Anti-Infective Therapy*, *11*(10), 1065–1077. https://doi.org/10.1586/14787210.2013.830413

Jarlier, V., & Nikaido, H. (1994). Mycobacterial cell wall: Structure and role in natural resistance to antibiotics. *FEMS Microbiology Letters*, *123*(1–2), 11–18. https://doi.org/10.1111/j.1574-6968.1994.tb07194.x

Jeffrey, B., Rose, S. J., Gilbert, K., Lewis, M., & Bermudez, L. E. (2017). Comparative analysis of the genomes of clinical isolates of Mycobacterium avium subsp. Hominissuis regarding virulence-related genes. *Journal of Medical Microbiology*, *66*(7), 1063–1075. https://doi.org/10.1099/jmm.0.000507

Johansen, M. D., Herrmann, J.-L., & Kremer, L. (2020). Non-tuberculous mycobacteria and the rise of Mycobacterium abscessus. *Nature Reviews Microbiology*, *18*(7), 392–407. https://doi.org/10.1038/s41579-020-0331-1

Jung, C. H., Ro, S.-H., Cao, J., Otto, N. M., & Kim, D.-H. (2010). MTOR regulation of autophagy. *FEBS Letters*, *584*(7), 1287–1295. https://doi.org/10.1016/j.febslet.2010.01.017

Kanoh, S., & Rubin, B. K. (2010). Mechanisms of Action and Clinical Application of Macrolides as Immunomodulatory Medications. *Clinical Microbiology Reviews*, *23*(3), 590–615. https://doi.org/10.1128/CMR.00078-09

Keown, D. A. (2010). *The role of cholesterol in the uptake and pathogenesis of Mycobacterium avium subspecies paratuberculosis in human monocytes*. https://doi.org/10.26021/6050

Khandia, R., Dadar, M., Munjal, A., Dhama, K., Karthik, K., Tiwari, R., Yatoo, Mohd. I., Iqbal, H. M. N., Singh, K. P., Joshi, S. K., & Chaicumpa, W. (2019). A Comprehensive Review of Autophagy and Its Various Roles in Infectious, Non-Infectious, and Lifestyle Diseases: Current Knowledge and Prospects for Disease Prevention, Novel Drug Design, and Therapy. *Cells*, *8*(7), 674. https://doi.org/10.3390/cells8070674

Kim, B.-R., Kim, B.-J., Kook, Y.-H., & Kim, B.-J. (2019). Phagosome Escape of Rough Mycobacterium abscessus Strains in Murine Macrophage via Phagosomal Rupture Can Lead to Type I Interferon Production and Their Cell-To-Cell Spread. *Frontiers in Immunology*, *10*, 125. https://doi.org/10.3389/fimmu.2019.00125

Kim, B.-R., Kim, B.-J., Kook, Y.-H., & Kim, B.-J. (2020). Mycobacterium abscessus infection leads to enhanced production of type 1 interferon and NLRP3 inflammasome activation in murine macrophages via mitochondrial oxidative stress. *PLOS Pathogens*, *16*(3), e1008294. https://doi.org/10.1371/journal.ppat.1008294

Kim, M.-J., Wainwright, H. C., Locketz, M., Bekker, L.-G., Walther, G. B., Dittrich, C., Visser, A., Wang, W., Hsu, F.-F., Wiehart, U., Tsenova, L., Kaplan, G., & Russell, D. G. (2010). Caseation of human tuberculosis granulomas correlates with elevated host lipid metabolism. *EMBO Molecular Medicine*, *2*(7), 258–274. https://doi.org/10.1002/emmm.201000079

Kim, S.-W., Subhadra, B., Whang, J., Back, Y. W., Bae, H. S., Kim, H.-J., & Choi, C. H. (2017). Clinical Mycobacterium abscessus strain inhibits autophagy flux and promotes its growth in murine macrophages. *Pathogens and Disease*, *75*(8), ftx107. https://doi.org/10.1093/femspd/ftx107

Klotz, D., Barth, S. A., Baumgärtner, W., & Hewicker-Trautwein, M. (n.d.). *Mycobacterium avium subsp. Hominissuis Infection in a Domestic Rabbit, Germany—Volume 24, Number 3—March 2018—Emerging Infectious Diseases journal—CDC*. https://doi.org/10.3201/eid2403.171692

Knight, M., Braverman, J., Asfaha, K., Gronert, K., & Stanley, S. (2018). Lipid droplet formation in Mycobacterium tuberculosis infected macrophages requires IFN-γ/HIF-1α signaling and supports host defense. *PLOS Pathogens*, *14*(1), e1006874. https://doi.org/10.1371/journal.ppat.1006874

Kuehnel, M. P., Goethe, R., Habermann, A., Mueller, E., Rohde, M., Griffiths, G., & Valentin-Weigand, P. (2001). Characterization of the intracellular survival of Mycobacterium avium ssp. paratuberculosis: Phagosomal pH and fusogenicity in J774 macrophages compared with other mycobacteria. *Cellular Microbiology*, *3*(8), 551–566. https://doi.org/10.1046/j.1462-5822.2001.00139.x

Kumar, S., Khan, M. Z., Khandelwal, N., Chongtham, C., Singha, B., Dabla, A., Behera, D., Singh, A., Gopal, B., Arimbasseri, G. A., Kamat, S. S., & Nandicoori, V. K. (2022). Mycobacterium tuberculosis Transcription Factor EmbR Regulates the Expression of Key Virulence Factors That Aid in Ex Vivo and In Vivo Survival. *MBio*, *13*(3), e03836-21. https://doi.org/10.1128/mbio.03836-21

Kumar, S. N., Prasad, T. S., Narayan, P. A., & Muruganandhan, J. (2013). Granuloma with langhans giant cells: An overview. *Journal of Oral and Maxillofacial Pathology : JOMFP*, *17*(3), 420–423. https://doi.org/10.4103/0973-029X.125211

Kurenuma, T., Kawamura, I., Hara, H., Uchiyama, R., Daim, S., Dewamitta, S. R., Sakai, S., Tsuchiya, K., Nomura, T., & Mitsuyama, M. (2009). The RD1 Locus in the Mycobacterium tuberculosis Genome Contributes to Activation of Caspase-1 via Induction of Potassium Ion Efflux in Infected Macrophages. *Infection and Immunity*, *77*(9), 3992–4001. https://doi.org/10.1128/IAI.00015-09

Kurtz, J. R., Goggins, J. A., & McLachlan, J. B. (2017). Salmonella infection: Interplay between the bacteria and host immune system. *Immunology Letters*, *190*, 42–50. https://doi.org/10.1016/j.imlet.2017.07.006

Langhans, Th. (1868). Ueber Riesenzellen mit wandständigen Kernen in Tuberkeln und die fibröse Form des Tuberkels. *Archiv für pathologische Anatomie und Physiologie und für klinische Medicin*, *42*(3), 382–404. https://doi.org/10.1007/BF02006420

Lappann, M., Claus, H., Van Alen, T., Harmsen, M., Elias, J., Molin, S., & Vogel, U. (2010). A dual role of extracellular DNA during biofilm formation of Neisseria meningitidis. *Molecular Microbiology*, *75*(6), 1355–1371. https://doi.org/10.1111/j.1365-2958.2010.07054.x

Lay, G., Poquet, Y., Salek-Peyron, P., Puissegur, M.-P., Botanch, C., Bon, H., Levillain, F., Duteyrat, J.-L., Emile, J.-F., & Altare, F. (2007). Langhans giant cells from M. tuberculosis-induced human granulomas cannot mediate mycobacterial uptake. *The Journal of Pathology*, *211*(1), 76–85. https://doi.org/10.1002/path.2092

Lee, H.-M., Yuk, J.-M., Kim, K.-H., Jang, J., Kang, G., Park, J. B., Son, J.-W., & Jo, E.-K. (2012). Mycobacterium abscessus activates the NLRP3 inflammasome

via Dectin-1–Syk and p62/SQSTM1. *Immunology and Cell Biology*, *90*(6), 601–610. https://doi.org/10.1038/icb.2011.72

Lee, W., VanderVen, B. C., Fahey, R. J., & Russell, D. G. (2013). Intracellular Mycobacterium tuberculosis Exploits Host-derived Fatty Acids to Limit Metabolic Stress*. *Journal of Biological Chemistry*, *288*(10), 6788–6800. https://doi.org/10.1074/jbc.M112.445056

Li, Y., Miltner, E., Wu, M., Petrofsky, M., & Bermudez, L. E. (2005). A Mycobacterium avium PPE gene is associated with the ability of the bacterium to grow in macrophages and virulence in mice. *Cellular Microbiology*, *7*(4), 539–548. https://doi.org/10.1111/j.1462-5822.2004.00484.x

Lin, Y.-C., Huang, D.-Y., Wang, J.-S., Lin, Y.-L., Hsieh, S.-L., Huang, K.-C., & Lin, W.-W. (2015). Syk is involved in NLRP3 inflammasome-mediated caspase-1 activation through adaptor ASC phosphorylation and enhanced oligomerization. *Journal of Leukocyte Biology*, *97*(5), 825–835. https://doi.org/10.1189/jlb.3HI0814-371RR

Liu, C., Yue, R., Yang, Y., Cui, Y., Yang, L., Zhao, D., & Zhou, X. (2016). AIM2 inhibits autophagy and IFN-β production during M. bovis infection. *Oncotarget*, *7*(30), 46972–46987. https://doi.org/10.18632/oncotarget.10503

Liu, N., Pang, X., Zhang, H., & Ji, P. (2022). The cGAS-STING Pathway in Bacterial Infection and Bacterial Immunity. *Frontiers in Immunology*, *12*. https://www.frontiersin.org/articles/10.3389/fimmu.2021.814709

Liu, X., Wang, C., Yan, B., Lyu, L., Takiff, H. E., & Gao, Q. (2020). The potassium transporter KdpA affects persister formation by regulating ATP levels in Mycobacterium marinum. *Emerging Microbes & Infections*, *9*(1), 129–139. https://doi.org/10.1080/22221751.2019.1710090

Lösslein, A. K., Lohrmann, F., Scheuermann, L., Gharun, K., Neuber, J., Kolter, J., Forde, A. J., Kleimeyer, C., Poh, Y. Y., Mack, M., Triantafyllopoulou, A., Dunlap, M. D., Khader, S. A., Seidl, M., Hölscher, A., Hölscher, C., Guan, X. L., Dorhoi, A., & Henneke, P. (2021). Monocyte progenitors give rise to multinucleated giant cells. *Nature Communications*, *12*(1), 2027. https://doi.org/10.1038/s41467-021-22103-5

Luberto, C., & Hannun, Y. A. (1998). Sphingomyelin Synthase, a Potential Regulator of Intracellular Levels of Ceramide and Diacylglycerol during SV40 Transformation: DOES SPHINGOMYELIN SYNTHASE ACCOUNT FOR THE PUTATIVE PHOSPHATIDYLCHOLINE-SPECIFIC PHOSPHOLIPASE C? *. *Journal of Biological Chemistry*, *273*(23), 14550–14559. https://doi.org/10.1074/jbc.273.23.14550

Luberto, C., Stonehouse, M. J., Collins, E. A., Marchesini, N., El-Bawab, S., Vasil, A. I., Vasil, M. L., & Hannun, Y. A. (2003). Purification, Characterization,

and Identification of a Sphingomyelin Synthase from Pseudomonas aeruginosa: PlcH IS A MULTIFUNCTIONAL ENZYME*. *Journal of Biological Chemistry*, *278*(35), 32733–32743. https://doi.org/10.1074/jbc.M300932200

Lugrin, J., & Martinon, F. (2018). The AIM2 inflammasome: Sensor of pathogens and cellular perturbations. *Immunological Reviews*, *281*(1), 99–114. https://doi.org/10.1111/imr.12618

Lunge, A., Gupta, R., Choudhary, E., & Agarwal, N. (2020). The unfoldase ClpC1 of Mycobacterium tuberculosis regulates the expression of a distinct subset of proteins having intrinsically disordered termini. *Journal of Biological Chemistry*, *295*(28), 9455–9473. https://doi.org/10.1074/jbc.RA120.013456

Ma, R., Ortiz Serrano, T. P., Davis, J., Prigge, A. D., & Ridge, K. M. (2020). The cGAS-STING pathway: The role of self-DNA sensing in inflammatory lung disease. *FASEB Journal : Official Publication of the Federation of American Societies for Experimental Biology*, *34*(10), 13156–13170. https://doi.org/10.1096/fj.202001607R

Madan-Lala, R., Peixoto, K. V., Re, F., & Rengarajan, J. (2011). Mycobacterium tuberculosis Hip1 Dampens Macrophage Proinflammatory Responses by Limiting Toll-Like Receptor 2 Activation. *Infection and Immunity*, *79*(12), 4828–4838. https://doi.org/10.1128/IAI.05574-11

Maphasa, R. E., Meyer, M., & Dube, A. (2021). The Macrophage Response to Mycobacterium tuberculosis and Opportunities for Autophagy Inducing Nanomedicines for Tuberculosis Therapy. *Frontiers in Cellular and Infection Microbiology*, *10*. https://doi.org/10.3389/fcimb.2020.618414

Matern, W. M., Bader, J. S., & Karakousis, P. C. (2018). Genome analysis of Mycobacterium avium subspecies hominissuis strain 109. *Scientific Data*, *5*, 180277. https://doi.org/10.1038/sdata.2018.277

Mayer-Barber, K. D., Barber, D. L., Shenderov, K., White, S. D., Wilson, M. S., Cheever, A., Kugler, D., Hieny, S., Caspar, P., Núñez, G., Schlueter, D., Flavell, R. A., Sutterwala, F. S., & Sher, A. (2010). Cutting Edge: Caspase-1 Independent IL-1β Production Is Critical for Host Resistance to Mycobacterium tuberculosis and Does Not Require TLR Signaling In Vivo. *The Journal of Immunology*, *184*(7), 3326–3330. https://doi.org/10.4049/jimmunol.0904189

McClean, C. M., & Tobin, D. M. (2020). Early cell-autonomous accumulation of neutral lipids during infection promotes mycobacterial growth. *PLOS ONE*, *15*(5), e0232251. https://doi.org/10.1371/journal.pone.0232251

McDonough, K. A., Florczyk, M. A., & Kress, Y. (2000). Intracellular passage within macrophages affects the trafficking of virulent tubercle bacilli upon

reinfection of other macrophages in a serum-dependent manner. *Tubercle and Lung Disease*, *80*(6), 259–271. https://doi.org/10.1054/tuld.2000.0268

McNamara, M., Danelishvili, L., & Bermudez, L. E. (2012). The Mycobacterium avium ESX-5 PPE protein, PPE25-MAV, Interacts with an ESAT-6 Family Protein, MAV_2921, and Localizes to the Bacterial Surface. *Microbial Pathogenesis*, *52*(4), 10.1016/j.micpath.2012.01.004. https://doi.org/10.1016/j.micpath.2012.01.004

Meng, A., Luberto, C., Meier, P., Bai, A., Yang, X., Hannun, Y. A., & Zhou, D. (2004). Sphingomyelin synthase as a potential target for D609-induced apoptosis in U937 human monocytic leukemia cells. *Experimental Cell Research*, *292*(2), 385–392. https://doi.org/10.1016/j.yexcr.2003.10.001

Meng, F., & Lowell, C. A. (1997). Lipopolysaccharide (LPS)-induced Macrophage Activation and Signal Transduction in the Absence of Src-Family Kinases Hck, Fgr, and Lyn. *The Journal of Experimental Medicine*, *185*(9), 1661–1670.

Mezouar, S., Diarra, I., Roudier, J., Desnues, B., & Mege, J. (2019). Tumor Necrosis Factor-alpha antagonist interferes with the formation of granulomatous multinucleated giant cells: New insights into Mycobacterium tuberculosis infection. *Frontiers in Immunology*, *10*. https://doi.org/10.3389/fimmu.2019.01947

Milde, R., Ritter, J., Tennent, G. A., Loesch, A., Martinez, F. O., Gordon, S., Pepys, M. B., Verschoor, A., & Helming, L. (2015). Multinucleated Giant Cells Are Specialized for Complement-Mediated Phagocytosis and Large Target Destruction. *Cell Reports*, *13*(9), 1937–1948. https://doi.org/10.1016/j.celrep.2015.10.065

Milhas, D., Andrieu-Abadie, N., Levade, T., Benoist, H., & Ségui, B. (2012). The Tricyclodecan-9-yl-xanthogenate D609 Triggers Ceramide Increase and Enhances FasL-Induced Caspase-Dependent and -Independent Cell Death in T Lymphocytes. *International Journal of Molecular Sciences*, *13*(7), 8834–8852. https://doi.org/10.3390/ijms13078834

Mishra, A., Vij, M., Kumar, D., Taneja, V., Mondal, A. K., Bothra, A., Rao, V., Ganguli, M., & Taneja, B. (2013). Integration Host Factor of Mycobacterium tuberculosis, mIHF, Compacts DNA by a Bending Mechanism. *PLoS ONE*, *8*(7), e69985. https://doi.org/10.1371/journal.pone.0069985

Mishra, B. B., Rathinam, V. A. K., Martens, G. W., Martinot, A. J., Kornfeld, H., Fitzgerald, K. A., & Sassetti, C. M. (2013a). Nitric oxide controls the immunopathology of tuberculosis by inhibiting NLRP3 inflammasome–dependent processing of IL-1β. *Nature Immunology*, *14*(1), 52–60. https://doi.org/10.1038/ni.2474

Mishra, B. B., Rathinam, V. A. K., Martens, G. W., Martinot, A. J., Kornfeld, H., Fitzgerald, K. A., & Sassetti, C. M. (2013b). Nitric oxide controls tuberculosis immunopathology by inhibiting NLRP3 inflammasome-dependent IL-1β processing. *Nature Immunology*, *14*(1), 52–60. https://doi.org/10.1038/ni.2474

Moscoso, M., García, E., & López, R. (2006). Biofilm Formation by Streptococcus pneumoniae: Role of Choline, Extracellular DNA, and Capsular Polysaccharide in Microbial Accretion. *Journal of Bacteriology*, *188*(22), 7785–7795. https://doi.org/10.1128/JB.00673-06

Murray, P. R., Elmore, C., & Krogstad, D. J. (1980). The Acid-Fast Stain: A Specific and Predictive Test for Mycobacterial Disease. *Annals of Internal Medicine*, *92*(4), 512–513. https://doi.org/10.7326/0003-4819-92-4-512

Ning, L., Wei, W., Wenyang, J., Rui, X., & Qing, G. (2020). Cytosolic DNA-STING-NLRP3 axis is involved in murine acute lung injury induced by lipopolysaccharide. *Clinical and Translational Medicine*, *10*(7), e228. https://doi.org/10.1002/ctm2.228

Oh, Y. K., & Straubinger, R. M. (1996). Intracellular fate of Mycobacterium avium: Use of dual-label spectrofluorometry to investigate the influence of bacterial viability and opsonization on phagosomal pH and phagosome-lysosome interaction. *Infection and Immunity*, *64*(1), 319–325.

Ohshimo, S., Guzman, J., Costabel, U., & Bonella, F. (2017). Differential diagnosis of granulomatous lung disease: Clues and pitfalls: Number 4 in the Series "Pathology for the clinician" Edited by Peter Dorfmüller and Alberto Cavazza. *European Respiratory Review*, *26*(145). https://doi.org/10.1183/16000617.0012-2017

Ojha, A., Anand, M., Bhatt, A., Kremer, L., Jacobs, W. R., & Hatfull, G. F. (2005). GroEL1: A Dedicated Chaperone Involved in Mycolic Acid Biosynthesis during Biofilm Formation in Mycobacteria. *Cell*, *123*(5), 861–873. https://doi.org/10.1016/j.cell.2005.09.012

Okino, N., Tani, M., Imayama, S., & Ito, M. (1998). Purification and Characterization of a Novel Ceramidase fromPseudomonas aeruginosa *. *Journal of Biological Chemistry*, *273*(23), 14368–14373. https://doi.org/10.1074/jbc.273.23.14368

Osada-Oka, M., Goda, N., Saiga, H., Yamamoto, M., Takeda, K., Ozeki, Y., Yamaguchi, T., Soga, T., Tateishi, Y., Miura, K., Okuzaki, D., Kobayashi, K., & Matsumoto, S. (2019). Metabolic adaptation to glycolysis is a basic defense mechanism of macrophages for Mycobacterium tuberculosis infection. *International Immunology*, *31*(12), 781–793. https://doi.org/10.1093/intimm/dxz048

Osman, M. M., Pagán, A. J., Shanahan, J. K., & Ramakrishnan, L. (2020). Mycobacterium marinum phthiocerol dimycocerosates enhance macrophage

phagosomal permeabilization and membrane damage. *PLOS ONE*, *15*(7), e0233252. https://doi.org/10.1371/journal.pone.0233252

Pandey, A. K., & Sassetti, C. M. (2008). Mycobacterial persistence requires the utilization of host cholesterol. *Proceedings of the National Academy of Sciences of the United States of America*, *105*(11), 4376–4380. https://doi.org/10.1073/pnas.0711159105

Peng, X., & Sun, J. (2016). Mechanism of ESAT-6 membrane interaction and its roles in pathogenesis of Mycobacterium tuberculosis. *Toxicon : Official Journal of the International Society on Toxinology*, *116*, 29–34. https://doi.org/10.1016/j.toxicon.2015.10.003

Peyron, P., Vaubourgeix, J., Poquet, Y., Levillain, F., Botanch, C., Bardou, F., Daffé, M., Emile, J.-F., Marchou, B., Cardona, P.-J., Chastellier, C. de, & Altare, F. (2008). Foamy Macrophages from Tuberculous Patients' Granulomas Constitute a Nutrient-Rich Reservoir for M. tuberculosis Persistence. *PLOS Pathogens*, *4*(11), e1000204. https://doi.org/10.1371/journal.ppat.1000204

Phillips, I. L., Danelishvili, L., & Bermudez, L. E. (2021). Macrophage Proteome Analysis at Different Stages of Mycobacterium avium Subspecies paratuberculosis Infection Reveals a Mechanism of Pathogen Dissemination. *Proteomes*, *9*(2), 20. https://doi.org/10.3390/proteomes9020020

Polotsky, V. Y., Belisle, J. T., Mikusova, K., Ezekowitz, R. A., & Joiner, K. A. (1997). Interaction of human mannose-binding protein with Mycobacterium avium. *The Journal of Infectious Diseases*, *175*(5), 1159–1168. https://doi.org/10.1086/520354

Prevots, D. R., & Marras, T. K. (2015). Epidemiology of Human Pulmonary Infection with Nontuberculous Mycobacteria: A Review. *Clinics in Chest Medicine*, *36*(1), 13–34. https://doi.org/10.1016/j.ccm.2014.10.002

Puissegur, M.-P., Botanch, C., Duteyrat, J.-L., Delsol, G., Caratero, C., & Altare, F. (2004). An in vitro dual model of mycobacterial granulomas to investigate the molecular interactions between mycobacteria and human host cells. *Cellular Microbiology*, *6*(5), 423–433. https://doi.org/10.1111/j.1462-5822.2004.00371.x

Py, B. F., Kim, M.-S., Vakifahmetoglu-Norberg, H., & Yuan, J. (2013). Deubiquitination of NLRP3 by BRCC3 Critically Regulates Inflammasome Activity. *Molecular Cell*, *49*(2), 331–338. https://doi.org/10.1016/j.molcel.2012.11.009

Qian, J., Chen, R., Wang, H., & Zhang, X. (2020). Role of the PE/PPE Family in Host–Pathogen Interactions and Prospects for Anti-Tuberculosis Vaccine and Diagnostic Tool Design. *Frontiers in Cellular and Infection Microbiology*, *10*. https://www.frontiersin.org/articles/10.3389/fcimb.2020.594288

Rastogi, S., & Briken, V. (2022). Interaction of Mycobacteria With Host Cell Inflammasomes. *Frontiers in Immunology*, *13*. https://www.frontiersin.org/article/10.3389/fimmu.2022.791136

Rastogi, S., Ellinwood, S., Augenstreich, J., Mayer-Barber, K. D., & Briken, V. (2021a). Mycobacterium tuberculosis inhibits the NLRP3 inflammasome activation via its phosphokinase PknF. *PLOS Pathogens*, *17*(7), e1009712. https://doi.org/10.1371/journal.ppat.1009712

Rastogi, S., Ellinwood, S., Augenstreich, J., Mayer-Barber, K. D., & Briken, V. (2021b). Mycobacterium tuberculosis inhibits the NLRP3 inflammasome activation via its phosphokinase PknF. *PLOS Pathogens*, *17*(7), e1009712. https://doi.org/10.1371/journal.ppat.1009712

Ratnatunga, C. N., Lutzky, V. P., Kupz, A., Doolan, D. L., Reid, D. W., Field, M., Bell, S. C., Thomson, R. M., & Miles, J. J. (2020). The Rise of Non-Tuberculosis Mycobacterial Lung Disease. *Frontiers in Immunology*, *11*. https://www.frontiersin.org/article/10.3389/fimmu.2020.00303

Reich, J. M., & Johnson, R. E. (1992). Mycobacterium avium Complex Pulmonary Disease Presenting as an Isolated Lingular or Middle Lobe Pattern: The Lady Windermere Syndrome. *Chest*, *101*(6), 1605–1609. https://doi.org/10.1378/chest.101.6.1605

Rivera-Calzada, A., Famelis, N., Llorca, O., & Geibel, S. (2021). Type VII secretion systems: Structure, functions and transport models. *Nature Reviews Microbiology*, *19*(9), 567–584. https://doi.org/10.1038/s41579-021-00560-5

Rocco, J. M., & Irani, V. R. (2011). Mycobacterium avium and modulation of the host macrophage immune mechanisms [Review article]. *The International Journal of Tuberculosis and Lung Disease*, *15*(4), 447–452. https://doi.org/10.5588/ijtld.09.0695

Rolando, M., & Buchrieser, C. (2019). A Comprehensive Review on the Manipulation of the Sphingolipid Pathway by Pathogenic Bacteria. *Frontiers in Cell and Developmental Biology*, *7*. https://doi.org/10.3389/fcell.2019.00168

Rose, S. J., Babrak, L. M., & Bermudez, L. E. (2015). Mycobacterium avium Possesses Extracellular DNA that Contributes to Biofilm Formation, Structural Integrity, and Tolerance to Antibiotics. *PLoS ONE*, *10*(5), e0128772. https://doi.org/10.1371/journal.pone.0128772

Rose, S. J., & Bermudez, L. E. (2014). Mycobacterium avium Biofilm Attenuates Mononuclear Phagocyte Function by Triggering Hyperstimulation and Apoptosis during Early Infection. *Infection and Immunity*, *82*(1), 405–412. https://doi.org/10.1128/IAI.00820-13

Rose, S. J., & Bermudez, L. E. (2016). Identification of Bicarbonate as a Trigger and Genes Involved with Extracellular DNA Export in Mycobacterial Biofilms. *MBio*, *7*(6). https://doi.org/10.1128/mBio.01597-16

ROY, S., GHATAK, D., DAS, P., & BOSEDASGUPTA, S. (2020). ESX secretion system: The gatekeepers of mycobacterial survivability and pathogenesis. *European Journal of Microbiology & Immunology*, *10*(4), 202–209. https://doi.org/10.1556/1886.2020.00028

Russell, D. G., Dant, J., & Sturgill-Koszycki, S. (1996). Mycobacterium avium- and Mycobacterium tuberculosis-containing vacuoles are dynamic, fusion-competent vesicles that are accessible to glycosphingolipids from the host cell plasmalemma. *The Journal of Immunology*, *156*(12), 4764–4773.

Sabir, N., Hussain, T., Shah, S. Z. A., Zhao, D., & Zhou, X. (2017). IFN-β: A Contentious Player in Host–Pathogen Interaction in Tuberculosis. *International Journal of Molecular Sciences*, *18*(12), 2725. https://doi.org/10.3390/ijms18122725

Saiga, H., Kitada, S., Shimada, Y., Kamiyama, N., Okuyama, M., Makino, M., Yamamoto, M., & Takeda, K. (2012). Critical role of AIM2 in Mycobacterium tuberculosis infection. *International Immunology, 24*(10), 637–644. https://doi.org/10.1093/intimm/dxs062

Sakai, H., Okafuji, I., Nishikomori, R., Abe, J., Izawa, K., Kambe, N., Yasumi, T., Nakahata, T., & Heike, T. (2012). The CD40–CD40L axis and IFN-γ play critical roles in Langhans giant cell formation. *International Immunology, 24*(1), 5–15. https://doi.org/10.1093/intimm/dxr088

Schoggins, J. W., MacDuff, D. A., Imanaka, N., Gainey, M. D., Shrestha, B., Eitson, J. L., Mar, K. B., Richardson, R. B., Ratushny, A. V., Litvak, V., Dabelic, R., Manicassamy, B., Aitchison, J. D., Aderem, A., Elliott, R. M., García-Sastre, A., Racaniello, V., Snijder, E. J., Yokoyama, W. M., … Rice, C. M. (2014). Pan-viral specificity of IFN-induced genes reveals new roles for cGAS in innate immunity. *Nature*, *505*(7485), 691–695. https://doi.org/10.1038/nature12862

Serafini, A., Tan, L., Horswell, S., Howell, S., Greenwood, D. J., Hunt, D. M., Phan, M., Schembri, M., Monteleone, M., Montague, C. R., Britton, W., Garza-Garcia, A., Snijders, A. P., VanderVen, B., Gutierrez, M. G., West, N. P., & de Carvalho, L. P. S. (2019). Mycobacterium tuberculosis requires glyoxylate shunt and reverse methylcitrate cycle for lactate and pyruvate metabolism. *Molecular Microbiology*, *112*(4), 1284–1307. https://doi.org/10.1111/mmi.14362

Shah, S., Bohsali, A., Ahlbrand, S. E., Srinivasan, L., Rathinam, V. A. K., Vogel, S. N., Fitzgerald, K. A., Sutterwala, F. S., & Briken, V. (2013). Cutting Edge: Mycobacterium tuberculosis but Not Nonvirulent Mycobacteria Inhibits IFN-

β and AIM2 Inflammasome–Dependent IL-1β Production via Its ESX-1 Secretion System. *The Journal of Immunology*, *191*(7), 3514–3518. https://doi.org/10.4049/jimmunol.1301331

Shin, D.-M., Jeon, B.-Y., Lee, H.-M., Jin, H. S., Yuk, J.-M., Song, C.-H., Lee, S.-H., Lee, Z.-W., Cho, S.-N., Kim, J.-M., Friedman, R. L., & Jo, E.-K. (2010). Mycobacterium tuberculosis Eis Regulates Autophagy, Inflammation, and Cell Death through Redox-dependent Signaling. *PLOS Pathogens*, *6*(12), e1001230. https://doi.org/10.1371/journal.ppat.1001230

Smith, D., Hänsch, H., Bancroft, G., & Ehlers, S. (1997). T-cell-independent granuloma formation in response to Mycobacterium avium: Role of tumour necrosis factor-α and interferon-γ. *Immunology*, *92*(4), 413–421. https://doi.org/10.1046/j.1365-2567.1997.00384.x

Sohaskey, C. D. Y. 2005. (n.d.). Regulation of nitrate reductase activity in Mycobacterium tuberculosis by oxygen and nitric oxide. *Microbiology*, *151*(11), 3803–3810. https://doi.org/10.1099/mic.0.28263-0

Song, N., Liu, Z.-S., Xue, W., Bai, Z.-F., Wang, Q.-Y., Dai, J., Liu, X., Huang, Y.-J., Cai, H., Zhan, X.-Y., Han, Q.-Y., Wang, H., Chen, Y., Li, H.-Y., Li, A.-L., Zhang, X.-M., Zhou, T., & Li, T. (2017). NLRP3 Phosphorylation Is an Essential Priming Event for Inflammasome Activation. *Molecular Cell*, *68*(1), 185-197.e6. https://doi.org/10.1016/j.molcel.2017.08.017

Speer, A., Sun, J., Danilchanka, O., Meikle, V., Rowland, J. L., Walter, K., Buck, B. R., Pavlenok, M., Hölscher, C., Ehrt, S., & Niederweis, M. (2015). Surface hydrolysis of sphingomyelin by the outer membrane protein Rv0888 supports replication of Mycobacterium tuberculosis in macrophages. *Molecular Microbiology*, *97*(5), 881–897. https://doi.org/10.1111/mmi.13073

Stamm, L. M., Morisaki, J. H., Gao, L.-Y., Jeng, R. L., McDonald, K. L., Roth, R., Takeshita, S., Heuser, J., Welch, M. D., & Brown, E. J. (2003). Mycobacterium marinum Escapes from Phagosomes and Is Propelled by Actin-based Motility. *The Journal of Experimental Medicine*, *198*(9), 1361–1368. https://doi.org/10.1084/jem.20031072

Stanley, S. A., Raghavan, S., Hwang, W. W., & Cox, J. S. (2003). Acute infection and macrophage subversion by Mycobacterium tuberculosis require a specialized secretion system. *Proceedings of the National Academy of Sciences of the United States of America*, *100*(22), 13001–13006. https://doi.org/10.1073/pnas.2235593100

Steele, S., Brunton, J., & Kawula, T. (2015). The role of autophagy in intracellular pathogen nutrient acquisition. *Frontiers in Cellular and Infection Microbiology*, *5*. https://www.frontiersin.org/article/10.3389/fcimb.2015.00051

Steele, S., Brunton, J., Ziehr, B., Taft-Benz, S., Moorman, N., & Kawula, T. (2013). Francisella tularensis Harvests Nutrients Derived via ATG5-Independent Autophagy to Support Intracellular Growth. *PLoS Pathogens*, *9*(8). https://doi.org/10.1371/journal.ppat.1003562

Stromhaug, P. E., & Klionsky, D. J. (2001). Approaching the Molecular Mechanism of Autophagy. *Traffic*, *2*(8), 524–531. https://doi.org/10.1034/j.1600-0854.2001.20802.x

Sturgill-Koszycki, S., Schlesinger, P. H., Chakraborty, P., Haddix, P. L., Collins, H. L., Fok, A. K., Allen, R. D., Gluck, S. L., Heuser, J., & Russell, D. G. (1994). Lack of acidification in Mycobacterium phagosomes produced by exclusion of the vesicular proton-ATPase. *Science*, *263*(5147), 678–681. https://doi.org/10.1126/science.8303277

Sun, Y., Zhang, W., Dong, C., & Xiong, S. (2020). Mycobacterium tuberculosis MmsA (Rv0753c) Interacts with STING and Blunts the Type I Interferon Response. *MBio*, *11*(6), e03254-19. https://doi.org/10.1128/mBio.03254-19

Swanson, K. V., Deng, M., & Ting, J. P.-Y. (2019). The NLRP3 inflammasome: Molecular activation and regulation to therapeutics. *Nature Reviews Immunology*, *19*(8), 477–489. https://doi.org/10.1038/s41577-019-0165-0

Sweet, L., & Schorey, J. S. (2006). Glycopeptidolipids from Mycobacterium avium promote macrophage activation in a TLR2- and MyD88-dependent manner. *Journal of Leukocyte Biology*, *80*(2), 415–423. https://doi.org/10.1189/jlb.1205702

Tambuyzer, B. R., & Nouwen, E. J. (2005). Inhibition of microglia multinucleated giant cell formation and induction of differentiation by GM-CSF using a porcine in vitro model. *Cytokine*, *31*(4), 270–279. https://doi.org/10.1016/j.cyto.2005.05.006

Teles, R. M. B., Graeber, T. G., Krutzik, S. R., Montoya, D., Schenk, M., Lee, D. J., Komisopoulou, E., Kelly-Scumpia, K., Chun, R., Iyer, S. S., Sarno, E. N., Rea, T. H., Hewison, M., Adams, J. S., Popper, S. J., Relman, D. A., Stenger, S., Bloom, B. R., Cheng, G., & Modlin, R. L. (2013). Type I Interferon Suppresses Type II Interferon–Triggered Human Anti-Mycobacterial Responses. *Science*, *339*(6126), 1448–1453. https://doi.org/10.1126/science.1233665

Tufariello, J. M., Chapman, J. R., Kerantzas, C. A., Wong, K.-W., Vilchèze, C., Jones, C. M., Cole, L. E., Tinaztepe, E., Thompson, V., Fenyö, D., Niederweis, M., Ueberheide, B., Philips, J. A., & Jacobs, W. R. (2016). Separable roles for Mycobacterium tuberculosis ESX-3 effectors in iron acquisition and virulence. *Proceedings of the National Academy of Sciences*, *113*(3), E348–E357. https://doi.org/10.1073/pnas.1523321113

Ufimtseva, E. (2015). Mycobacterium-Host Cell Relationships in Granulomatous Lesions in a Mouse Model of Latent Tuberculous Infection. *BioMed Research International*, *2015*, e948131. https://doi.org/10.1155/2015/948131

van der Niet, S., van Zon, M., de Punder, K., Grootemaat, A., Rutten, S., Moorlag, S. J. C. F. M., Houben, D., van der Sar, A. M., Bitter, W., Brosch, R., Hernandez Pando, R., Pena, M. T., Peters, P. J., Reits, E. A., Mayer-Barber, K. D., & van der Wel, N. N. (2021). IL-1R1-Dependent Signals Improve Control of Cytosolic Virulent Mycobacteria In Vivo. *MSphere*, *6*(3), e00153-21. https://doi.org/10.1128/mSphere.00153-21

Vega-Dominguez, P., Peterson, E., Pan, M., Di Maio, A., Singh, S., Umapathy, S., Saini, D. K., Baliga, N., & Bhatt, A. (2020). Biofilms of the non-tuberculous Mycobacterium chelonae form an extracellular matrix and display distinct expression patterns. *The Cell Surface*, *6*, 100043. https://doi.org/10.1016/j.tcsw.2020.100043

Via, L. E., Deretic, D., Ulmer, R. J., Hibler, N. S., Huber, L. A., & Deretic, V. (1997). Arrest of Mycobacterial Phagosome Maturation Is Caused by a Block in Vesicle Fusion between Stages Controlled by rab5 and rab7 *. *Journal of Biological Chemistry*, *272*(20), 13326–13331. https://doi.org/10.1074/jbc.272.20.13326

Vinod, V., Pushkaran, A. C., Kumar, A., Mohan, C. G., & Biswas, R. (2021). Interaction mechanism of Mycobacterium tuberculosis GroEL2 protein with macrophage Lectin-like, oxidized low-density lipoprotein receptor-1: An integrated computational and experimental study. *Biochimica et Biophysica Acta (BBA) - General Subjects*, *1865*(1), 129758. https://doi.org/10.1016/j.bbagen.2020.129758

Volkman, H. E., Clay, H., Beery, D., Chang, J. C. W., Sherman, D. R., & Ramakrishnan, L. (2004). Tuberculous Granuloma Formation Is Enhanced by a Mycobacterium Virulence Determinant. *PLoS Biology*, *2*(11). https://doi.org/10.1371/journal.pbio.0020367

Wagner, D., Sangari, F. J., Kim, S., Petrofsky, M., & Bermudez, L. E. (2002). Mycobacterium avium infection of macrophages results in progressive suppression of interleukin-12 production in vitro and in vivo. *Journal of Leukocyte Biology*, *71*(1), 80–88. https://doi.org/10.1189/jlb.71.1.80

Wang, C. H., Lin, H. C., Liu, C. Y., Huang, K. H., Huang, T. T., Yu, C. T., & Kuo, H. P. (2001). Upregulation of inducible nitric oxide synthase and cytokine secretion in peripheral blood monocytes from pulmonary tuberculosis patients. *The International Journal of Tuberculosis and Lung Disease*, *5*(3), 283–291.

Wang, J., Pan, X.-L., Ding, L.-J., Liu, D.-Y., Lei, D.-P., & Jin, T. (2013). Aberrant Expression of Beclin-1 and LC3 Correlates with Poor Prognosis of Human

Hypopharyngeal Squamous Cell Carcinoma. *PLOS ONE*, *8*(7), e69038. https://doi.org/10.1371/journal.pone.0069038

Wassermann, R., Gulen, M. F., Sala, C., Perin, S. G., Lou, Y., Rybniker, J., Schmid-Burgk, J. L., Schmidt, T., Hornung, V., Cole, S. T., & Ablasser, A. (2015). Mycobacterium tuberculosis Differentially Activates cGAS- and Inflammasome-Dependent Intracellular Immune Responses through ESX-1. *Cell Host & Microbe*, *17*(6), 799–810. https://doi.org/10.1016/j.chom.2015.05.003

Watson, R. O., Bell, S. L., MacDuff, D. A., Kimmey, J. M., Diner, E. J., Olivas, J., Vance, R. E., Stallings, C. L., Virgin, H. W., & Cox, J. S. (2015). The Cytosolic Sensor cGAS Detects Mycobacterium tuberculosis DNA to Induce Type I Interferons and Activate Autophagy. *Cell Host & Microbe*, *17*(6), 811–819. https://doi.org/10.1016/j.chom.2015.05.004

Weiss, G., & Schaible, U. E. (2015). Macrophage defense mechanisms against intracellular bacteria. *Immunological Reviews*, *264*(1), 182–203. https://doi.org/10.1111/imr.12266

Whiteley, L., Meffert, T., Haug, M., Weidenmaier, C., Hopf, V., Bitschar, K., Schittek, B., Kohler, C., Steinmetz, I., West, T. E., & Schwarz, S. (2017). Entry, Intracellular Survival, and Multinucleated-Giant-Cell-Forming Activity of Burkholderia pseudomallei in Human Primary Phagocytic and Nonphagocytic Cells. *Infection and Immunity*, *85*(10), e00468-17. https://doi.org/10.1128/IAI.00468-17

Wilburn, K. M., Fieweger, R. A., & VanderVen, B. C. (2018). Cholesterol and fatty acids grease the wheels of Mycobacterium tuberculosis pathogenesis. *Pathogens and Disease*, *76*(fty021). https://doi.org/10.1093/femspd/fty021

Wilińska, E., & Szturmowicz, M. (2010). Lung mycobacteriosis—Clinical presentation, diagnostics and treatment. *Advances in Respiratory Medicine*, *78*(2), 138–147. https://doi.org/10.5603/ARM.27742

Wong, K.-W., & Jacobs Jr, W. R. (2011). Critical role for NLRP3 in necrotic death triggered by Mycobacterium tuberculosis. *Cellular Microbiology*, *13*(9), 1371–1384. https://doi.org/10.1111/j.1462-5822.2011.01625.x

Wu, M.-F., Shu, C.-C., Wang, J.-Y., Yan, B.-S., Lai, H.-C., Chiang, B.-L., Wu, L. S.-H., & Yu, C.-J. (2019). NLRP3 inflammasome is attenuated in patients with Mycobacterium avium complex lung disease and correlated with decreased interleukin-1β response and host susceptibility. *Scientific Reports*, *9*(1), 12534. https://doi.org/10.1038/s41598-019-47609-3

Xiong, M., Wang, S., Wang, Y.-Y., & Ran, Y. (2018). The Regulation of cGAS. *Virologica Sinica*, *33*(2), 117–124. https://doi.org/10.1007/s12250-018-0005-6

Xu, F., Qi, H., Li, J., Sun, L., Gong, J., Chen, Y., Shen, A., & Li, W. (2020). Mycobacterium tuberculosis infection up-regulates MFN2 expression to promote NLRP3 inflammasome formation. *The Journal of Biological Chemistry*, *295*(51), 17684–17697. https://doi.org/10.1074/jbc.RA120.014077

Yamazaki, Y., Danelishvili, L., Wu, M., Hidaka, E., Katsuyama, T., Stang, B., Petrofsky, M., Bildfell, R., & Bermudez, L. E. (2006). The ability to form biofilm influences Mycobacterium avium invasion and translocation of bronchial epithelial cells. *Cellular Microbiology*, *8*(5), 806–814. https://doi.org/10.1111/j.1462-5822.2005.00667.x

Yunna, C., Mengru, H., Lei, W., & Weidong, C. (2020). Macrophage M1/M2 polarization. *European Journal of Pharmacology*, *877*, 173090. https://doi.org/10.1016/j.ejphar.2020.173090

Zheng, X.-F., Hong, Y.-X., Feng, G.-J., Zhang, G.-F., Rogers, H., Lewis, M. A. O., Williams, D. W., Xia, Z.-F., Song, B., & Wei, X.-Q. (2013). Lipopolysaccharide-Induced M2 to M1 Macrophage Transformation for IL-12p70 Production Is Blocked by Candida albicans Mediated Up-Regulation of EBI3 Expression. *PLoS ONE*, *8*(5), e63967. https://doi.org/10.1371/journal.pone.0063967

Zhou, R., Tardivel, A., Thorens, B., Choi, I., & Tschopp, J. (2010). Thioredoxin-interacting protein links oxidative stress to inflammasome activation. *Nature Immunology*, *11*(2), 136–140. https://doi.org/10.1038/ni.1831

Zimmermann, P., Ziesenitz, V. C., Curtis, N., & Ritz, N. (2018). The Immunomodulatory Effects of Macrolides—A Systematic Review of the Underlying Mechanisms. *Frontiers in Immunology*, *9*. https://www.frontiersin.org/articles/10.3389/fimmu.2018.00302

Appendix

Appendix 1. Abstract of Additional Manuscript

Amikacin Liposome Inhalation Suspension (ALIS) Penetrates Non-tuberculous Mycobacterial Biofilms and Enhances Amikacin Uptake Into Macrophages

Authors: Jimin Zhang, Franziska Leifer, Sasha Rose, Dung Yu Chun, Jill Thaisz, Tracey Herr, Mary Nashed, Jayanthi Joseph, Walter R. Perkins and Keith DiPetrillo.

Journal: Frontiers in Microbiology. May 16, 2018.

Abstract:

Non-tuberculous mycobacteria (NTM) cause pulmonary infections in patients with structural lung damage, impaired immunity, or other risk factors. Delivering antibiotics to the sites of these infections is a major hurdle of therapy because pulmonary NTM infections can persist in biofilms or as intracellular infections within macrophages. Inhaled treatments can improve antibiotic delivery into the lungs, but efficient nebulization delivery, distribution throughout the lungs, and penetration into biofilms and macrophages are considerable challenges for this approach. Therefore, we developed amikacin liposome inhalation suspension (ALIS) to overcome these challenges. Nebulization of ALIS has been shown to provide particles within the respirable size range that distribute to both central and peripheral lung compartments in humans. The *in vitro* and *in vivo* efficacy of ALIS against NTM has been demonstrated previously. The key mechanistic questions are whether ALIS penetrates NTM biofilms and enhances amikacin uptake into macrophages. We found that ALIS effectively penetrated throughout NTM biofilms and concentration-dependently reduced the number of viable mycobacteria. Additionally, we found that ALIS improved amikacin uptake by ~4-fold into cultured macrophages compared with free amikacin. In rats, inhaled ALIS increased amikacin concentrations in pulmonary

macrophages by 5- to 8-fold at 2, 6, and 24 h post-dose and retained more amikacin at 24 h in airways and lung tissue relative to inhaled free amikacin. Compared to intravenous free amikacin, a standard-of-care therapy for refractory and severe NTM lung disease, ALIS increased the mean area under the concentration-time curve in lung tissue, airways, and macrophages by 42-, 69-, and 274-fold. These data demonstrate that ALIS effectively penetrates NTM biofilms, enhances amikacin uptake into macrophages, both *in vitro* and *in vivo*, and retains amikacin within airways and lung tissue. An ongoing Phase III trial, adding ALIS to guideline-based therapy, met its primary endpoint of culture conversion by month six. ALIS represents a promising new treatment approach for patients with refractory NTM lung disease.